RECLAMATION

*Managing Water in the West*

Desalination and Water Purification Research and Development Program Report No. 170

# Development and Testing of a Copper-Charged Cellulose Acetate Membrane for Biofilm Control

U.S. Department of the Interior
Bureau of Reclamation

December 2013

| REPORT DOCUMENTATION PAGE | *Form Approved* *OMB No. 0704-0188* |
|---|---|



**1. REPORT DATE** *(DD-MM-YYYY)*
25 Nov 2013

**2. REPORT TYPE**
Final

**3. DATES COVERED** *(From - To)*
Oct 2011 to Nov 2013

**4. TITLE AND SUBTITLE**
Development and Testing of a Copper-Charged Cellulose Acetate Membrane for Biofilm Control

**5a. CONTRACT NUMBER**
Agreement No. R11AC81536

**5b. GRANT NUMBER**

**5c. PROGRAM ELEMENT NUMBER**

**6. AUTHOR(S)**
Isabel C. Escobar
Cyndee L. Gruden
Sunitha Asapu

**5d. PROJECT NUMBER**

**5e. TASK NUMBER**
Task IV

**5f. WORK UNIT NUMBER**

**7. PERFORMING ORGANIZATION NAME(S) AND ADDRESS(ES)**
The University of Toledo
2801 W. Bancroft Street
Toledo, OH 43606-3390

**8. PERFORMING ORGANIZATION REPORT NUMBER**

**9. SPONSORING/MONITORING AGENCY NAME(S) AND ADDRESS(ES)**
U.S. Department of the Interior, Bureau of Reclamation
Technical Service Center, Environmental Services Division
Water Treatment Engineering and Research Group, 86-68230
PO Box 25007, Denver, CO 80225-0007

**10. SPONSOR/MONITOR'S ACRONYM(S)**
BOR

**11. SPONSOR/MONITOR'S REPORT NUMBER(S)**
DWPR Report No. 170

**12. DISTRIBUTION/AVAILABILITY STATEMENT**
Available from the National Technical Information Service (NTIS), Operations Division, 5285 Port Royal Road, Springfield, VA 22161

**13. SUPPLEMENTARY NOTE**
Report can be downloaded from Reclamation Web site:
www.usbr.gov/pmts/water/publications/reports.html

**14. ABSTRACT**
The goal of this project was to develop low-biofouling membranes through the functionalization of cellulose acetate (CA) membranes with metal chelating ligands charged with biocidal metal ions, i.e., copper ions. To this end, glycidyl methacrylate, an epoxy, was used to attach a chelating agent, iminodiacetic acid (IDA), to facilitate the charging of copper to the membrane surface. CA and copper-charged membranes were characterized chemically and structurally. Permeation experiments were conducted with distilled (DI) water and then subjected to protein rejection measurements. The permeation of the copper-charged membrane was initially lower than the CA membrane during the filtration of DI water. The membranes were then subjected to bovine serum albumin (BSA) and lipase filtration. The copper-charged membrane showed higher permeation values for of both proteins as compared to CA membranes. This resulted from increased resistance from the IDA and copper on the surface during DI water filtration, and later, from reduced fouling from both proteins. The rejection of BSA and lipase was the same for both the copper-charged and CA membranes. Therefore, the modified membranes have a potential to be used as low-biofouling membranes in the future.

**15. SUBJECT TERMS**
biofouling, cellulose acetate, reverse osmosis, nanofiltration, surface functionalization, copper

| 16. SECURITY CLASSIFICATION OF: | | | 17. LIMITATION OF ABSTRACT | 18. NUMBER OF PAGES | 19a. NAME OF RESPONSIBLE PERSON |
|---|---|---|---|---|---|
| | | | | | John Walp |
| a. REPORT | b. ABSTRACT | a. THIS PAGE | | | 19b. TELEPHONE NUMBER *(Include area code)* |
| U | U | U | SAR | | 303-445-2871 |

**Standard Form 298 (Rev. 8/98)**
Prescribed by ANSI Std. Z39.18

Desalination and Water Purification Research and Development Program Report No. 170

# Development and Testing of a Copper-Charged Cellulose Acetate Membrane for Biofilm Control

Prepared for Reclamation Under Agreement No. R110AC81536

*by*

**Isabel C. Escobar**
**Cyndee L. Gruden**

U.S. Department of the Interior
Bureau of Reclamation

December 2013

# MISSION STATEMENTS

The U.S. Department of the Interior protects America's natural resources and heritage, honors our cultures and tribal communities, and supplies the energy to power our future.

The mission of the Bureau of Reclamation is to manage, develop, and protect water and related resources in an environmentally and economically sound manner in the interest of the American public.

## Disclaimer

The views, analyses, recommendations, and conclusions in this report are those of the authors and do not represent official or unofficial policies or opinions of the U.S. Government, and the United States takes no position with regard to any findings, conclusions, or recommendations made. As such, mention of trade names or commercial products does not constitute their endorsement by the U.S. Government.

## Acknowledgements

The research reported herein was made possible by a grant from the Bureau of Reclamation's Desalination and Water Purification Research and Development Program (Cooperative Agreement No. R11AC81537). The contents do not necessarily reflect the views and policies of the sponsors nor does the mention of trade names or commercial products constitute endorsement or recommendation for use. The authors wish to express their appreciation for the advice and assistance of Frank Leitz and Andrew Tiffenbach, the Bureau of Reclamation project officers. The authors are especially grateful to Mr. Jonathan Daly and his staff at the City of Corona, specifically Mr. Justin Amon, Mr. Tom Moody, and the operators at the Temescal Desalter, for providing facilities for the pilot testing and assisting with set up and decommissioning of the equipment. Further thanks go to GE Infrastructure Water and Process Technologies, who provided some pilot equipment at a reduced cost, and to Mr. Jeff Mosher and the Southern California Salinity Coalition who also provided some financial assistance for the project.

# ACRONYMS AND ABBREVIATIONS

| | |
|---|---|
| ATCC | American Type Culture Collection |
| BSA | bovine serum albumin |
| CA | cellulose acetate |
| CCMP | Center for Cultivation of Marine Phytoplankton |
| DI | distilled |
| DMSO | dimethyl sulfoxide |
| DNA | deoxyribonucleic acid |
| DOM | dissolved organic matter |
| EDS | energy dispersive X-ray spectroscopy |
| EDTA | ethylenediaminetetraacetic acid |
| EPS | extracellular polymeric substance |
| FTIR | Fourier transform infrared spectroscopy |
| g/L | grams per liter |
| GMA | glycidyl methacrylate |
| IDA | iminodiacetic acid |
| IMA | immobilized metal affinity |
| M | moles per liter |
| MF | microfiltration |
| mg/L | milligrams per liter |
| mL | milliliter |
| mM | millimole |
| Mw | molecular weight |
| NaCl | sodium chloride |
| NF | nanofiltration |
| nm | nanometer |
| NMP | N-methyl-2-pyrrolidinone |
| NOM | natural organic matter |
| PA | polyamide |
| PEG | polyethylene glycol |
| pI | isoelectric points |
| PP | polypropylene |
| ppm | parts per million |
| PS | polysulfone |
| RO | reverse osmosis |
| SEM | scanning electron microscopy |
| TEP | transparent exopolymeric particles |
| TFC | thin film composite |
| TOC | total organic carbon |
| UF | ultrafiltration |
| wt% | weight percent |

**Symbols**

| | |
|---|---|
| °C | degrees Celsius |
| > | greater than |
| µm | micron |
| # | number |
| % | percent |
| ± | plus or minus |

# CONTENTS

# Tables



# Figures

# Appendices

Appendix

# EXECUTIVE SUMMARY

Implementation of nanofiltration and reverse osmosis (RO) processes in treating traditional water sources can provide a steady-state level of removal that eliminates the need for regeneration of ion exchange resins or granular activated carbon. Moreover, RO can help meet future potable water demands through desalination of seawater and brackish waters. Many of these applications use membranes in a spiral-wound configuration that contains a feed spacer between the envelopes. The productivity of membrane filtration is severely lowered by fouling, which is caused by the accumulation of foreign substances on the surface and/or within pores of membranes. Microbial fouling, or biofouling, is the growth of micro-organisms on the membrane surface and on the feed spacer. The fouling of membranes has demanded and continues to demand considerable attention from industry and research communities.

The goal of this project was to develop low-biofouling membranes through the functionalization of cellulose acetate (CA) membranes with metal chelating ligands charged with biocidal metal ions, i.e., copper ions. The use of low-biofouling membranes would reduce the cost associated with chemical pretreatment and cleaning as well as chemical storage. To this end, glycidyl methacrylate (GMA), an epoxy, was used to attach a chelating agent, iminodiacetic acid (IDA) to facilitate the charging of copper to the membrane surface. Both CA and CA-GMA membranes were cast using the phase-inversion method. The CA-GMA membranes were then charged with copper ions to make them resistant to microbial growth. The pore size distribution analysis of CA and copper-charged membranes were conducted using various molecular weights of polyethylene glycol. CA and copper-charged membranes were characterized using Fourier transform infrared spectroscopy for chemistry, scanning electron microscopy for copper dispersion on the membrane surface, and contact angle for hydrophilicity changes. The permeation experiments were conducted with distilled (DI) water and protein solutions followed by protein rejection measurements. The permeation of the copper-charged membrane was initially lower than the CA membrane during the filtration of DI water. The membranes were then subjected to bovine serum albumin (BSA) and lipase filtration. The copper-charged membrane showed higher permeation values for both proteins as compared to CA membranes. The lower permeation with DI resulted from increased resistance from the IDA and copper on the surface during DI water filtration, and later, higher permeation resulted from reduced fouling from both proteins. The rejection of BSA and lipase was the same for both the copper-charged and CA membranes. Therefore, the modified membranes have a potential to be used as low-biofouling membranes in the future.

# BACKGROUND AND INTRODUCTION

Currently, about one-half of the world's population suffers from water shortages, and over the next 25 years, the number of people affected by severe water shortages is expected to increase fourfold [1]. In the developing countries that are most affected, 80 - 90 percent (%) of all diseases and 30% of all deaths result from poor water quality [2]. In addition, modern economies cannot develop and thrive without sufficient access to water. There is growing recognition by governments and corporations that future peace and prosperity is intimately tied to the availability of clean, fresh water [3, 4].

Membranes possess the ability to treat a wide variety of source waters, such as brackish and seawater for desalination, as well as low quality surface water and even wastewater. They can produce water that is of higher quality than traditional water treatment processes such as coagulation, flocculation, sedimentation, sand filtration, etc. For this reason, membranes and membrane processes have gained much popularity in recent years. Furthermore, like any high-tech product, membrane performance has been consistently increasing while membrane cost has been consistently decreasing [5]. Ultimately, dwindling freshwater resources, more stringent water treatment standards, and the need to augment existing water supplies in growing urban areas are all driving factors for the expansion of membrane processes [6].

Membranes for water treatment are usually characterized into four main classifications that can be based solely on pore size. These classifications are, from the largest pore size (approximately 1 micron [µm] ) to the smallest (approximately 0.001 µm): microfiltration (MF) and ultrafiltration (UF), which are considered low-pressure membranes, and nanofiltration (NF) and reverse osmosis (RO), which are considered high-pressure membranes. RO membranes have also been considered to be nonporous membranes resulting in a solution-diffusion based separation. Much advancement has been made in membrane performance, permeability, and durability, but there are still many problems with membrane performance and lifetime, which restrict them from more widespread uses. One such challenge, which is common to both low- and high-pressure systems, is membrane fouling [7]. Fouling can be described as the undesirable accumulation and/or formation of deposits at the membrane surfaces, on the membrane pores, or within the pores. Just as it is with membrane classifications, there are four main categories of membrane fouling: colloidal fouling, inorganic fouling, organic fouling, and biological fouling, which is often referred to as biofouling. The accumulation of foulants hinder the membrane filtration process by decreasing the flux of permeate and increasing the hydraulic resistance of mass transport. This accumulation can come in the form of cake/gel layer formation, concentration polarization, or physical pore blocking.

Biofouling is the accumulation and growth of micro-organisms on the membrane surface and on the feed spacer present between the envelopes in spiral-wound RO membrane modules. This accumulation of micro-organisms, along with the presence of nutrients that are common in many membrane applications, forms biofilms. For spiral-wound RO and NF membranes, biofouling is the major type of fouling leading to pressure drop [8–10]. It has been shown that biofouling causes a flux decline by increasing hydraulic resistance and by hindering back diffusion of salts, which further increases the concentration polarizations phenomenon [11, 12]. Furthermore, biofouling is particularly significant because membrane replacement due to fouling is the single largest operating cost in water separation [7]. For this reason, research on altering the chemical, and possibly antimicrobial, properties of the feed spacer is the focus of much attention.

In biofilms, organisms are embedded in a matrix of microbial origin consisting of extracellular polymeric substances (EPS). These matrices are often very complex and difficult to remove. For this reason, much effort goes into the prevention of biofilm growth rather than its removal. This prevention is usually attempted through the use of pretreatments, nutrient removal, maximizing shear forces at the membrane surface, and back-flushing. The problem with pretreatment methods is that even if 99.9% of micro-organisms are removed, those left remaining can proliferate and cause irreversible fouling. Furthermore, biocides, such as free or combined chlorine, can only be used with certain chlorine-resistant membranes. Since biofouling is such a common problem, this has its downfalls. Biofouling often starts at the membrane/feed spacer interface, suggesting that biofouling might be a feed spacer problem [13].

The goal of this project was to develop low-biofouling membranes through the functionalization of the membrane surface. The functionalized membrane contained a metal chelating ligand, iminodiacetic acid (IDA). Many studies have been conducted on the use of copper ions to disinfect water against microbial biofilms [14, 15]. These ions are believed to interfere with enzymes involved in cellular respiration and bind deoxyribonucleic acid (DNA) at specific sites [16]. For this reason, the metal chelating ligands were charged with copper ions to increase biofouling resistance.

## Membrane Materials

The majority of RO and NF membranes are found in a spiral-wound configuration and are polyamide (PA) thin-film composite (TFC) membranes, although cellulose acetate (CA) and cellulose triacetate are also used [17]. Other commercial materials of NF/RO membranes include sulfonated polysulfone, sulfonated polyether sulfone, piperazine polyamide, and polyvinyl alcohol [18]. The TFC RO membrane usually consists of three structural components: polyester fabric, polysulfone (PS) support, and PA dense film layer [19]. This type of membrane provides high flux and strength, coming from a loose and porous, yet mechanically strong, support layer and high rejection due to the thin selective polyamide layer.

# Membrane Fouling

## Colloidal Fouling

Feed water to membranes is generally pretreated for larger particles. Hence, colloids are generally the reason for particulate fouling in membrane systems. As its definition implies, when the term colloid is used in fouling, it covers a myriad of different materials or aggregates of materials, including organic, inorganic, and biological materials. Low-pressure membranes such as MF and UF are usually discussed when colloid fouling is of concern. This is because these sorts of filtration are designed to reject such particles. The rejections of these particles result in cake/gel layers on or in the membrane pores. The layer has characteristics that may depend on the system operation parameters (flux and velocity levels), membrane characteristics (surface roughness and charge), solution chemistry (pH, ionic strength, ionic composition), and the characteristics of the colloids (size, shape, charge, and hydrophobicity). Particulate fouling has obvious impacts on the performance of a membrane system. The increase in deposition of materials on the surface can form a compact layer that decreases flux and increases the pressure required for operation [20]. Colloidal fouling is typically assessed or evaluated in terms of transport, which is determined by convective forces, such as permeate flux and cross-flow velocity, and attachment, which is determined by electrostatic, van der Waals, and hydrophobic interactions [21]. Colloidal fouling is most commonly dealt with via pretreatment of the feed stream and back-flushing of the membranes, but sometimes pH adjustment is used as well. Overall, little can be done to prevent colloidal fouling on a long-term basis because, as previously mentioned, it is what some membranes are intended to reject [22, 23].

## Inorganic Fouling

Inorganic fouling is caused by any material of inorganic origin. It may be the sole source of fouling, but more commonly, it is in concert with other types of fouling [24]. This type of fouling is usually thought of as the precipitation of dissolved, sparingly soluble metals as metal hydroxides, salts, and minerals onto membrane surfaces, which results in scaling. Inorganic fouling is usually encountered in desalination systems where salt concentrations and their rejections are high. The phenomenon known as concentration polarization plays a large part in inorganic fouling and, more specifically, mineral scaling [25, 26]. In a concentration polarization layer, the concentration of chemical species (the inorganic compounds in this case) is higher at the membrane surface than in the bulk solution. Concentration polarization occurs because the rate of arrival of an inorganic species at the surface is larger than that of the diffusion of it back into the bulk solution. As Elimelech and Bhattacharjee [26] have shown, concentration polarization can affect membrane performance adversely outright, but what is more important is its role in the formation of mineral scaling. Mineral scale formation is almost always initiated within the concentration polarization boundary layer. This is due to the elevated salt concentrations in the concentration polarization layer relative to those in the bulk solution, which can result in precipitation [26]. This precipitation and the subsequent mineral scaling occur when rejected salts or minerals become so concentrated at the membrane surface that they exceed their solubility limit. As is common with most types of fouling, the properties of this scale are dependent on the chemistry of the bulk solution.

More often than not though, the scaling is considered to be a hard or rock-like structure that grows from an initial nucleation site. This scale can contain its own microenvironment that can result in difficult removal and flow obstructions. There are many different forms of mineral scale that can occur simultaneously in a system and this can result in the formation of a very complex scale. Because of this, the chemistry of mineral scale removal is poorly understood and currently the topic of much research. pH adjustment through acid addition and the use of antiscalants are the two most widely used pretreatment methods to avoid scaling in NF and RO processes [27]. Due to the weak pH dependence of the solubility of barium and calcium sulfate, it is difficult to control scaling due to it in membrane systems through pH adjustment alone. In these cases, antiscalants are required to prevent mineral scale formation. The mechanisms through which an antiscalant works relies on its ability to interfere with the two principle mechanisms of scale formation: nucleation and crystal growth [27]. The four mechanisms through which this may occur are interference with the clustering process, dispersion, crystal distortion, and chelation, which results in a soluble salt [28].

Polycarboxylates and phosphonates, two types of polymeric organic compounds, are the most common antiscalants used in membrane treatment [27]. Metallic ions have also been proposed to be an efficient antiscalant for feed streams prone to calcium carbonate precipitation [29]. As far as pH adjustment goes, the most common form is acid addition to control inorganic scaling. However, alkalization has been utilized as another form of pretreatment [30].

## Organic Fouling

Organic fouling generally results from the adsorption of dissolved organic matter (DOM) on the membrane surface but can also result from deposition of colloidal organic matter. It is usually the first form and primary cause of chronic membrane fouling in most membrane systems. Organic foulants can include natural organic matter (NOM), algogenic organic matter, organic macromolecules, organic colloids, biopolymers, and microbially derived cellular debris. Organic fouling is a ubiquitous problem throughout all membrane processes. Studies have shown that organic matter is the most prevalent membrane foulant, having accounted for nearly one-half of the foulants that were identified in membrane autopsies [28].

Organic fouling occurs through a variety of mechanisms, including adsorption, attachment, pore blockage, and cake/gel layer formation. The occurrence and progression of these different mechanisms are influenced by a host of parameters, including the properties of the organic matter, such as size, hydrophobicity, and charge; membrane characteristics such as hydrophobicity, charge, surface roughness, and pore size; water chemistry; and operation parameters [31, 32]. Since adsorption is the mechanism most commonly associated with organic fouling, interaction between the membrane surface and organic foulant is of supreme significance. It is this interaction that has become the focus of much organic fouling control. As previously mentioned, surface characteristics play a large role in the adsorption of organic materials. If these can be altered, then the fouling can be controlled. Two membrane surface characteristics that have shown promising results are decreases in surface roughness and increases in membrane hydrophilicity. Both have shown the ability to decrease organic fouling, probably by lessening the effect of adsorption of organic matter [33, 34].

## Biofouling

Biofouling, which is the accumulation and growth of micro-organisms and biofilms on the membrane surface and on the feed spacer, causes a significant increase in differential pressure, is difficult to eliminate by routine cleaning procedures, and is ultimately endemic [35]. Biofouling can cause a flux decline by two methods: (i) an increase of the hydraulic resistance over the membrane and (ii) hindering the back diffusion of salts [36]. Micro-organisms are present in nearly all water systems [37], and because of this, biofouling and its control remains a major operating problem for many RO plants, as it occurs despite the use of pretreatment systems and the addition of disinfectants. Biofouling is especially problematic because biofilms occurring in membrane systems may cause severe loss of performance and the use of costly cleaning procedures to maintain output and quality. Frequently, the fouling can be so severe that operation cannot be maintained, and membrane replacement is needed [35]. In spirally wound elements, biofouling is especially problematic due to the possibility for some sections of the flow channel to become blocked. Furthermore, biofouling can lead to other types of fouling, such as inorganic fouling, as these channeling issues cause rapid salt concentration in the affected areas. This leads to the precipitation of sparingly soluble salts and, ultimately, scaling [38].

### *Biofouling Mechanism*

Biofouling of membrane surfaces occurs in a few general phases. Initially, the surface to which the biofilm attaches becomes conditioned with a range of organic molecules that rapidly adsorb to the surface upon exposure to an aqueous environment. These molecules can include proteins, polysaccharides, nucleic acids, humic acids, lipids, fatty acids, pollutants, etc. [39] Then, primary colonization occurs where adhesion is essentially proportional to the cell density in the water phase and occurs owing to weak physicochemical interactions. It is thought that the cells that initially attach during this phase are often in starvation/survival phase and tend to be smaller in size and secreting a higher ratio of extracellular polysaccharides [39]. It has been shown that higher amounts of EPS are directly related to cellular adhesion [40]. This primary colonization is then followed by the logarithmical growth phase, when cell growth on the surface contributes more to biofilm accumulation than does the adhesion of planktonic cells. Essentially, the cells which have attached to the conditioned surface can now feed off the nutrients which are concentrated at the membrane surface, due to rejection by the membrane's selective layer, and multiply [37]. Finally, a plateau phase, when biofilm growth (adhesion and cell multiplication) and cell detachment are in balance, occurs. This phase is controlled by the nutrient concentration and the resultant growth rate, the mechanical stability of the biofilm, and the effective shear forces. Also, it is independent of the concentration of cells in the raw water. It is also thought that during this stage subsequent production of extracellular polymers occurs [41].

### *Role of Transparent Exopolymeric Particles in Biofouling*

The most abundant and widely available water sources today are saline waters, including estuarine, brackish, and seawater. However, fouling of membranes can be very problematic during seasonal algal blooms [42–44]. Potential membrane foulants present in saline feed water include, but are not limited to, micro-organisms (e.g., bacteria and algae) and their fragments, EPS, soluble microbial products, and NOM. Recent data suggest that transparent exopolymeric particles (TEP), which exist as individual amorphous particles with a varied size range (0.4 to 100 µm) and in concentrations up to 5,000 $mL^{-1}$ during algal blooms may facilitate membrane fouling [45, 46, 47–49]. Similar to EPS, TEP can form from soluble microbial products (e.g., sugars) excreted by plankton or bacteria and have varied composition [50, 51]. TEP have been largely overlooked in membrane research due to the fact that these particles are invisible. They are operationally defined as particles that are visible when stained with the cationic dye, alcian blue, which detects sulfated and carboxylated polysaccharides. Their presence and abundance have been established in saline environments [52–55], and their characteristics may alter our previously held views on the process of membrane fouling and biofouling during desalination [56–58].

Many case studies [59–62] have previously established the major stages of biofilm formation, including transport to the solid-liquid interface, initial deposition, adhesion facilitated by EPS excreted from the biofoulants, biofoulant proliferation, and biofilm formation. Recent studies indicate that this model may not be complete since TEP present in the feed water can play a significant role in fouling and biofilm formation [55, 56, 63]. TEP are considered very surface active or sticky. Berman and Holenberg [64] suggested that TEP adhered to membrane surfaces could provide a nutritious substrate for microbial growth and establishment of biofilm. Using cross-flow filtration with lake water on a UF membrane, Berman found that active, live bacteria excreting EPS were not required, but rather TEP in the feed water were adhered to the membrane surface at biofilm initiation [65]. Previous studies have demonstrated TEP deposition as well as reversible and irreversible fouling by TEP in UF, MF, and RO membrane processes [55, 57, 58].

RO membrane desalination facilities have been adversely impacted by the onset of massive algal blooms [42–44]. These seasonal events generate high concentrations of cells (up to millions of cells per milliliter [mL]) and organic substances, which wreak havoc on desalination processes by causing membrane fouling. Although some desalination biofoulants have been previously considered extensively, including cellular organisms (e.g., bacteria or algae) and cellular debris, including algae skeletons [44, 66, 67], the impact of abundant TEP on fouling in desalination facilities has only recently been documented [56–58, 63, 68, 69]. TEP, present in extremely high concentrations (up to $10^3$ particles per milliliter) during an algal bloom, can occur from DOM (e.g., sugars) excreted by plankton or bacteria and from abiotic colloidal polysaccharides and are considered surface active or “sticky” [47, 50, 53, 54]. Due perhaps to the fact that they are invisible, these particles have only recently been implicated in organic fouling [63, 69] as well as the initiation of biofilms on UF water membranes [70].

### *Traditional Biofouling Control*

Biofilm formation and biofouling are essentially unavoidable, as some small percentage of micro-organisms present can survive physical pretreatment processes like coagulation, flocculation, sand filtration, UF and cartridge filtration [71]. More recent developments have led to technologies such as UF membrane and ultraviolet pretreatment, but the former has a high capital and operational cost, and the latter can lead to scale formation and has no residual effects. Both of these technologies are also ultimately incapable of completely removing micro-organisms. As a result, chemical pretreatment of RO membrane units is required but is also shown to be ineffective in removing and/or completely destroying the complex multicellular structures [72]. Some common chemicals such as chlorine and ozone by alkaline treatment, tensides, enzyme, or complex-forming substances [73] have been used, as have been biodispersants [74]. Chlorine containing substances are notorious for chemical corrosion of RO membranes and can also form toxic disinfectant byproducts [41]. Recently, modifications to the membrane to prevent biofouling have been explored. These modifications usually look to reduce the formation of the conditioning layer, via an increase in hydrophilicity [33, 75, 76] and a decrease in surface roughness [34], or by coating/impregnating the membrane is antimicrobial metals [77, 78]. Conventional cleaning with toxic chemicals has an effect on the occurrence of biofouling in RO systems, but is not effective in really cleaning the RO system [71], as the biomass must be physically removed [79]. Because of this, methods of physically removing the biofilm layer have been investigated. Such methods include back-flushing the membrane, air sparging [13, 80], and, more recently, modifications to the membrane feed spacer's size and geometry to increase shear forces[81].

## Charging Membranes with Copper

Grafting of unsaturated vinyl monomers onto polypropylene (PP) is a convenient route to develop new polymeric materials with synergistic properties [82]. Polymer-metal complexes have been extensively studied and successfully employed in several fields [83]. As in low-molecular-weight compounds, a polymer ligand must donate unshared electrons to the metal ion to form metal-ligand bonds. Among the multidentate ligands, IDA possesses one aminopolycarboxylate and provides a reactive secondary amine hydrogen to react with alternate functional groups [83]. Hence, IDA can be more easily introduced to the side chain of a polymer or vinyl monomer via what is proposed to be an SN2 epoxy group reaction of glycidyl methacrylate (GMA) and IDA [84]. This reaction has two advantages: (1) GMA is a commercial industrial material that is cheaper than any other vinyl monomers that possess an epoxy ring in the side chain and (2) it produces a vinyl monomer that can be polymerized in the presence of an initiator and can be grafted to activated polymer surfaces. The chemical modification of PP feed spacers to allow metal chelation, increase antimicrobial properties, and ultimately control membrane biofouling has been studied [84, 85]. In these studies, PP was functionalized with copper to demonstrate that copper-charged PP could be used to make low-biofouling feed spacers for spiral-wound elements. The functionalized PP contained grafted GMA with the metal chelating ligand (IDA) to which copper was chelated [84].

Many studies have been conducted on the use of copper ions to disinfect water against microbial biofilms with effective dosages of a few tenths of 1 milligram per liter (mg/L) [14]. Copper is thought to be cytotoxic by causing changes in the plasma membrane permeability or efflux of intracellular $K^+$ during the entry of $Cu^{2+}$ ions [86]. Copper is known to coordinate with cysteine residues, which in turn may lead to changes in enzyme activity and intracellular trafficking [87]. It can also participate in Fenton-like reactions, generating reactive hydroxyl radicals, which can cause cellular damage imparted via oxidative stress [86]. Copper may damage many proteins, both on the micro-organism envelope or within the cell. Conformational changes in the protein structure or in the protein active site may occur, resulting in the inhibition or neutralization of the proteins' biological activities [88]. Silver ions also possess antimicrobial properties, as they are known to have strong interactions with thiol (sulfydryl, -SH) groups [89]. Cytoplasmic proteins and DNA are targets of silver through interaction with these thiol groups in proteins, causing enzymatic inactivation [90]. Additionally, cytosines in DNA form stable C-Ag-C structures [91].

# CONCLUSIONS AND RECOMMENDATIONS

The initial goal of this project was to develop a copper-charged CA membrane that could potentially be used in desalination applications. To this end, CA was functionalized with metal affinity ligands. Infrared spectroscopy verified that CA was successfully modified to become CA-GMA-IDA. A scanning electron microscopy (SEM) and elemental analyses were used to show that the CA-GMA-IDA was uniformly charged with copper (II). The modification method utilized simple a reaction apparatus, inexpensive straightforward techniques, and commonly used, readily available chemicals.

A second goal of this project was to show that this method was able to control membrane biofouling. As mentioned, CA membranes were functionalized with metal affinity ligands that could be charged with biocidal metals such as copper. This modification gave antimicrobial properties to the CA membrane without affecting its hydrophilicity. The chelation of copper to the CA membrane was determined to be preferential to Fe(II), ethylenediaminetetraacetic acid (EDTA), and DOM in cross-flow leaching studies. Thus, environmental impacts from copper leaching when using copper-charged membranes would be minimal. More significantly, use of the copper-charged membrane led to a consistently lower rate of flux decline during filtration of BSA and lipase proteins.

During cross-flow filtration experiments, the copper-charged membrane resulted in a decrease in flux decline over a 24-hour period when compared to unmodified membranes in the presence of a biofoulant. In addition, the amount of biofilm on the copper-charged membrane was significantly less than on the unmodified membranes. Dead-end filtration experiments were carried out with algae organic matter, specifically TEP. Using Fourier transform infrared spectroscopy (FTIR), we were able to detect protein and polysaccharides on the fouled membranes following TEP filtration. We discovered that the copper-charged membrane experienced less flux decline in the presence of TEP. Therefore, the use of copper-charged membrane has the potential to increase membrane life and decrease chemical cleanings associated with detrimental biofouling of membranes.

# EQUIPMENT AND METHODS

## Materials

The polymer dope used to cast flat sheet membranes was made of CA (average $M_N$ 30,000) with an acetyl content of 39.8 weight% (wt%) purchased from Sigma-Aldrich and GMA (average $M_N$ 142.16) purchased from Alfa Aesar, in N-methyl-2-pyrrolidinone( >99%, Alfa Aesar) solvent. GMA was polymerized with toluene (99.9%, 92.14) purchased from Fisher Scientific and benzoyl peroxide (97%) purchased from Sigma-Aldrich. Iminodiacetate dibasic hydrate

98% was purchased from Aldrich Chemistry (St. Louis, Missouri). Dimethyl sulfoxide (DMSO) 99%, copper sulfate, acetone, and hydrochloric acid were purchased from Fisher Scientific (Hampton, New Hampshire). Bovine serum albumin (BSA), lipase, glycerol, glucose, sucrose, fructose, and polyethylene glycol (PEG) were purchased from Sigma-Aldrich.

# Methods

The preparation of the copper-charged membrane involved three steps. Figure 1 shows the reaction scheme. In the first step, GMA was homopolymerized separately and added as a blend to the polymer dope. The flat sheet membranes were then cast using the phase inversion method. In the second step, the metal chelating ligand IDA was attached to the membrane surface via the spacer arm of GMA. Lastly, the membrane was charged with copper ions by covalently binding the copper ions to the chelation group of IDA and attached to the surface of the membrane.

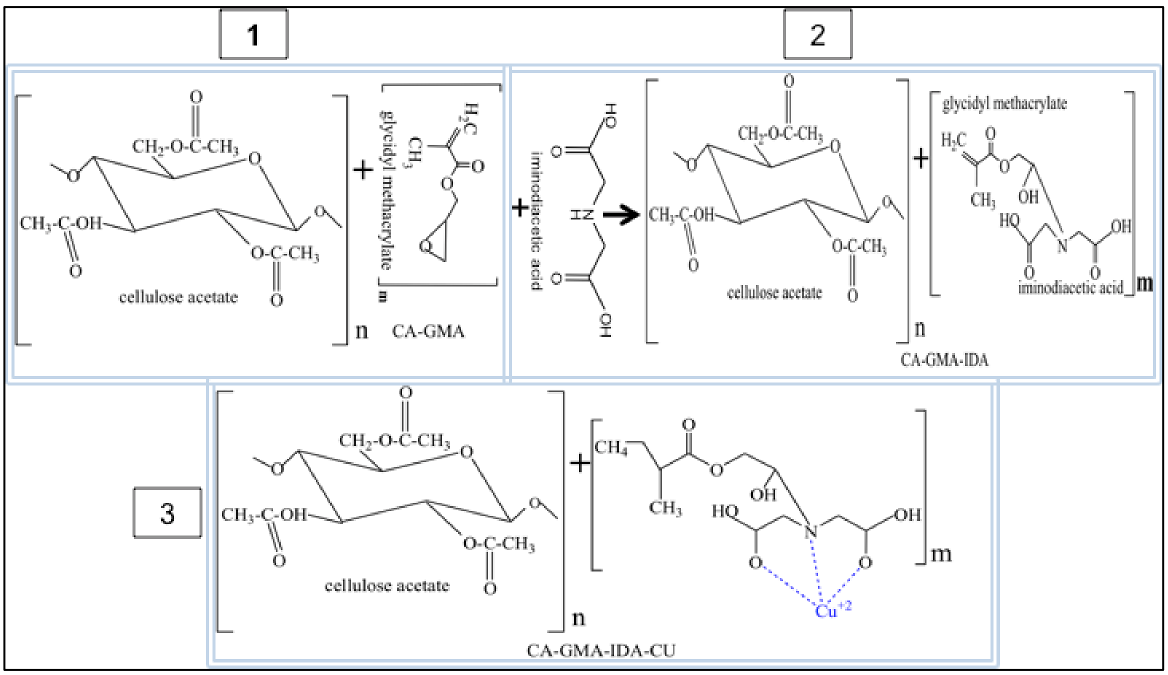


**Figure 1.—Reaction scheme of the modification [92].**

## Polymerization of Glycidal Methacrylate

The polymerization of GMA was done with a mixture of 15 mL of GMA monomer, 35 mL of toluene, and 0.100 gram benzoyl peroxide with a stir bar in a round bottom flask. The polymerization reaction was completed in a nitrogen-rich environment and maintained at 70 degrees Celsius (°C) with continuous stirring for 3 hours. The GMA polymer was removed from the round bottom flask, placed in a glass petri dish, dried, and crushed. The drying process in this experiment took 4 days to air dry and then an additional 4 days of drying in a fume hood before it was suitable to be blended into the polymer dope solutions.

## Phase Inversion

The phase inversion process induced by immersion precipitation is a well-known technique for preparing asymmetric polymer membranes. Flat sheet membranes were cast with the polymer dope solution of 21/77/2 wt% ratio of CA/NMP/GMA using the phase inversion method. The polymeric dope solution was poured on a glass mirror, and the flat sheets were cast using the doctor's blade at a thickness of 130 µm. These were then immersed in a water bath to allow interaction of the solvent in the casting solution film with the nonsolvent in the precipitation media. This process resulted in an asymmetric membrane with a dense top layer and a porous sublayer.

## Iminodiacetic Acid and Copper Application

The metal chelating ligand IDA was attached to the epoxy group of GMA by treating the flat sheet membranes with 0.5M IDA dissolved in a 50/50% water/DMSO mixture for approximately 2-4 hours at a constant temperature between 50–55 °C. Then the membranes were washed with distilled (DI) water and placed in 0.6M copper sulfate solution for 24 hours.

## *Pseudomonas fluorescens Migula* (ATCC #12842)

For the analysis of the biofilm formation on membranes, *Pseudomonas fluorescens Migula (ATCC #12842)* was purchased from ATCC and grown in Luria-Bertani broth. PicoGreen was used to nonspecifically stain all organisms green, and the stained sample was mounted on a slide using immersion oil. Slides of samples were counted using fluorescent microscopy for (1000× magnification) the analysis of bacteria growth in the medium at different intervals of time (figure 2). A 27-hour incubation time was determined for bacteria growth at the exponential phase. Bacteria from the exponential phase were included at a final concentration of $10^4$ cells/mL.

## The Marine Algae, *Chaetoceros affinis* (CCMP 158)

The presence of marine algae in feed water can drastically change the behavior in the formation of bioflim on the membrane. For this analysis, *Chaetoceros affinis* (CCMP 158) was purchased from the National Center for Marine Algae and Microbiota. *C. affinis* is being grown on f/2-si medium in green house chamber at the University of Toledo. The algae cultures are incubated at 20 ± 2 °C room temperature under an artificial light source (fluorescent lamp) at a 12/12-hour light/dark regime and a continuous slow mixing condition over a shaker. Light intensity was set at 40–50 µmol/$m^2$s. The cell concentrations of algae are measured every 2–4 days with the help of a counting chamber and

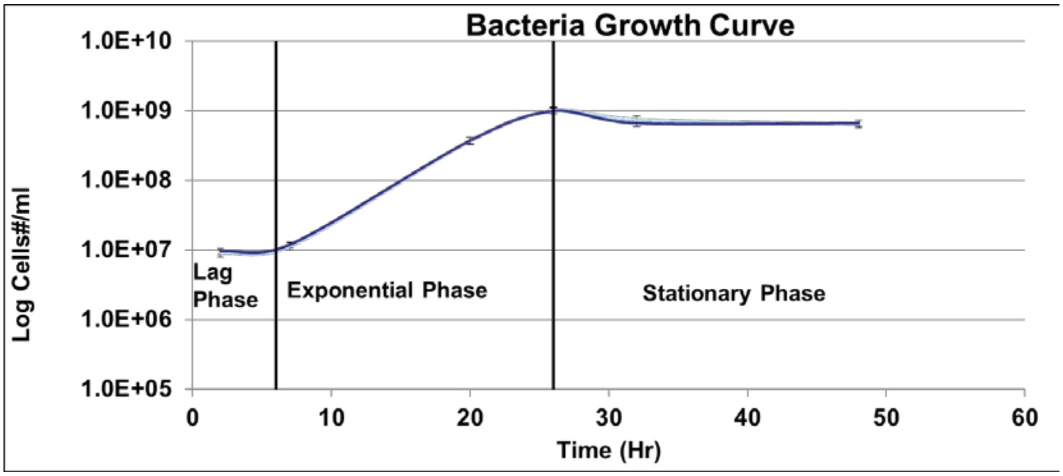


**Figure 2.—Biofoulant (*P. fluorescens)* growth curve.**

light microscopy (figure 3). The growth curve for algae has been developed (figure 4). Peak concentration occurs after approximately 15 days of incubation. The corresponding TEP concentration was measured during *C. affinis* growth. Notably, the TEP concentration continues to increase while the *C. affinis* are in the death/dying phase.

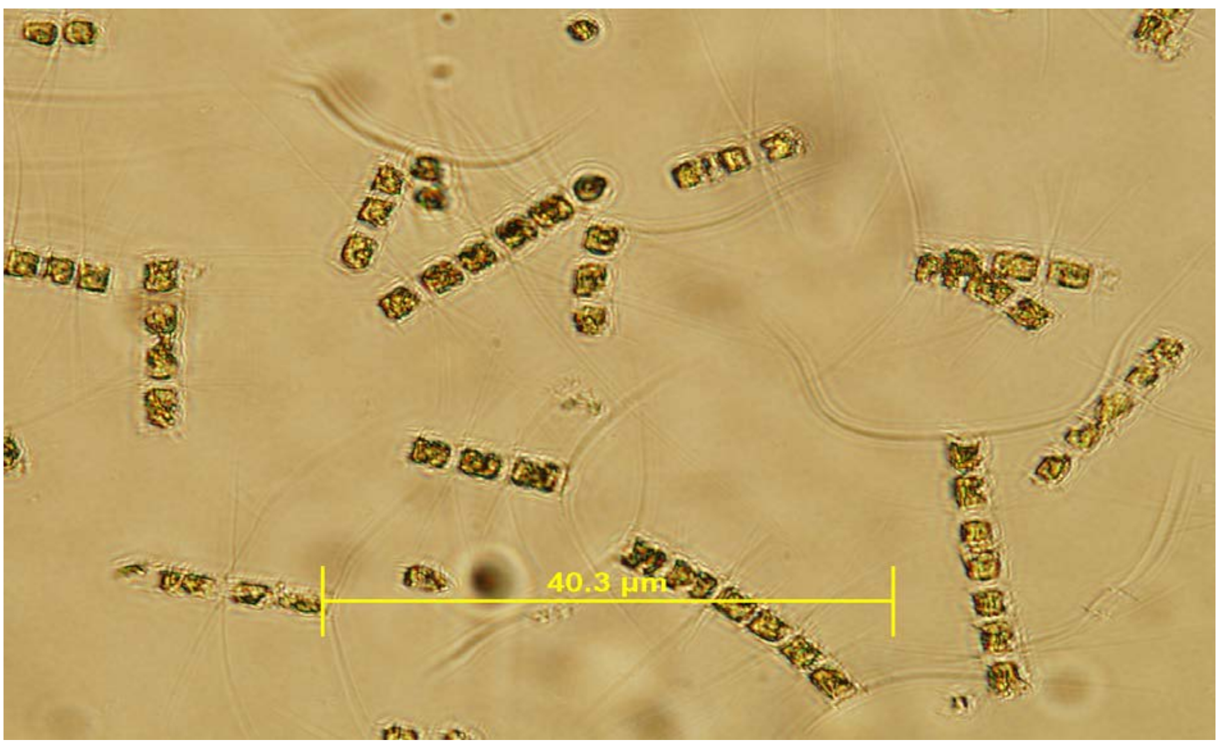


**Figure 3.—*C. affinis* observed with light microscopy at 5 days of incubation.**

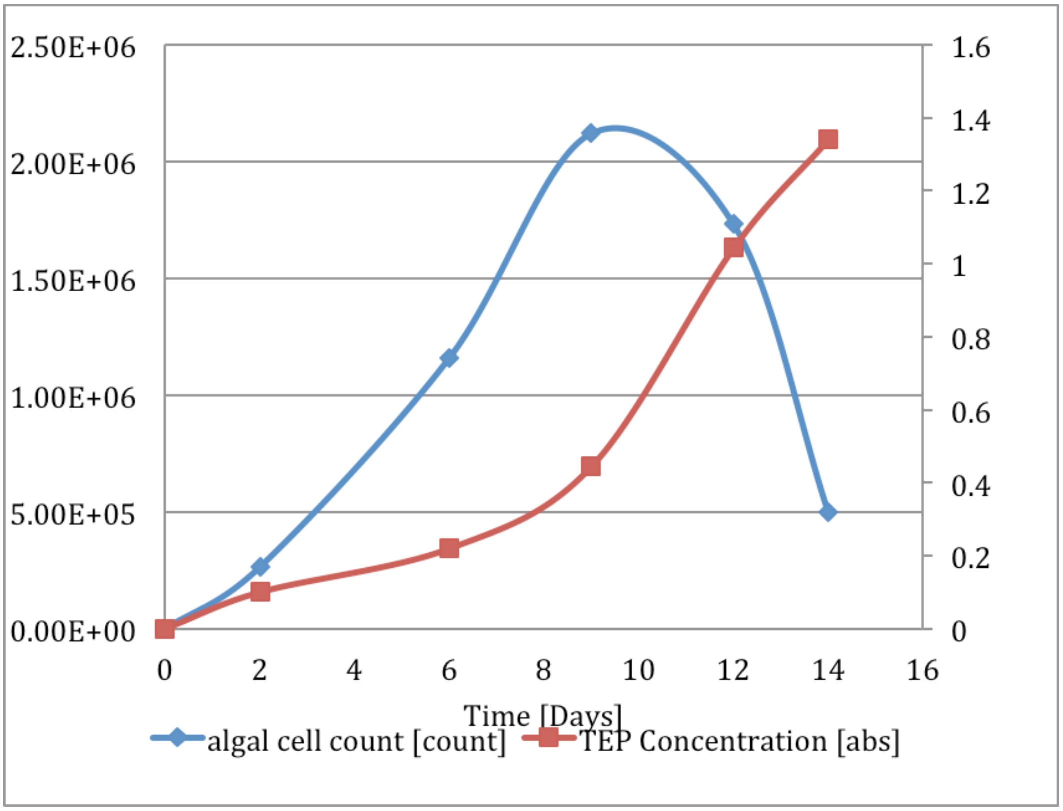


**Figure 4.—Algae growth curve and the corresponding TEP concentration.**

To detect the TEP present in the samples, filtered *C. affinis* were stained with 0.02% alcian blue for 7 minutes and gently rinsed twice by dipping in distilled water. The stained samples were then mounted on slides using immersion oil and viewed under bright field illumination to reveal adhesion of TEP to the surface (figure 5).

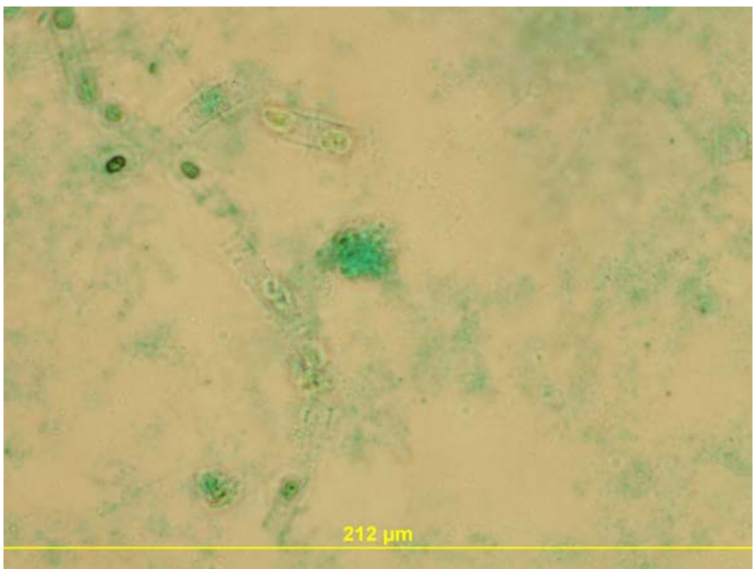


**Figure 5.—TEP stained with alcian blue (20×).**

# Characterization

## Fourier Transform Infrared Spectroscopy Analysis

FTIR data were acquired using an attenuated total reflection Fourier transform infrared spectrometer (ATR-FTIR, Digilab UMA 600 FT-IT microscope with a Pike HATR adapter and an Excalibur FTS 400 spectrometer). Four random areas of the membrane were analyzed, and the data received were averaged.

## Scanning Electron Microscopy Analyses

The surface of the membrane was dusted with a thin layer of palladium-gold using a Cressington 108 auto sputtering device. To view the surface structure, and distribution of copper on the surface, these samples were studied using a Hitachi S-4800 SEM.

## Contact Angle Measurements

The hydrophobicity of the copper-charged membrane was compared with that of CA membranes by measuring the contact angle using a Cam-Plus micro contact angle meter. The flat sheet membranes were placed on the device, and a water droplet was dropped on the membrane. The contact angle of the droplet was measured through the micro contact angle meter as shown (figure 6).

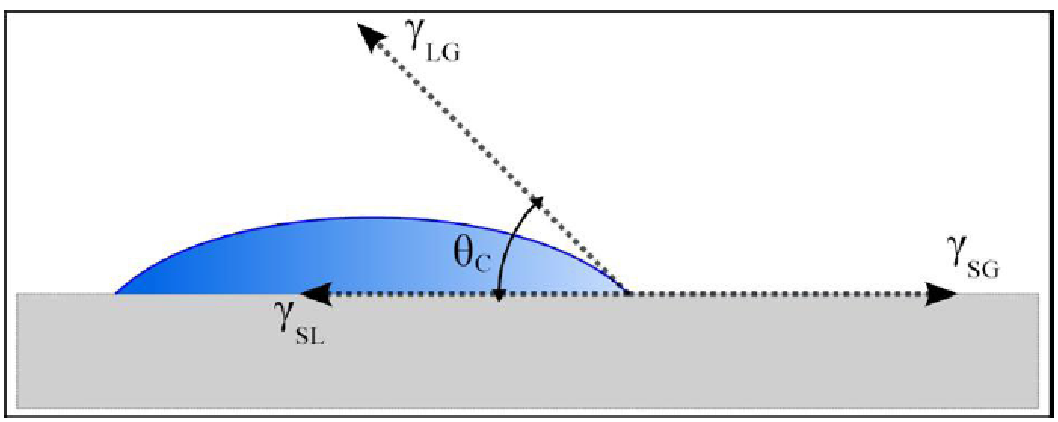


**Figure 6.—Contact angle measurement.**

## Pore Size Distribution

The pore size distribution analyses of CA and copper-charged membranes were conducted using 200 parts per million (ppm) of glycerol, glucose, sucrose, various molecular weights of PEG, and dextrans. The solutions were filtered through CA membranes. The total organic carbon (TOC) of both feed and permeate solutions were measured using a Tekmar Phoenix 8000 TOC analyzer. The rejection of solutes R(%) was calculated using the equation below:

$$R = \left(1 - \frac{C_p}{C_f}\right) \times 100\%$$

where $C_p$ is the concentration of the solute in the permeate and $C_f$ is the concentration of solute in the feed solution. The various solute samples that were used in this study, along with their Stokes-Einstein radii, are shown in table 1. The rejection values of all solutes were used to determine the mean effective pore size.

Table 1.—Neutral solutes used for pore size distribution analysis

| Solute | Molecular weight (gram/mol) | Stokes-Einstein radius (nm) |
|---|---|---|
| Glycerol | 92.09 | 0.26 |
| Glucose | 180.16 | 0.37 |
| Sucrose | 342.30 | 0.47 |
| Raffinose | 504.42 | 0.58 |
| PEG 600 | 600.00 | 0.61 |
| PEG 1000 | 1,000.00 | 0.80 |
| PEG 2000 | 2,000.00 | 1.14 |
| PEG 4600 | 4,600.00 | 1.75 |
| PEG 8000 | 8,000.00 | 2.31 |
| Dextran 10 | 10,000.00 | 2.30 |
| Dextran 40 | 40,000.00 | 4.50 |
| Dextran 70 | 70,000.00 | 6.00 |

## Copper Leaching Cross-Flow Studies

The copper leaching studies were conducted using cross-flow experiments as shown on figure 7. The apparatus consists of a feed bottle, which is filled with the solution of interest; a pump to flow the solution through a flow cell that contains the copper-charged membrane; and a collection bottle to collect nearly all of the solution that has passed over the copper-charged membrane (containing an average amount of copper leached).

Five separate solutions were prepared in DI water: one containing 5 mM EDTA at a pH of 11, one containing 35 g/L of sodium chloride (NaCl), one containing 10 mg/L ferrous sulfate, and one containing 8 ppm of DOM solutions comprised of 4 ppm of humic acid and 4 ppm of tannic acid. These solutions

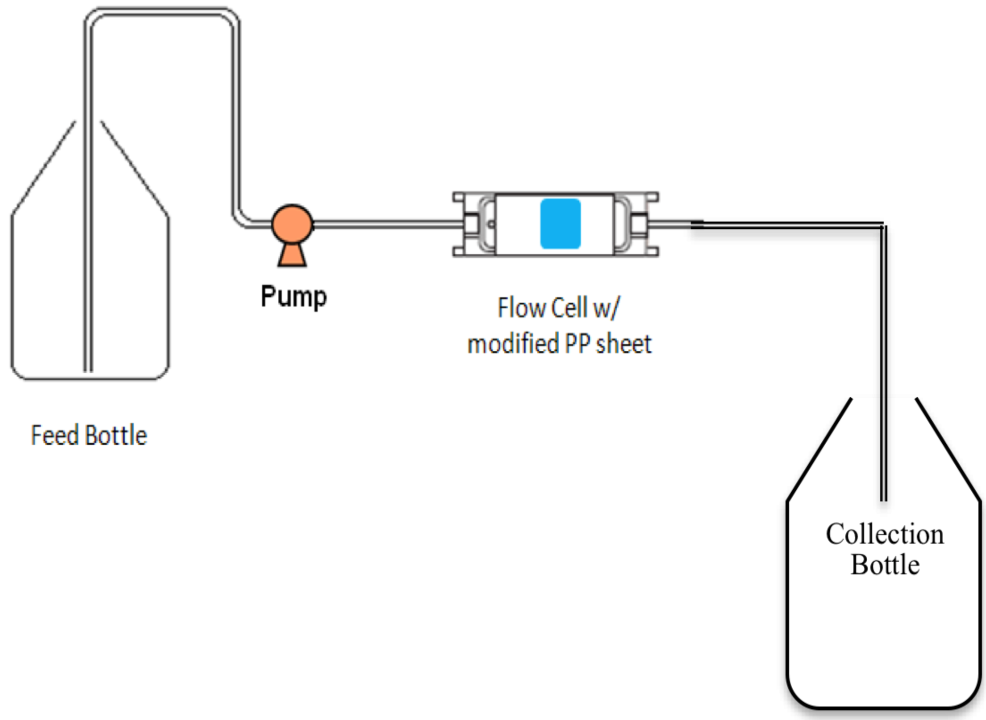


**Figure 7.—Cross-flow experiment apparatus used for copper leaching studies.**

were then pumped for 24 hours, at a flow rate of 0.6 milliliter/minute, through a flow cell (24 mm × 40 mm × 8 mm deep; Stovall Life Sciences Incorporated, Greensboro, North Carolina), which contained samples of copper-charged membranes. As mentioned, the solution that had flowed through the cell was sent to a collection bottle, and the membrane samples were collected at different intervals of times. Analyses of the samples were performed using energy dispersive X-ray spectroscopy (EDS) to measure the wt% of copper on the membrane surface.

These solutions were chosen because the first solution is the most common cleaning solution; the second is the typical salt concentration found in brackish water; the third contains a divalent metal ion that could compete with copper for IDA chelation sites, causing the potential copper to be displaced; and the last solution is the possible competition between copper complexation with DOM and copper chelation to IDA.

# Filtration Experiments

Cross-flow filtration was used to test the performance of RO membranes, both commercial and those developed here (i.e., copper-charged membrane) in the presence of a biofoulant (*p. fluorescens*). Feed water (table 2) was pumped from the reservoir to the cell membrane (GE Water Sepa CF, Minnetonka, Minnesota). Both the concentrate and permeate were recycled to the reservoir.

Table 2.—Compositions of synthetic brackish water

| Component | Concentration (mg/L) |
|---|---|
| $Na^+$ | 849.00 |
| $Ca^{2+}$ | 1,330.00 |
| $Mg^{2+}$ | 514.00 |
| $Ba^{2+}$ | 2.00 |
| $Fe^{3+}$ | 2.30 |
| $Cl^-$ | 3,933.00 |
| $SO_4^{2-}$ | 991.00 |
| $NO_3^-$ | 89.00 |
| Alkalinity (as $CaCO_3$) | 780.00 |
| Total dissolved solids | 8,790.00 |

The remaining filtration experiments were conducted using an Amicon dead-end filtration cell (figure 8) with an effective cross sectional area of 4.1 square centimeters at an operating pressure of 70 pounds per square inch. The membranes were tested by precompacting with DI water for the first 8 hours followed by protein permeations using BSA for 8–16 hours and lipase for 16–24 hours. Filtration experiments were also performed with saltwater (35 g/L NaCl) and TEP (1 mg/L) in saltwater (35 g/L NaCl).

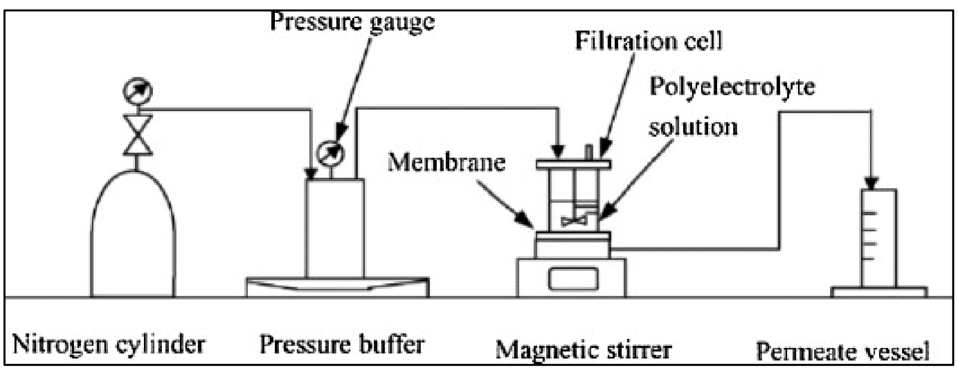


**Figure 8.—Schematic of dead-end filtration cell [93].**

## Surface Area Coverage Analysis

Surface area coverage of the formed biofilm on the modified and unmodified membranes was calculated using software Image J 1.41 (figure 9). The commercially available software was downloaded (http://rsbweb.nih.gov/ij/) to use as a direct observation method to detect biofilm coverage (area) on membranes.

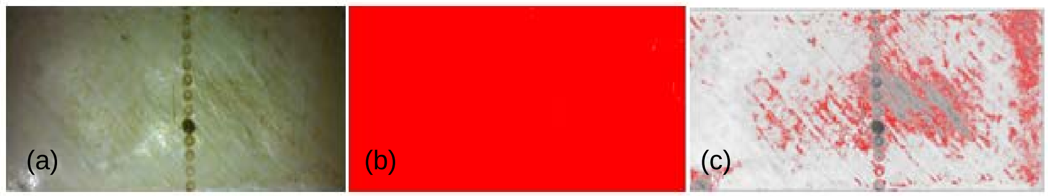


**Figure 9.—Bioflim surface area coverage assessment using Image J. (a) Biofouled membrane; (b) clean membrane; and (c) biofouled membrane.**

# RESULTS

## Chemical Characterization of CA, CA-GMA, and CA-GMA-IDA Membranes

Data were acquired using an attenuated total reflection Fourier transform infrared spectrometer. Four random areas of the membrane were analyzed, and the data received were averaged as shown on figure 10 (CA versus CA-GMA) and figure 11 (CA versus CA-GMA-IDA) and tables 3 and 4, respectively. Characteristic FTIR absorption bands were observed at 860cm$^{-1}$, 955cm$^{-1}$, and 2,990cm$^{-1}$ for the modified dope (i.e., CA/GMA/NMP dope) and IDA treated membranes.

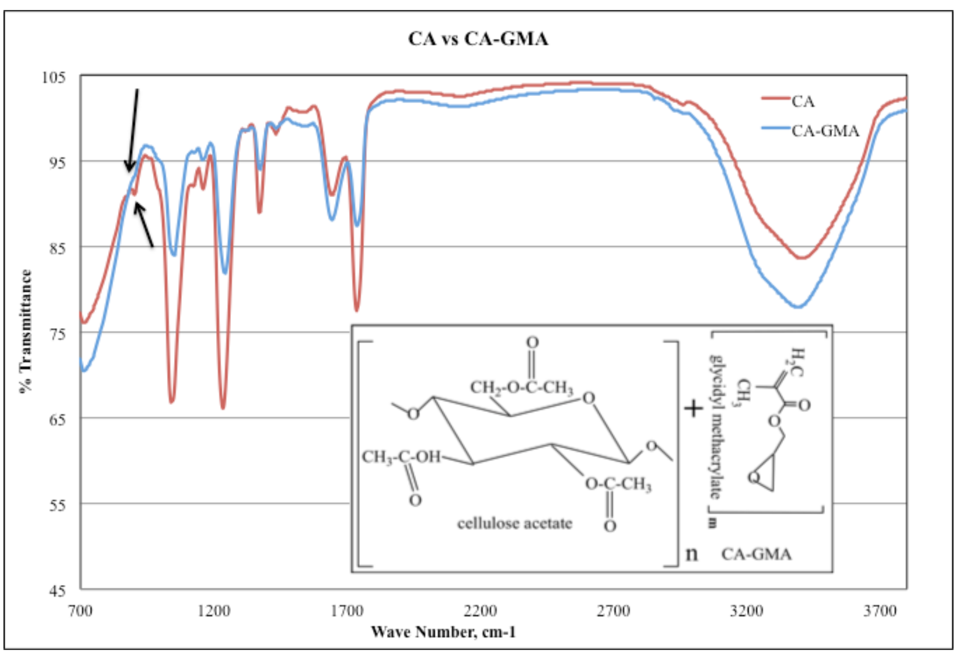


**Figure 10.—FTIR spectra comparing pure CA membranes with CA-GMA membranes.**

Table 3.—FTIR peak descriptions

| Wavenumber ($cm^{-1}$) | Band assignment | Associated biomolecule | References |
|---|---|---|---|
| 860 | =C-H Bending | Methylene bending vibrations | [94], [95] |

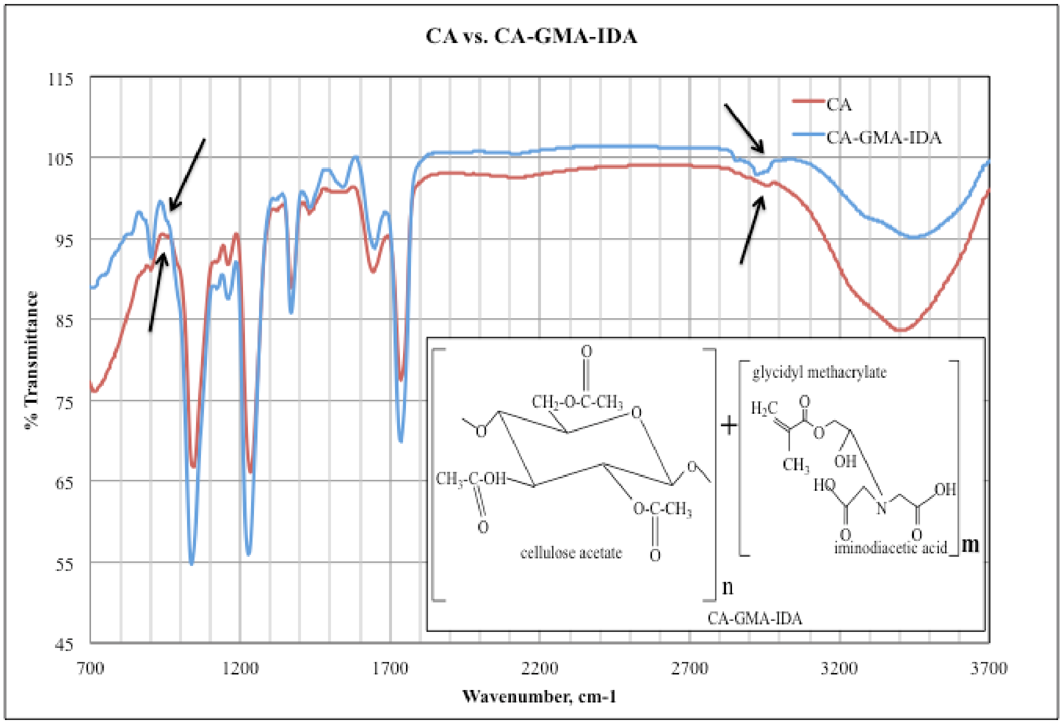


**Figure 11.—FTIR spectra comparing pure CA membranes with CA-GMA-IDA membranes.**

Table 4.—FTIR peak descriptions

| Wavenumber ($cm^{-1}$) | Band assignment | Associated biomolecule | References |
|---|---|---|---|
| 955, 2990 | -C-H bend, O-H stretch | Alkenes, carboxylic acids | [94], [95] |

# Morphological Characterization of Cellulose Acetate and Copper-charged Membranes

Membranes were cast and treated with IDA and copper in order to determine optimal IDA dosage to maximize copper chelation. The SEM (figure 12) and EDS (figure 13) images show a uniform distribution of copper on the surface of the treated membrane.

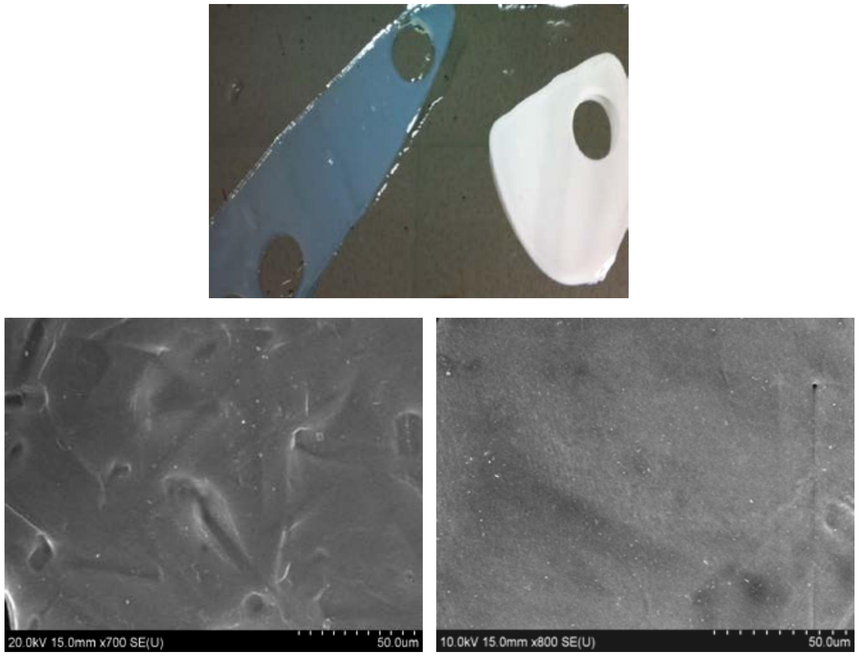


**Figure 12.—SEM images of the treated membrane (left) and nontreated membranes (right).**

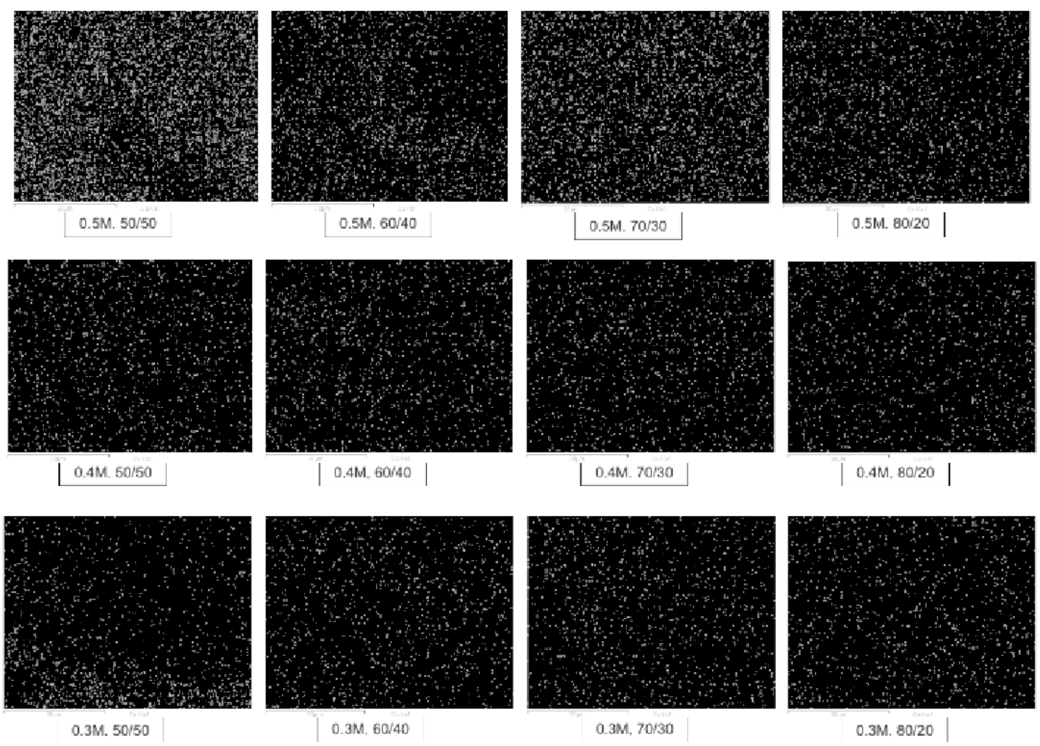


**Figure 13.—EDS images of the copper-charged membrane.**

# Hydrophilicity of Cellulose Acetate and Copper-charged Membranes

The contact angle was measured on three different areas of each membrane, and averages and standard deviations were compared for CA and copper-charged membranes (figure 14).

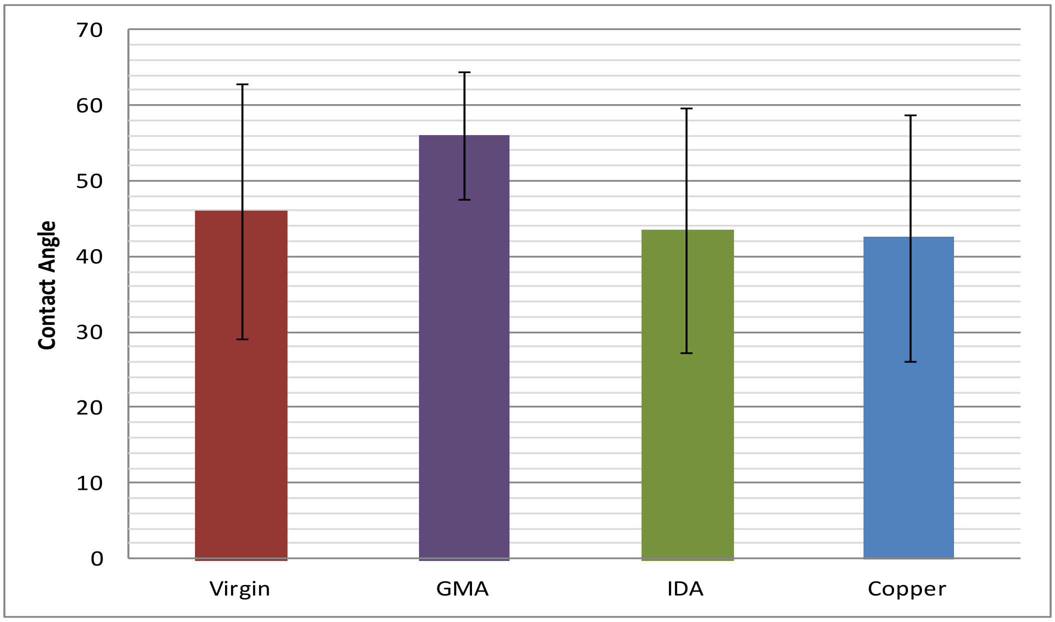


**Figure 14.—Contact angle of membranes.**

# Pore Size Distribution Analysis

Solutions of different sizes (listed in table 1) were filtered through both the CA and copper-charged membranes. The effective mean pore size for each membrane sample was calculated for each membrane, and the pore size distributions are shown on figure 15.

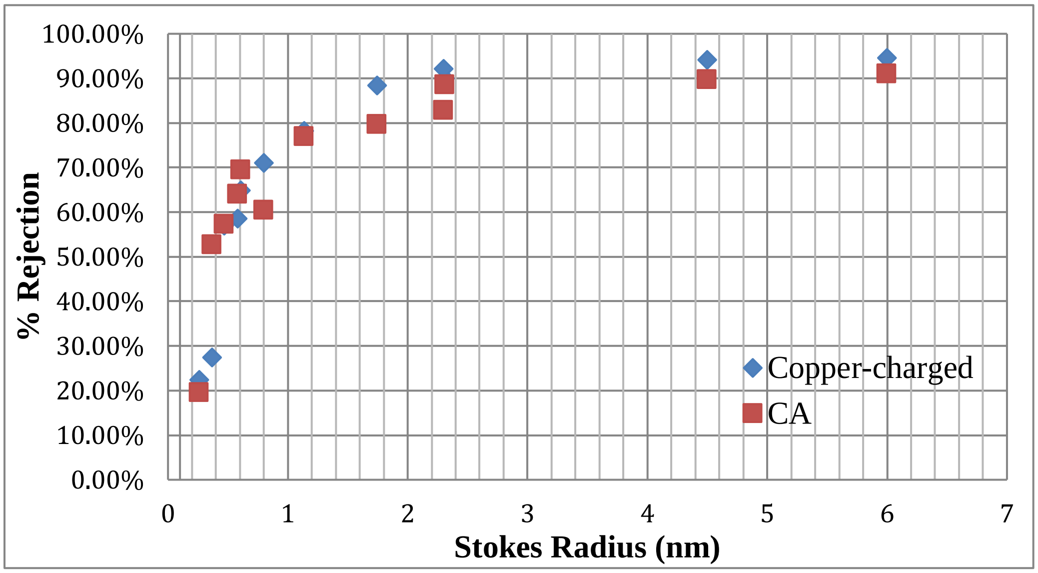


**Figure 15.—Contact angle of membranes.**

## Copper Leaching – Cross-Flow Study

The results obtained from the cross-flow leaching experiments are shown on figure 16. The points on the graph represent wt% of the copper on the membrane surface at different intervals of time.

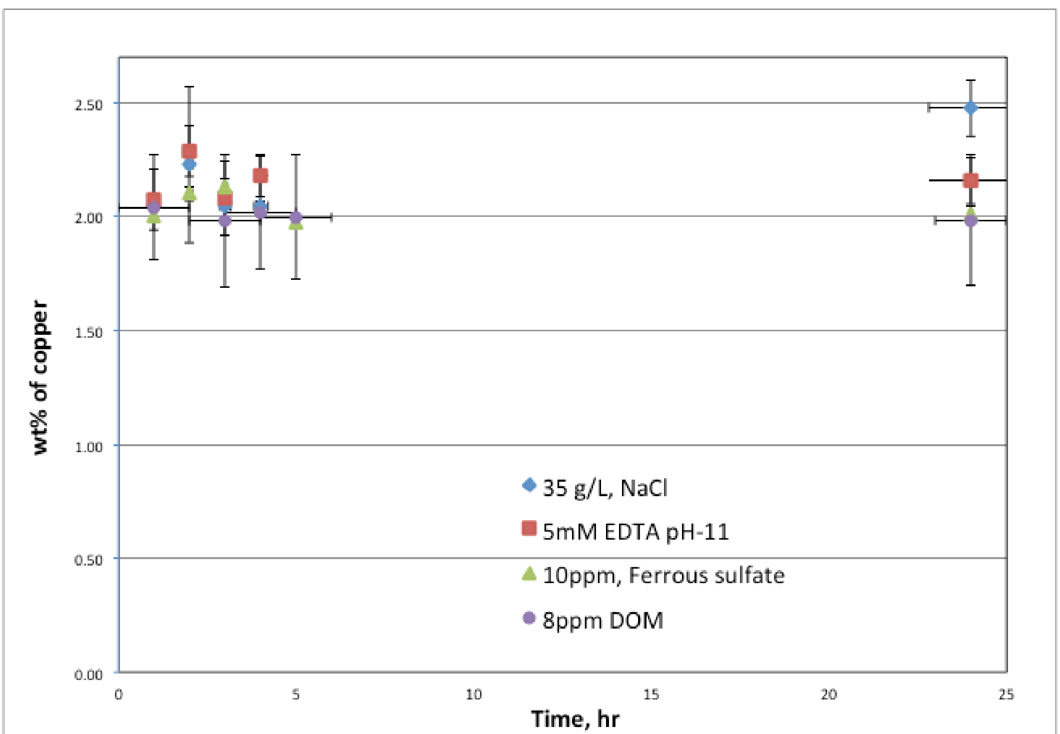


**Figure 16.—Cross-flow copper leaching results.**

# Filtration Experiments

Flux measurements for CA membranes and copper-charged membranes are shown on figure 17. The membranes were tested for the first 24 hours by pre-compaction for 0–8 hours with DI water, followed by the filtration of a BSA solution for 8–16 hours and a lipase solution for 16–24 hours (figure 17).

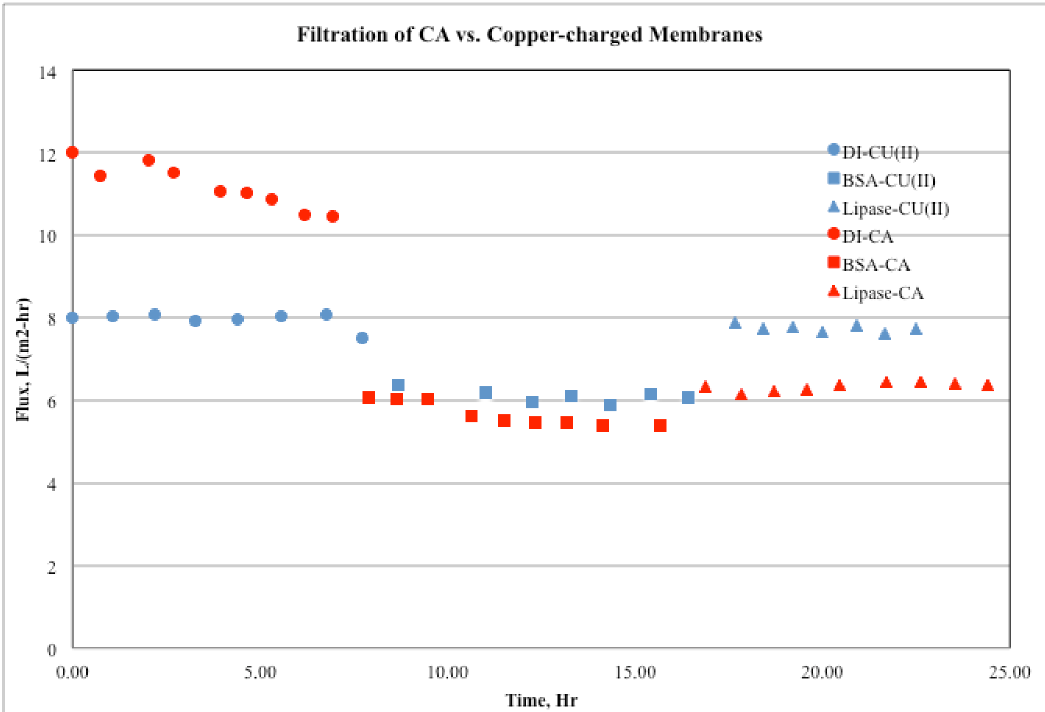


**Figure 17.—Permeation measurements with DI water (0–8 hours), BSA (8–16 hours), and lipase (16–24 hours).**

The protein rejections of the BSA and lipase were determined using ultraviolet-visible spectroscopy of both the CA and copper-charged membranes. The results are shown in table 5.

Table 5.—Protein rejections of CA and copper-charged membranes

| Membrane | BSA rejection (%) | Lipase rejection (%) |
|---|---|---|
| CA | 95.7 | 88.9 |
| Copper-charged | 95.1 | 88.0 |

Flux decline using cross-flow filtration was measured in the presence of the biofoulant *P. fluorescens*. Modified membranes resulted in less flux decline when compared to unmodified membranes (figure 18).

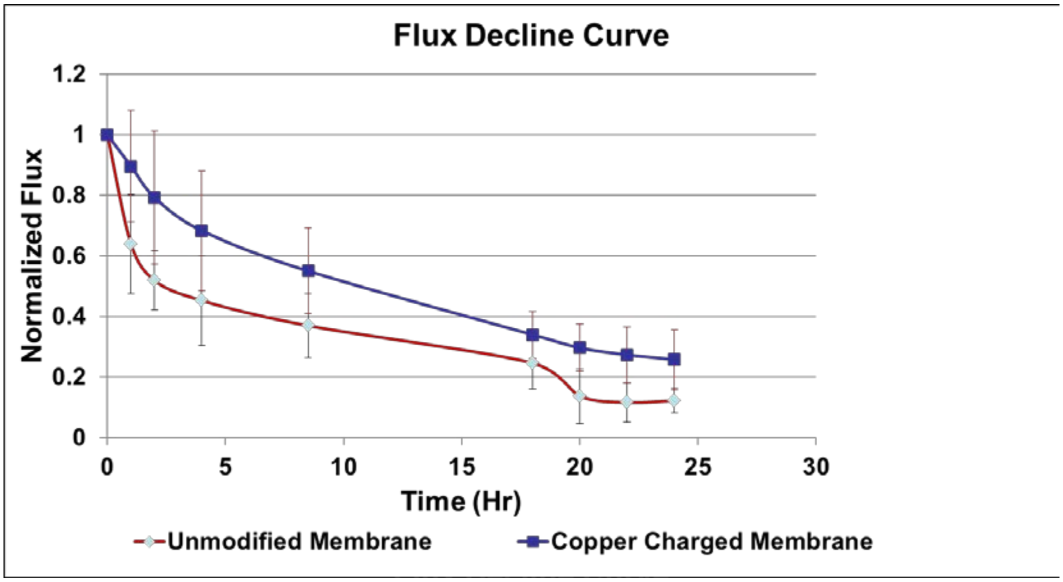


**Figure 18.—Flux decline in 24-hour cross-flow filtration studies with biofoulant.**

Copper-charged surface membranes showed that the biofilm surface area was significantly less than the biofilm surface area formed on unmodified membranes, suggesting that the modified membranes can reduce biofilm formation (table 6).

Table 6.—Biofilm surface area coverage using Image J

| Samples | Unmodified membrane Biofilm surface area coverage (%) | Copper-charged surface Biofilm surface area coverage (%) |
|---|---|---|
| 1 | 91.7 | 63.8 |
| 2 | 94.5 | 67.8 |
| 3 | 93.4 | 72.3 |
| **Average** | **93.2** | **68.0** |

We carried out similar experiments in the presence of algae organic matter, specifically TEP, since TEP are shown to cause significant fouling of desalination membranes. Sample flux measurements for modified (copper-charged) and unmodified membranes are shown on figure 19. The membranes tested were first precompacted with DI water, followed by filtering with saltwater only or TEP in

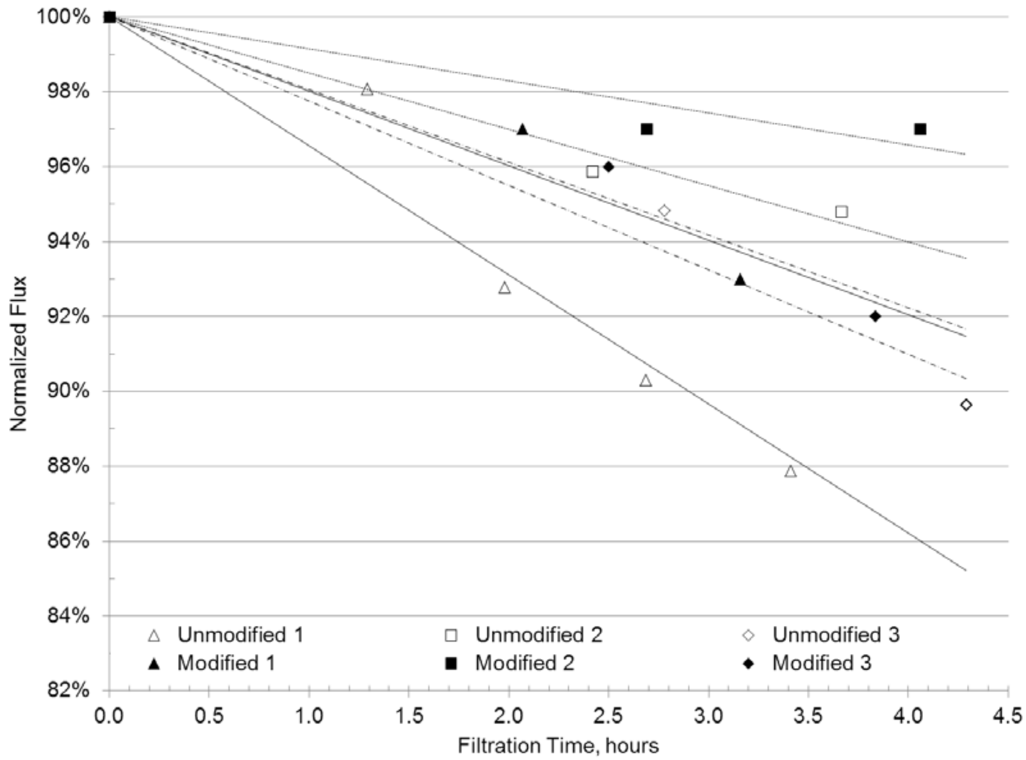


**Figure 19.—Flux decline data with TEP (1 mg/L) in saline water (35 g/L NaCl).**

saltwater. As shown on figure 19, all filtrations led to decreases in flux during operation. Salt-only runs resulted in approximately a 5–7% decline in flux. The samples, including TEP, resulted in a statistically significant increase in flux decline to almost 10–13%, while the maximum decline for the modified membranes was just over 8%.

FTIR was used to characterize the type of functional groups present on the surface of clean membranes and fouled membranes (Figure 20) [96]. There were distinct peaks present between 950 and 1,450 $cm^{-1}$on the membranes fouled with TEP when compared to membranes fouled with only saltwater. The distinct infrared peaks on the TEP fouled membranes include polysaccharides and proteins (table 7).

Table 7.—FTIR peak descriptions

| Wavenumber ($cm^{-1}$) | Band assignment | Associated molecule | Reference |
|---|---|---|---|
| 970 | C-O stretch | Polysaccharides | [97] |
| 1052 | C-O or C-O-C stretch | Polysaccharides | [98] |
| 1,350–1,450 | Amide III | Protein | [99] |

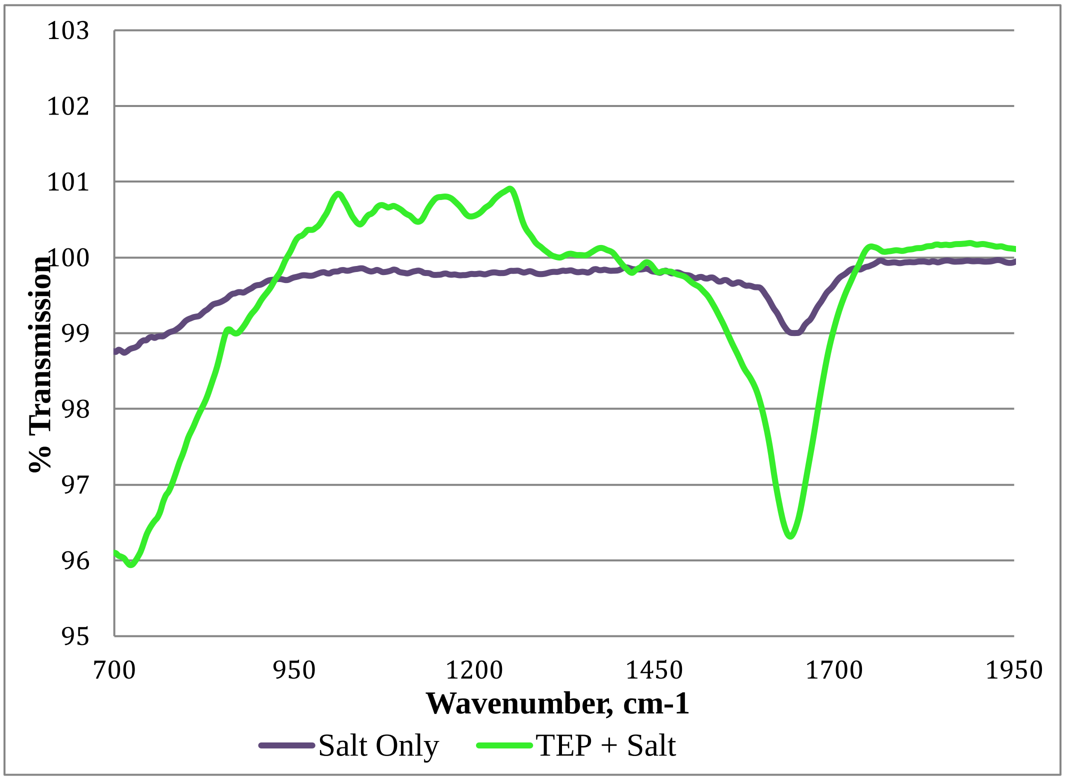


**Figure 20.—FTIR spectra comparing clean membranes and fouled membranes.**

# Discussion of Results

The FTIR analyses of the CA, CA-GMA, and CA-GMA-IDA membranes (see figures 10 and 11) showed characteristic FTIR absorption bands at 860cm$^{-1}$, 955cm$^{-1}$, and 2,990cm$^{-1}$. These bands were absent from the CA sample, which confirms the GMA presence in the modified doped polymer solution, and IDA addition was verified by peaks for -C-H bend and –O-H stretch, associated with the presence of alkenes and carboxylic acid (tables 3 and 4).

IDA-treated membranes were tested with 0.5M, 0.4M and 0.3M IDA in 50/50, 60/40, 70/30, and 80/20 water/DMSO mixtures. All samples were then treated with copper sulfate solution and analyzed for copper loading using EDS (see figure 13). The maximum copper loading was found on the membrane treated with 0.5M in 50/50 water/DMSO solution with a copper loading of 2.27 ± 0.74% by weight on the surface in a uniform fashion (figure 13). The EDS analysis of the copper-charged membrane validates the experimental procedure of the surface modification.

The contact angle analyses showed that copper-charging did not affect the hydrophobicity of the membranes (figure 14). This is important since changing the hydrophobicity of the membranes could have a negative effect on permeation flux and fouling if the membranes had become more hydrophobic.

The mean pore size was the pore size in which 50% solute rejection was achieved. The typical rejection curves for neutral solutes (see table 1) were analyzed with trend lines (figure 15). The effective mean pore radius for the CA membrane was determined to be 0.43 nm, whereas the copper-charged membrane had a mean pore radius of 0.525 nm.

The copper leaching studies showed that very little copper leached from the surface of the membranes (see figure 16). The membranes were collected after 24 hours of filtration. The average copper that leached into the NaCl solution was 0.10 wt%, into the EDTA solution was 0.11 wt%, into the Fe(II) solution was 0.22 wt%, and into the DOM solution was 0.26 wt%. Therefore, little copper leached from the copper-charged membrane. The copper that leached from the surface was slightly higher in the Fe(II) and DOM solutions compared to NaCl and EDTA, which is hypothesized due to the higher affinity of the iron and DOM for the IDA chelation causing displacement of copper from the membrane surface.

During filtration, membrane precompaction using DI water showed lower flux values for the copper-charged membrane as compared to the CA membranes (see figure 17). This is believed to be due to the additional resistance to filtration offered by GMA and IDA. On the other hand, the filtration of proteins showed slightly higher fluxes for copper-charged membrane compared to CA membranes. Other researchers have shown that protein permeation is strongly affected by pH and solution conductivity ([100–102]). They have shown that proteins were electrostatically excluded by both negatively and positively charged membranes at a solution pH away from their isoelectric points (pI). Filtration was performed at neutral pH values, which is away from the isoelectric points of BSA (pI = 4.7) and lipase (pI = 4.5). CA membranes are uncharged; therefore, an accumulation of protein was hypothesized to form a fouling layer on the membrane, which led to a flux decline. The positive copper-charged membrane would lead to electrostatic exclusion of proteins, so no proteins accumulated on the surface, which led to a minimal flux decline. Similar protein rejections of both the BSA and lipase were noticed for the copper-charged membrane compared to CA membranes (see table 5), indicating that modification of the membranes did not affect rejection ability.

Cross-flow filtration experiments using the bacterial biofoulant *P. fluorscens* indicated that the copper-charged membrane was effective at mitigating biofilm formation. This was concluded due to a lower observed flux decline to approximately 25% as compared to 15% during 24 hours of filtration. The lower flux decline is likely attributed to the biofilm coverage, which was significantly lower (66%) on the copper-charged membrane as compared to the unmodified membranes (93%). The positive charge of the copper-charged membrane is believed to cause an oxidizing atmosphere, which can lead to cell lysis and cell death [103]. Other studies have shown that a positive charge can also increase bacterial surface mobility, which prevents bacteria from attaching [104].

This project also commenced studying the impact of TEP commonly found in sea water desalination systems and attributed to algae. In dead-end filtration studies, TEP in the salt feed water did result in an increase in flux decline (10–13%) for unmodified membranes during approximately 6 hours of filtration as compared to modified membrane (2–8.5%) filtration experiments. FTIR analyses of the membranes showed distinct IR peaks present in the TEP filtration studies. These peaks may be attributed to polysaccharides and proteins, which are commonly present in TEP [56, 58, 96]. Polysaccharides are common in biofilms, and their contribution to biofilm formation on membranes has been well studied and presented in EPS literature [105, 106]. The objective with TEP studies going forward will be to characterize the proteins and polysaccharides present. These have been shown to vary with the life cycle stage of an organism [96]. The components of the TEP may be used to predict incidents of increased flux decline and to develop strategies for membrane cleaning during algal blooms.

# REFERENCES

[1] Engelman R; Cincotta RP; Dye B; Gardner-Outlaw T; Wisnewski J, *People in the Balance Population and Natural Resources at the Turn of the Millennium*. 2000, 1300 19th Street, NW Second Floor. Washington, DC 20036 USA: Population Action. 32.

[2] Leitner, G.F., *Is there a water crisis?* Int. Desalination and Water Reuse Quart., 1998. **7**(4): p. 10–21.

[3] Maude Barlow, T.C., *Blue Gold*. 2002, New York, NY: News Press.

[4] Rothfeder, J., *Every Drop for Sale: Our Desperate Battle Over Water*. 2001, New York, NY: Tarcher.

[5] J. Birkett, R.T., *A Figure of Merit for Appreciating Improvements in RO Membrane Performance.* International Desalination Association News, 2007. **16**.

[6] Safrik, J., D.P., *Final Report for Department of Water Resources Project: Role of Microfiltration (MF) Cake Layer Composition and Stability in Desalination Efficiency*, C.D.o.W. Resources, Editor 2005: Sacramento.

[7] Escobar I.C., E.H., C. Gabelich, F. DiGiano, Y. Le Gouellec, P. Berube, K. Howe, J. Allen, K. Atasi, M. Benjamin, P. Brandhuber, J. Brant, Y. Chang, M. Chapman, A. Childress, W. Conlon, T. Cooke, I. Crossley, G. Crozes, P. Huck, S. Kommineni, J. Jacangelo, A. Karimi, J. Kim, D. Lawler, Q. Li, L. Schideman, S. Sethi, J. Tobiason, T. Tseng, S. Veerapaneni, and A. Zander, *American Water Works Association Membrane Technology Research Committee Report: Membrane Fouling – Recent Advances and Research Needs.* American Water Works Association, 2005. **97**(8): p. 78–89.

[8] Characklis, W.G., Marshall, K.C., *Biofilms*. 1990, New York, NY: John Wiley & Sons.

[9] Ridgeway, H.F., H.C.F., *Membrane Biofouling*, in *Water Treatment: Membrane Processes*, P.E.O. J. Mallevialle, M. R. Weisner, Editor 1996, McGraw-Hill: New York, NY. p. 6.1–6.62.

[10] Patching, J.W., G.T.A.F., *Industrial biofilm: formation, problems and control*, in *Biofilms in medicine, industry and environmental biotechnology: characteristics, analysis and control*, P. Lens, Editor 2003, IWA Publishing: London. p. 568–590.

[11] Herzberg, M. and M. Elimelech, *Biofouling of reverse osmosis membranes: Role of biofilm-enhanced osmotic pressure.* Journal of Membrane Science, 2007. **295**(1-2): p. 11–20.

[12] Chong, T.H., F.S. Wong, and A.G. Fane, *The effect of imposed flux on biofouling in reverse osmosis: Role of concentration polarisation and biofilm enhanced osmotic pressure phenomena.* Journal of Membrane Science, 2008. **325**(2): p. 840–850.

[13] Cornelissen, E.R., et al., *Periodic air/water cleaning for control of biofouling in spiral wound membrane elements.* Journal of Membrane Science, 2007. **287**(1): p. 94–101.

[14] Kim, B.R., et al., *Literature review - efficacy of various disinfectants against Legionella in water systems.* Water Research, 2002. **36**(18): p. 4433–4444.

[15] Roe, D., et al., *Antimicrobial surface functionalization of plastic catheters by silver nanoparticles.* Journal of Antimicrobial Chemotherapy, 2008. **61**(4): p. 869–876.

[16] Landeen, L.K., M.T. Yahya, and C.P. Gerba, *Efficacy of Copper and Silver Ions and Reduced Levels of Free Chlorine in Inactivation of Legionella-Pneumophila.* Applied and Environmental Microbiology, 1989. **55**(12): p. 3045–3050.

[17] Kwak, S.Y., *Relationship of relaxation property to reverse osmosis permeability in aromatic polyamide thin-film-composite membranes.* Polymer, 1999. **40**(Copyright © 2011 American Chemical Society (ACS). All Rights Reserved.): p. 6361–6368.

[18] Driol, E.M., Francesca, *Membrane Research, Membrane Production and Membrane Application in China*, 2008, ITM-CNR - Italy: Institute on Membrane Technology.

[19] Jin, Y. and Z. Su, *Effects of polymerization conditions on hydrophilic groups in aromatic polyamide thin films.* J. Membr. Sci., 2009. **330**(Copyright © 2011 American Chemical Society (ACS). All Rights Reserved.): p. 175–179.

[20] Gabelich, C.J., et al., *Effects of aluminum sulfate and ferric chloride coagulant residuals on polyamide membrane performance.* Desalination, 2002. **150**(1): p. 15–30.

[21] Park, C., et al., *Effect of cake layer structure on colloidal fouling in reverse osmosis membranes.* Desalination, 2008. **220**(1-3): p. 335–344.

[22] Moftah, K., *For water treatment consider high-pH reverse osmosis.* Chemical Engineering, 2003. **110**(9): p. 62–69.

[23] Niriella, D. and R.P. Carnahan, *Influence of operating parameters on clay fouling of a RO membrane.* Separation Science and Technology, 2006. **41**(1): p. 25–41.

[24] Hoek, E.M.V. and M. Elimelech, *Cake-Enhanced Concentration Polarization: A New Fouling Mechanism for Salt-Rejecting Membranes.* Environmental Science & Technology, 2003. **37**(24): p. 5581–5588.

[25] Kim, S. and E.M.V. Hoek, *Modeling concentration polarization in reverse osmosis processes.* Desalination, 2005. **186**(1-3): p. 111–128.

[26] Elimelech, M. and S. Bhattacharjee, *A novel approach for modeling concentration polarization in crossflow membrane filtration based on the equivalence of osmotic pressure model and filtration theory.* Journal of Membrane Science, 1998. **145**(2): p. 223–241.

[27] Tzotzi, C., et al., *A study of CaCO3 scale formation and inhibition in RO and NF membrane processes.* Journal of Membrane Science, 2007. **296**(1-2): p. 171–184.

[28] Darton, E.G. and E. Buckley, *Thirteen years' experiences treating a seawater RO plant.* Desalination, 2001. **134**(1-3): p. 55–62.

[29] Lisitsin, D., et al., *Inhibition of CaCO3 scaling on RO membranes by trace amounts of zinc ions.* Desalination, 2005. **183**(1-3): p. 289–300.

[30] Hafez, A.I., M.S. El-Manharawy, and M.A. Khedr, *RO membrane removal of unreacted chromium from spent tanning effluent. A pilot-scale study, part 2.* Desalination, 2002. **144**(1-3): p. 237–242.

[31] Taniguchi, M., J.E. Kilduff, and G. Belfort, *Modes of natural organic matter fouling during ultrafiltration.* Environmental Science & Technology, 2003. **37**(8): p. 1676–1683.

[32] Zularisam, A.W., A.F. Ismail, and R. Salim, *Behaviours of natural organic matter in membrane filtration for surface water treatment - a review.* Desalination, 2006. **194**(1-3): p. 211–231.

[33] Gullinkala, T. and I. Escobar, *Study of the hydrophilic-enhanced ultrafiltration membrane.* Environmental Progress, 2008. **27**(2): p. 210–217.

[34] Chennamsetty, R. and I. Escobar, *Effect of Ion Beam Irradiation on Two Nanofiltration Water Treatment Membranes.* Separation Science and Technology, 2008. **43**(16): p. 4009–4029.

[35] Baker, J.S. and L.Y. Dudley, *Biofouling in membrane systems - a review.* Water Supply, 1999. **17**(Copyright © 2011 American Chemical Society (ACS). All Rights Reserved.): p. 173–181.

[36] Vrouwenvelder, J.S., et al., *Biofouling of spiral-wound nanofiltration and reverse osmosis membranes: A feed spacer problem.* Water Res., 2009. **43**(Copyright © 2011 American Chemical Society (ACS). All Rights Reserved.): p. 583–594.

[37] Flemming, H.-C., *Reverse osmosis membrane biofouling.* Exp. Therm. Fluid Sci., 1997. **14**(Copyright © 2011 American Chemical Society (ACS). All Rights Reserved.): p. 382–391.

[38] Amjad, Z. *Scale inhibition in desalination applications: an overview.* 1996. NACE International.

[39] Geesey, G.G., et al., *Biofouling and Biocorrosion in Industrial Water Systems*. 1994: Lewis. 297 pp.

[40] Tsuneda, S., et al., *Extracellular polymeric substances responsible for bacterial adhesion onto solid surface.* FEMS Microbiol. Lett., 2003. **223**(Copyright (C) 2011 American Chemical Society (ACS). All Rights Reserved.): p. 287–292.

[41] Kim, D., et al., *Biocide application for controlling biofouling of SWRO membranes - an overview.* Desalination, 2009. **238**(Copyright (C) 2011 American Chemical Society (ACS). All Rights Reserved.): p. 43–52.

[42] Caron, D.A., et al., *Harmful algae and their potential impacts on desalination operations off southern California.* Water Research, 2010. **44**(2): p. 385–416.

[43] Kwon, B., N. Park, and J. Cho, *Effect of algae on fouling and efficiency of UF membranes.* Desalination, 2005. **179**(1-3): p. 203–214.

[44] Ladner, D.A., D.R. Vardon, and M.M. Clark, *Effects of shear on microfiltration and ultrafiltration fouling by marine bloom-forming algae.* Journal of Membrane Science, 2010. **356**(1-2): p. 33–43.

[45] Villacorte, L.O., et al., *The fate of Transparent Exopolymer Particles (TEP) in integrated membrane systems: Removal through pre-treatment processes and deposition on reverse osmosis membranes.* Water Research, 2009. **43**(20): p. 5039–5052.

[46] Bar-Zeev, E., et al., *Transparent exopolymer particles:Potential agents for fouling and bioflim formation in desalination and water treatment plants.* Desalination and Water Treatment, 2009. **3**: p. 136–142.

[47] Alldredge, A.L., U. Passow, and S.H.D. Haddock, *The characteristics and transparent exopolymer particle (TEP) content of marine snow formed from thecate dinoflagellates.* Journal of Plankton Research, 1998. **20**(3): p. 393–406.

[48] Passow, U. and A.L. Alldredge, *Distribution, Size and Bacterial-Colonization of Transparent Exopolymer Particles (Tep) in the Ocean.* Marine Ecology-Progress Series, 1994. **113**(1-2): p. 185–198.

[49] Passow, U. and A.L. Alldredge, *Abiotic Formation of Transparent Exopolymer Particles (TEP) from Polysaccharides Excreted by Phytoplankton.* Abstracts of Papers of the American Chemical Society, 1994. **207**: p. 178-GEOC.

[50] Mari, X. and T. Kiorboe, *Abundance, size distribution and bacterial colonization of transparent exopolymeric particles (TEP) during spring in the Kattegat.* Journal of Plankton Research, 1996. **18**(6): p. 969–986.

[51] Passow, U., et al., *The origin of transparent exopolymer particles (TEP) and their role in the sedimentation of particulate matter.* Continental Shelf Research, 2001. **21**(4): p. 327–346.

[52] Berman, T., *Biofouling: TEP - a major challenge for water filtration.* Filtration & Separation, 2010. **47**(2): p. 20–22.

[53] Passow, U., *Transparent exopolymer particles (TEP) in aquatic environments.* Progress in Oceanography, 2002. **55**(3-4): p. 287–333.

[54] Passow, U., *Production of transparent exopolymer particles (TEP) by phyto- and bacterioplankton.* Marine Ecology-Progress Series, 2002. **236**: p. 1–12.

[55] Van Nevel, S., et al., *Transparent exopolymer particle removal in different drinking water production centers.* Water Res, 2012. **46**(11): p. 3603–3611.

[56] Bar-Zeev, E., et al., *Transparent exopolymer particles (TEP) link phytoplankton and bacterial production in the Gulf of Aqaba.* Aquatic Microbial Ecology, 2009. **56**(2-3): p. 217–225.

[57] Villacorte, L.O., et al., *The fate of Transparent Exopolymer Particles (TEP) in integrated membrane systems: Removal through pre-treatment processes and deposition on reverse osmosis membranes.* Water Res, 2009. **43**(20): p. 5039–5052.

[58] Villacorte, L.O., et al., *Measuring transparent exopolymer particles (TEP) as indicator of the (bio)fouling potential of RO feed water.* Desalination and Water Treatment, 2009. **5**(1-3): p. 207–212.

[59] Al-Ahmad, M., et al., *Biofuoling in RO membrane systems Part 1: Fundamentals and control.* Desalination, 2000. **132**(1-3): p. 173–179.

[60] Bos, R., H.C. van der Mei, and H.J. Busscher, *Physico-chemistry of initial microbial adhesive interactions - its mechanisms and methods for study.* Fems Microbiology Reviews, 1999. **23**(2): p. 179–230.

[61] Escobar, I.C., et al., *Committee Report: Recent advances and research needs in membrane fouling.* Journal of the American Water Works Association, 2005. **97**(8): p. 79–89.

[62] Ivnitsky, H., et al., *Characterization of membrane biofouling in nanofiltration processes of wastewater treatment.* Desalination, 2005. **185**(1-3): p. 255–268.

[63] Villacorte, L.O., et al., *The fate of Transparent Exopolymer Particles (TEP) in integrated membrane systems: Removal through pre-treatment processes and deposition on reverse osmosis membranes (vol. 43, pg. 5039, 2009).* Water Res, 2011. **45**(2): p. 960–960.

[64] Berman, T. and M. Holenberg, *Don't fall foul of biofilm through high TEP levels.* Filtration + Separation, 2005. **42**(4): p. 30–32.

[65] Berman, T., *Biofouling: TEP – a major challenge for water filtration.* Filtration + Separation, 2010. **47**(2): p. 20–22.

[66] Brant, J.a.P.K., *State-of-the-Science Review of Membrane Fouling: Organic, Inorganic, and Biological*, in *Water Reuse Foundation Report No. WRF-06-010A*2010, WateReuse Foundation: Alexandria, VA.

[67] Farooque, A.M., Al-Amoudi, A.S., Saeed, M.O., Al-Muaili, F. A., *Impact of Fouling on Performance of Different Hff Membranes Operated at Different Coasts*, International Desalination and Water Reuse Quarterly, 2004(14): p. 19–24.

[68] Berman, T., *Don't fall foul of biofilm through high TEP levels.* Filtration & Separation, 2005. **42**(4): p. 30–32.

[69] Villacorte, L.O., et al., *The fate of transparent exopolymer particles (TEP) in seawater UF-RO system: A pilot plant study in Zeeland, The Netherlands.* Desalination and Water Treatment, 2010. **13**(1-3): p. 109–119.

[70] Berman, T., R. Mizrahi, and C.G. Dosoretz, *Transparent exopolymer particles (TEP): A critical factor in aquatic biofilm initiation and fouling on filtration membranes.* Desalination, 2011. **276**(1–3): p. 184–190.

[71] Bereschenko, L.A., et al., *Effect of conventional chemical treatment on the microbial population in a biofouling layer of reverse osmosis systems.* Water Res., 2011. **45**(Copyright (C) 2011 American Chemical Society (ACS). All Rights Reserved.): p. 405–416.

[72] Flemming, H.C., *Biofouling in water systems - cases, causes and countermeasures.* Appl. Microbiol. Biotechnol., 2002. **59**(Copyright © 2011 American Chemical Society (ACS). All Rights Reserved.): p. 629–640.

[73] Turakhia, M.H., K.E. Cooksey, and W.G. Characklis, *Influence of a calcium-specific chelant on biofilm removal.* Appl. Environ. Microbiol., 1983. **46**(Copyright © 2011 American Chemical Society (ACS). All Rights Reserved.): p. 1236–1238.

[74] Whitekettle, W.K., J. Jiang, and X. Huang, *Method for reduction of microbial biofilms on surfaces in aquatic systems by adding polyalkyleneoxide polysiloxane surfactants*, 2010, General Electric Company, USA . p. 20pp.; Chemical Indexing Equivalent to 153:78822 (US).

[75] Gullinkala, T., *Evaluation of Poly (Ethylene Glycol) Grafting as a Tool for Improving Membrane Performance*, in *Chemical and Environmental Engineering*, 2010, University of Toledo: Toledo, OH.

[76] Liu, C.X., et al., *Modification of membrane surface for anti-biofouling performance: Effect of anti-adhesion and anti-bacteria approaches.* J. Membr. Sci., 2010. **346**(Copyright (C) 2011 American Chemical Society (ACS). All Rights Reserved.): p. 121–130.

[77] Zodrow, K., et al., *Polysulfone ultrafiltration membranes impregnated with silver nanoparticles show improved biofouling resistance and virus removal.* Water Res., 2009. **43**(Copyright © 2011 American Chemical Society (ACS). All Rights Reserved.): p. 715–723.

[78] Yang, H.L., J.C.T. Lin, and C. Huang, *Application of nanosilver surface modification to RO membrane and spacer for mitigating biofouling in seawater desalination.* Water Res., 2009. **43**(Copyright © 2011 American Chemical Society (ACS). All Rights Reserved.): p. 3777–3786.

[79] Vrouwenvelder, J.S. and van der Kooij, D.. *Diagnosis, prediction and prevention of biofouling of NF and RO membranes*. 2001. American Water Works Association.

[80] Willems, P., et al., *Bubbles in spacers: Direct observation of bubble behavior in spacer filled membrane channels.* J. Membr. Sci., 2009. **333**(Copyright © 2011 American Chemical Society (ACS). All Rights Reserved.): p. 38–44.

[81] Koutsou, C.P., S.G. Yiantsios, and A.J. Karabelas, *Direct numerical simulation of flow in spacer-filled channels: Effect of spacer geometrical characteristics.* J. Membr. Sci., 2007. **291**(Copyright © 2011 American Chemical Society (ACS). All Rights Reserved.): p. 53–69.

[82] Picchioni, F., J.G.P. Goossens, and M. van Duin, *Solid-state modification of polypropylene (PP): grafting of styrene on atactic PP.* Macromolecular Symposia, 2001. **176**(1): p. 245–264.

[83] Chen, C.Y. and C.Y. Chen, *Stability constants of polymer-bound iminodiacetate-type chelating agents with some transition-metal ions.* J. Appl. Polym. Sci., 2002. **86**(Copyright © 2011 American Chemical Society (ACS). All Rights Reserved.): p. 1986–1994.

[84] Hausman, R., T. Gullinkala, and I.C. Escobar, *Development of low-biofouling polypropylene feedspacers for reverse osmosis.* J. Appl. Polym. Sci., 2009. **114**(Copyright © 2011 American Chemical Society (ACS). All Rights Reserved.): p. 3068–3073.

[85] Hausman, R., T. Gullinkala, and I.C. Escobar, *Development of copper-charged polypropylene feedspacers for biofouling control.* J. Membr. Sci., 2010. **358**(Copyright (C) 2011 American Chemical Society (ACS). All Rights Reserved.): p. 114–121.

[86] Selvaraj, S., et al., *Toxicity of free and various aminocarboxylic ligands sequestered copper(II) ions to Escherichia coli.* Journal of Hazardous Materials, 2009. **166**(2-3): p. 1403–1409.

[87] Massaro, E.J., *Handbook of Copper Pharmacology and Toxicology*. 2002, Totowa, New Jersey: Humana Press Inc.

[88] Borkow, G. and J. Gabbay, *Copper, An Ancient Remedy Returning to Fight Microbial, Fungal and Viral Infections.* Current Chemical Biology, 2009. **3**(3): p. 272–278.

[89] Belly, R.T. and G.C. Kydd, *Silver resistance in microorganisms.* Dev. Ind. Microbiol., 1982. **23**: p. 567–577.

[90] Pradeep, T. and Anshup, *Noble metal nanoparticles for water purification: A critical review.* Thin Solid Films, 2009. **517**(24): p. 6441–6478.

[91] Dattagupta, N.C., Donald M., *Solution structural studies of the Ag(I)-DNA complex.* Nucleic Acids Research, 1981. **9**(12): p. 2971–2985.

[92] Appaw, C., *Rheology and Microstructure of Cellulose Acetate in Mixed Solvent Systems.* 2005.

[93] Zhao, Q., et al., *Polyelectrolyte complex membranes for pervaporation, nanofiltration and fuel cell applications.* Journal of Membrane Science, 2011. **379**(1-2): p. 19-45.

[94] Silverstein, R.M., G.C. Bassler, and T.C. Morrill, *Spectrometric identification of organic compounds*. 5th ed. 1991, New York: John Wiley and Sons, Inc. 419 p.

[95] Meyers, R.A., *Encyclopedia of analytical chemistry : applications, theory and instrumentation*. 2011, Chichester, West Sussex, U.K.: John Wiley and Sons, Inc.

[96] Villacorte, L.O., et al., *Characterisation of transparent exopolymer particles (TEP) produced during algal bloom: a membrane treatment perspective.* Desalination and Water Treatment, 2013. **51**(4-6): p. 1021–1033.

[97] Osiro, D., et al., *A kinetic model for Xylella fastidiosa adhesion, biofilm formation, and virulence.* Fems Microbiology Letters, 2004. **236**(2): p. 313–318.

[98] Schmitt, J., et al., *Changes of biofilm properties in response to sorbed substances - An FTIR-ATR study.* Water Science and Technology, 1995. **32**(8): p. 149–155.

[99] Mayo D.W., M.F.A.a.H.R.W., *Course Notes On The Interpretation of Infrared and Raman Spectra*, 2004, New Jersey: John Wiley & Sons Inc.

[100] Lucas, D., et al., *Role of the physico-chemical environment on ultrafiltration of lysozyme with modified inorganic membrane.* Colloids and Surfaces a-Physicochemical and Engineering Aspects, 1998. **136**(1-2): p. 109–122.

[101] Nakao, S., et al., *Separation of Proteins by Charged Ultrafiltration Membranes.* Desalination, 1988. **70**(1-3): p. 191–205.

[102] Saksena, S. and A.L. Zydney, *EFFECT OF SOLUTION PH AND IONIC-STRENGTH ON THE SEPARATION OF ALBUMIN FROM IMMUNOGLOBULINS (IGG) BY SELECTIVE FILTRATION.* Biotechnology and Bioengineering, 1994. **43**(10): p. 960–968.

[103] Shim, S., et al., *Prevention of Pseudomonas aeruginosa adhesion by electric currents.* Biofouling, 2011. **27**(2): p. 217–24.

[104] de Lannoy, C.F., et al., *Aquatic biofouling prevention by electrically charged nanocomposite polymer thin film membranes.* Environ Sci Technol, 2013. **47**(6): p. 2760–8.

[105] Kim, D., et al., *Biocide application for controlling biofouling of SWRO membranes - an overview.* Desalination, 2009. **238**(1-3): p. 43–52.

[106] Tsuneda, S., et al., *Extracellular polymeric substances responsible for bacterial adhesion onto solid surface.* Fems Microbiology Letters, 2003. **223**(2): p. 287–292.

# APPENDICES

A Bacterial Growth Data

B Fourier Transform Infrared Spectroscopy (FTIR) Peak Data

C Flux Data

# APPENDIX A

## Bacterial Growth Data

The acronyms, abbreviations, and units of measure as they appear in this appendix are defined as follows:

| | |
|---|---|
| h | hour |
| # | number |
| mL | milliliter |
| $mm^2$ | square millimeter |

Table A-1.—Biofoulant (*Pseudomonas fluorescens)* growth curve data for figure 2

| Time (h) | 2 (dilution 1:10) | | 7 (dilution 1:10) | | 20 (dilution 1:100) | | 26 (dilution 1:400) | | 32 (dilution 1:400) | | 48 (dilution 1:400) | |
|---|---|---|---|---|---|---|---|---|---|---|---|---|
| | **S-01** | **S-02** | **S-01** | **S-02** | **S-01** | **S-02** | **S-01** | **S-02** | **S-01** | **S-02** | **S-01** | **S-02** |
| | 21 | 18 | 24 | 24 | 85 | 79 | 51 | 54 | 42 | 35 | 26 | 41 |
| | 22 | 22 | 21 | 25 | 90 | 74 | 49 | 49 | 40 | 31 | 34 | 31 |
| | 18 | 21 | 20 | 32 | 79 | 83 | 60 | 52 | 36 | 42 | 36 | 38 |
| | 21 | 24 | 30 | 26 | 75 | 93 | 55 | 55 | 43 | 35 | 34 | 36 |
| | 16 | 18 | 22 | 24 | 81 | 80 | 58 | 59 | 37 | 29 | 35 | 27 |
| | 20 | 19 | 27 | 20 | 76 | 75 | 61 | 52 | 44 | 36 | 39 | 35 |
| | 17 | 23 | 26 | 29 | 73 | 81 | 48 | 54 | 41 | 43 | 38 | 41 |
| **Average** | 19.29 | 20.71 | 24.29 | 25.71 | 79.86 | 80.71 | 54.57 | 53.57 | 40.43 | 35.86 | 34.57 | 35.57 |
| **Cells#/mL** | 9,004,693 | 9,671,707 | 11,339,243 | 12,006,257 | 372,860,986 | 376,863,071 | 1,019,197,829 | 1,000,521,429 | 755,060,171 | 669,682,343 | 645,669,829 | 664,346,229 |
| **Standard Deviation** | 1,068,612 | 1,134,578 | 1,677,290 | 1,802,585 | 28,070,129 | 29,371,359 | 99,329,155 | 57,924,088 | 55,880,778 | 96,702,503 | 79,132,374 | 96,358,365 |

Table A-2.—Algae growth curve and corresponding transparent exopolymeric particles concentration data for figure 4

| | Algae count day 2 | | | | Algae count day 6 | | | |
|---|---|---|---|---|---|---|---|---|
| **Samples** | **A** | **B** | **C** | **D** | **A** | **B** | **C** | **D** |
| | 1 | 1 | 2 | 2 | 7 | 3 | 10 | 7 |
| | 3 | 0 | 3 | 2 | 7 | 1 | 11 | 8 |
| | 3 | 1 | 4 | 1 | 4 | 3 | 9 | 12 |
| | 3 | 2 | 0 | 3 | 11 | 1 | 10 | 9 |
| | 1 | 0 | 1 | 4 | 10 | 5 | 13 | 10 |
| | 3 | 1 | 2 | 3 | 8 | 4 | 8 | 10 |
| | 2 | 1 | 1 | 2 | 13 | 3 | 10 | 8 |
| | 2 | 1 | 2 | 2 | 9 | 4 | 12 | 12 |
| | 2 | 2 | 3 | 1 | 10 | 2 | 7 | 8 |
| | 1 | 2 | 1 | 1 | 11 | 5 | 10 | 10 |
| Total | 21 | 11 | 19 | 21 | 90 | 31 | 100 | 94 |
| Average | 2.1 | 1.1 | 1.9 | 2.1 | 9 | 3.1 | 10 | 9.4 |
| Average of counts | | 1.8 | | | | 7.875 | | |
| Standard deviation | 0.8756 | 0.7379 | 1.1972 | 0.9944 | 2.5820 | 1.4491 | 1.7638 | 1.7127 |
| Average of standard deviation | | 0.9513 | | | | 1.8769 | | |
| Algal cell number in batch culture | 308,824 | 161,765 | 279,412 | 308,824 | 1,323,529 | 455,882 | 1,470,588 | 1,382,353 |
| Algal cell number in average | | 264,706 | | | Average count | 1,158,088 | | |
| Algal cell number in standard deviation | | 70,014 | | | Standard deviation | 472,022 | | |
| Area of field ($mm^2$) | 0.0068 | | | | | | | |
| Area of chamber ($mm^2$) | 1,000 | | Standard deviation | 70,014 | 472,022 | 363,605 | 226,673 | 283732.1 |
| # of fields | 147,059 | | Counts | 265,000 | 1,160,000 | 2,120,000 | 1,730,000 | 4.96E+05 |

Table A-2.—Algae growth curve and corresponding transparent exopolymeric particles concentration data for figure 4

| | Algae count day 9 | | | | Algae count day 12 | | | |
|---|---|---|---|---|---|---|---|---|
| **Samples** | **A** | **B** | **C** | **D** | **A** | **B** | **C** | **D** |
| | 8 | 19 | 23 | 11 | 5 | 16 | 21 | 10 |
| | 8 | 13 | 19 | 12 | 6 | 10 | 15 | 11 |
| | 11 | 22 | 17 | 20 | 9 | 19 | 14 | 14 |
| | 12 | 9 | 18 | 14 | 13 | 6 | 15 | 12 |
| | 8 | 19 | 14 | 12 | 12 | 18 | 11 | 8 |
| | 14 | 13 | 14 | 20 | 16 | 13 | 12 | 12 |
| | 14 | 15 | 17 | 12 | 15 | 13 | 13 | 8 |
| | 14 | 13 | 14 | 13 | 11 | 9 | 11 | 9 |
| | 11 | 18 | 18 | 20 | 11 | 13 | 13 | 12 |
| | 9 | 14 | 12 | 12 | 8 | 8 | 11 | 8 |
| Total | 109 | 155 | 166 | 146 | 106 | 125 | 136 | 104 |
| Average | 10.9 | 15.5 | 16.6 | 14.6 | 10.6 | 12.5 | 13.6 | 10.4 |
| Average of counts | | 14.4 | | | | 11.775 | | |
| Standard deviation | 2.5582 | 3.8944 | 3.2042 | 3.8064 | 3.6271 | 4.3012 | 3.0258 | 2.1187 |
| Average of standard deviation | | 3.3658 | | | | 3.2682 | | |
| Algal cell number in batch culture | 1,602,941 | 2,279,412 | 2,441,176 | 2,147,059 | 1,558,824 | 1,838,235 | 2,000,000 | 1,529,412 |
| Algal cell number in average | Average count | 2,117,647 | Standard deviation | 363,605 | | | 1,731,618 | 226,673 |

Table A-2.—Algae growth curve and corresponding transparent exopolymeric particles concentration data for figure 4

| | **Algae count day 14** | | | | | | | |
|---|---|---|---|---|---|---|---|---|
| A | B | C | D | | | | | |
| 6 | 1 | 4 | 9 | | | | | |
| 2 | 0 | 8 | 1 | | | | | |
| 3 | 2 | 5 | 2 | | | | | |
| 3 | 0 | 4 | 2 | | | | | |
| 3 | 1 | 3 | 4 | | | | | |
| 4 | 2 | 3 | 4 | | | | | |
| 3 | 0 | 3 | 5 | | | | | |
| 3 | 0 | 4 | 3 | | | | | |
| 3 | 0 | 5 | 4 | | | | | |
| 4 | 1 | 13 | 8 | **TEP ABSORBANCE** | | | | |
| 34 | 7 | 52 | 42 | | | | | |
| 3.4 | 0.7 | 5.2 | 4.2 | **Day 2** | **Day 6** | **Day 9** | **Day 12** | **Day 14** |
| | 3.375 | | | 0.087 | 0.302 | 0.389 | 0.869 | 1.238 |
| 1.0750 | 0.8233 | 3.1198 | 2.5734 | 0.102 | 0.187 | 0.434 | 1.207 | 0.905 |
| | 1.8979 | | | 0.106 | 0.205 | 0.451 | 1.424 | 1.992 |
| 500,000 | 102,941 | 764,706 | 617,647 | 0.113 | 0.192 | 0.511 | 0.676 | 1.23 |
| Average count | 496,324 | | | 0.102 | 0.2215 | 0.44625 | 1.044 | 1.34125 |
| Standard deviation | 283,732 | | | 0.0110 | 0.0542 | 0.0505 | 0.3352 | 0.4607 |

# APPENDIX B

## Fourier Transform Infrared Spectroscopy (FTIR) Peak Data

The acronyms, abbreviations, and units of measure as they appear in this appendix are defined as follows:

| | |
|---|---|
| CA | cellulose acetate |
| GMA | glycidyl methacrylate |
| IDA | iminodiacetic acid |

Table B-1.—FTIR data of the CA versus CA-GMA membranes presented on figure 10 and CA versus CA-GMA-IDA presented on figure 11

| CA | | | CA-GMA | | | CA-GMA-IDA | |
|---|---|---|---|---|---|---|---|
| XLabel | Wavenumber | | XLabel | Wavenumber | | XLabel | Wavenumber |
| YLabel | %Transmittance | | YLabel | %Transmittance | | YLabel | %Transmittance |
| FileType | %Transmittance | | FileType | %Transmittance | | FileType | %Transmittance |
| DisplayDirection | 20300 | | DisplayDirection | 20300 | | DisplayDirection | 20300 |
| PeakDirection | 20311 | | PeakDirection | 20311 | | PeakDirection | 20311 |
| 698.229749 | 77.213422 | | 698.229749 | 71.908354 | | 698.229749 | 89.149662 |
| 702.087372 | 76.716946 | | 702.087372 | 71.301447 | | 702.087372 | 88.963939 |
| 705.944995 | 76.357376 | | 705.944995 | 70.840765 | | 705.944995 | 88.864142 |
| 709.802618 | 76.081096 | | 709.802618 | 70.466265 | | 709.802618 | 88.843364 |
| 713.660241 | 76.099947 | | 713.660241 | 70.455209 | | 713.660241 | 89.013894 |
| 717.517864 | 76.144453 | | 717.517864 | 70.51183 | | 717.517864 | 89.164904 |
| 721.375487 | 76.247974 | | 721.375487 | 70.64156 | | 721.375487 | 89.392905 |
| 725.23311 | 76.446583 | | 725.23311 | 70.835512 | | 725.23311 | 89.736288 |
| 729.090733 | 76.679637 | | 729.090733 | 71.041124 | | 729.090733 | 90.079603 |
| 732.948356 | 76.887763 | | 732.948356 | 71.236973 | | 732.948356 | 90.358116 |
| 736.805979 | 77.072039 | | 736.805979 | 71.434373 | | 736.805979 | 90.535445 |
| 740.663602 | 77.241105 | | 740.663602 | 71.628588 | | 740.663602 | 90.539587 |
| 744.521224 | 77.490136 | | 744.521224 | 71.914813 | | 744.521224 | 90.483505 |
| 748.378847 | 77.769819 | | 748.378847 | 72.239153 | | 748.378847 | 90.496407 |
| 752.23647 | 78.068034 | | 752.23647 | 72.606491 | | 752.23647 | 90.595896 |
| 756.094093 | 78.400185 | | 756.094093 | 73.019807 | | 756.094093 | 90.765109 |
| 759.951716 | 78.75 | | 759.951716 | 73.466629 | | 759.951716 | 91.082043 |
| 763.809339 | 79.074123 | | 763.809339 | 73.900711 | | 763.809339 | 91.565114 |
| 767.666962 | 79.38794 | | 767.666962 | 74.314602 | | 767.666962 | 92.091533 |
| 771.524585 | 79.740635 | | 771.524585 | 74.746828 | | 771.524585 | 92.531619 |
| 775.382208 | 80.116261 | | 775.382208 | 75.180775 | | 775.382208 | 92.833189 |
| 779.239831 | 80.465645 | | 779.239831 | 75.57081 | | 779.239831 | 93.020697 |
| 783.097454 | 80.818481 | | 783.097454 | 75.977886 | | 783.097454 | 93.190111 |
| 786.955077 | 81.193314 | | 786.955077 | 76.45951 | | 786.955077 | 93.401013 |
| 790.8127 | 81.593104 | | 790.8127 | 77.004282 | | 790.8127 | 93.651289 |
| 794.670323 | 82.029402 | | 794.670323 | 77.572884 | | 794.670323 | 93.914243 |
| 798.527945 | 82.481735 | | 798.527945 | 78.136501 | | 798.527945 | 94.158479 |
| 802.385568 | 82.945167 | | 802.385568 | 78.719089 | | 802.385568 | 94.390548 |
| 806.243191 | 83.422842 | | 806.243191 | 79.340638 | | 806.243191 | 94.641164 |
| 810.100814 | 83.900752 | | 810.100814 | 79.969119 | | 810.100814 | 94.905755 |
| 813.958437 | 84.368045 | | 813.958437 | 80.582752 | | 813.958437 | 95.150075 |
| 817.81606 | 84.831023 | | 817.81606 | 81.195112 | | 817.81606 | 95.36558 |
| 821.673683 | 85.295778 | | 821.673683 | 81.809085 | | 821.673683 | 95.530895 |
| 825.531306 | 85.753575 | | 825.531306 | 82.427629 | | 825.531306 | 95.596827 |
| 829.388929 | 86.185297 | | 829.388929 | 83.041792 | | 829.388929 | 95.543255 |

Table B-1.—FTIR data of the CA versus CA-GMA membranes presented on figure 10 and CA versus CA-GMA-IDA presented on figure 11

| CA | | | CA-GMA | | | CA-GMA-IDA | |
|---|---|---|---|---|---|---|---|
| 833.246552 | 86.610498 | | 833.246552 | 83.654408 | | 833.246552 | 95.433564 |
| 837.104175 | 87.078257 | | 837.104175 | 84.294391 | | 837.104175 | 95.429708 |
| 840.961798 | 87.619971 | | 840.961798 | 84.988168 | | 840.961798 | 95.673617 |
| 844.819421 | 88.224941 | | 844.819421 | 85.732164 | | 844.819421 | 96.175175 |
| 848.677043 | 88.857619 | | 848.677043 | 86.514036 | | 848.677043 | 96.846426 |
| 852.534666 | 89.449197 | | 852.534666 | 87.288902 | | 852.534666 | 97.514194 |
| 856.392289 | 89.924483 | | 856.392289 | 87.984532 | | 856.392289 | 98.006433 |
| 860.249912 | 90.259594 | | 860.249912 | 88.572001 | | 860.249912 | 98.258882 |
| 864.107535 | 90.509628 | | 864.107535 | 89.112163 | | 864.107535 | 98.285646 |
| 867.965158 | 90.700078 | | 867.965158 | 89.648085 | | 867.965158 | 98.102087 |
| 871.822781 | 90.812511 | | 871.822781 | 90.158109 | | 871.822781 | 97.75516 |
| 875.680404 | 90.918634 | | 875.680404 | 90.632453 | | 875.680404 | 97.425877 |
| 879.538027 | 91.143277 | | 879.538027 | 91.115559 | | 879.538027 | 97.291292 |
| 883.39565 | 91.459343 | | 883.39565 | 91.621522 | | 883.39565 | 97.23215 |
| 887.253273 | 91.699081 | | 887.253273 | 92.096342 | | 887.253273 | 96.921821 |
| 891.110896 | 91.725506 | | 891.110896 | 92.478371 | | 891.110896 | 96.08641 |
| 894.968519 | 91.497816 | | 894.968519 | 92.735433 | | 894.968519 | 94.685405 |
| 898.826141 | 91.175798 | | 898.826141 | 92.910178 | | 898.826141 | 93.24269 |
| 902.683764 | 91.090636 | | 902.683764 | 93.126947 | | 902.683764 | 92.591349 |
| 906.541387 | 91.411323 | | 906.541387 | 93.48736 | | 906.541387 | 93.074492 |
| 910.39901 | 92.037481 | | 910.39901 | 93.994583 | | 910.39901 | 94.407641 |
| 914.256633 | 92.763069 | | 914.256633 | 94.556746 | | 914.256633 | 96.010815 |
| 918.114256 | 93.423172 | | 918.114256 | 95.073054 | | 918.114256 | 97.339931 |
| 921.971879 | 93.985196 | | 921.971879 | 95.505873 | | 921.971879 | 98.252198 |
| 925.829502 | 94.487237 | | 925.829502 | 95.872277 | | 925.829502 | 98.891151 |
| 929.687125 | 94.930851 | | 929.687125 | 96.188095 | | 929.687125 | 99.321635 |
| 933.544748 | 95.278468 | | 933.544748 | 96.431269 | | 933.544748 | 99.504079 |
| 937.402371 | 95.502091 | | 937.402371 | 96.59415 | | 937.402371 | 99.415909 |
| 941.259994 | 95.593091 | | 941.259994 | 96.693701 | | 941.259994 | 99.073723 |
| 945.117617 | 95.543731 | | 945.117617 | 96.729774 | | 945.117617 | 98.498659 |
| 948.97524 | 95.387035 | | 948.97524 | 96.704209 | | 948.97524 | 97.792151 |
| 952.832862 | 95.232275 | | 952.832862 | 96.647435 | | 952.832862 | 97.222309 |
| 956.690485 | 95.204956 | | 956.690485 | 96.611761 | | 956.690485 | 96.985519 |
| 960.548108 | 95.292104 | | 960.548108 | 96.60743 | | 960.548108 | 96.892137 |
| 964.405731 | 95.285834 | | 964.405731 | 96.563723 | | 964.405731 | 96.522594 |
| 968.263354 | 95.00867 | | 968.263354 | 96.423659 | | 968.263354 | 95.664191 |
| 972.120977 | 94.48937 | | 972.120977 | 96.207281 | | 972.120977 | 94.417675 |
| 975.9786 | 93.866275 | | 975.9786 | 95.953191 | | 975.9786 | 92.98986 |
| 979.836223 | 93.24027 | | 979.836223 | 95.682603 | | 979.836223 | 91.528991 |
| 983.693846 | 92.637388 | | 983.693846 | 95.41943 | | 983.693846 | 90.118755 |

Table B-1.—FTIR data of the CA versus CA-GMA membranes presented on figure 10 and CA versus CA-GMA-IDA presented on figure 11

| CA | | | CA-GMA | | | CA-GMA-IDA | |
|---|---|---|---|---|---|---|---|
| 987.551469 | 92.094813 | | 987.551469 | 95.195248 | | 987.551469 | 88.865642 |
| 991.409092 | 91.702261 | | 991.409092 | 95.04895 | | 991.409092 | 87.898681 |
| 995.266715 | 91.42932 | | 995.266715 | 94.994361 | | 995.266715 | 87.144169 |
| 999.124338 | 91.024705 | | 999.124338 | 94.946828 | | 999.124338 | 86.194771 |
| 1002.98196 | 90.274693 | | 1002.98196 | 94.795292 | | 1002.98196 | 84.634666 |
| 1006.839583 | 89.140029 | | 1006.839583 | 94.496688 | | 1006.839583 | 82.306342 |
| 1010.697206 | 87.554422 | | 1010.697206 | 94.004646 | | 1010.697206 | 79.17367 |
| 1014.554829 | 85.406856 | | 1014.554829 | 93.273077 | | 1014.554829 | 75.276205 |
| 1018.412452 | 82.623516 | | 1018.412452 | 92.274345 | | 1018.412452 | 70.792993 |
| 1022.270075 | 79.211873 | | 1022.270075 | 90.955311 | | 1022.270075 | 66.02138 |
| 1026.127698 | 75.337014 | | 1026.127698 | 89.299695 | | 1026.127698 | 61.349765 |
| 1029.985321 | 71.448292 | | 1029.985321 | 87.444124 | | 1029.985321 | 57.446549 |
| 1033.842944 | 68.466069 | | 1033.842944 | 85.817198 | | 1033.842944 | 55.172103 |
| 1037.700567 | 67.057215 | | 1037.700567 | 84.860534 | | 1037.700567 | 54.70867 |
| 1041.55819 | 66.775418 | | 1041.55819 | 84.468419 | | 1041.55819 | 55.326026 |
| 1045.415813 | 66.874464 | | 1045.415813 | 84.199284 | | 1045.415813 | 56.455685 |
| 1049.273436 | 67.337073 | | 1049.273436 | 83.944822 | | 1049.273436 | 58.175174 |
| 1053.131058 | 68.604625 | | 1053.131058 | 84.015841 | | 1053.131058 | 60.658958 |
| 1056.988681 | 70.798341 | | 1056.988681 | 84.682913 | | 1056.988681 | 63.75659 |
| 1060.846304 | 73.308506 | | 1060.846304 | 85.770709 | | 1060.846304 | 66.822109 |
| 1064.703927 | 75.435105 | | 1064.703927 | 86.85297 | | 1064.703927 | 69.282935 |
| 1068.56155 | 77.203421 | | 1068.56155 | 87.807924 | | 1068.56155 | 71.254194 |
| 1072.419173 | 78.999895 | | 1072.419173 | 88.794742 | | 1072.419173 | 73.211067 |
| 1076.276796 | 80.899606 | | 1076.276796 | 89.85152 | | 1076.276796 | 75.321718 |
| 1080.134419 | 82.762943 | | 1080.134419 | 90.885693 | | 1080.134419 | 77.49377 |
| 1083.992042 | 84.548171 | | 1083.992042 | 91.85944 | | 1083.992042 | 79.699014 |
| 1087.849665 | 86.330015 | | 1087.849665 | 92.804619 | | 1087.849665 | 81.984169 |
| 1091.707288 | 88.090781 | | 1091.707288 | 93.722531 | | 1091.707288 | 84.264055 |
| 1095.564911 | 89.682293 | | 1095.564911 | 94.558657 | | 1095.564911 | 86.313871 |
| 1099.422534 | 90.900301 | | 1099.422534 | 95.210111 | | 1099.422534 | 87.870009 |
| 1103.280156 | 91.6404 | | 1103.280156 | 95.613089 | | 1103.280156 | 88.791519 |
| 1107.137779 | 91.990356 | | 1107.137779 | 95.819918 | | 1107.137779 | 89.159333 |
| 1110.995402 | 92.123478 | | 1110.995402 | 95.932639 | | 1110.995402 | 89.188378 |
| 1114.853025 | 92.147272 | | 1114.853025 | 96.000709 | | 1114.853025 | 89.049917 |
| 1118.710648 | 92.10078 | | 1118.710648 | 96.015563 | | 1118.710648 | 88.855689 |
| 1122.568271 | 92.055665 | | 1122.568271 | 95.969415 | | 1122.568271 | 88.743917 |
| 1126.425894 | 92.180873 | | 1126.425894 | 95.927842 | | 1126.425894 | 88.885945 |
| 1130.283517 | 92.606314 | | 1130.283517 | 95.992788 | | 1130.283517 | 89.365688 |
| 1134.14114 | 93.223708 | | 1134.14114 | 96.165015 | | 1134.14114 | 90.022247 |
| 1137.998763 | 93.785381 | | 1137.998763 | 96.346221 | | 1137.998763 | 90.52607 |

Table B-1.—FTIR data of the CA versus CA-GMA membranes presented on figure 10 and CA versus CA-GMA-IDA presented on figure 11

| CA | | | CA-GMA | | | CA-GMA-IDA | |
|---|---|---|---|---|---|---|---|
| 1141.856386 | 94.076551 | | 1141.856386 | 96.409275 | | 1141.856386 | 90.561522 |
| 1145.714009 | 93.903319 | | 1145.714009 | 96.218525 | | 1145.714009 | 89.944033 |
| 1149.571632 | 93.239879 | | 1149.571632 | 95.777728 | | 1149.571632 | 88.905223 |
| 1153.429255 | 92.386329 | | 1153.429255 | 95.305259 | | 1153.429255 | 88.00742 |
| 1157.286877 | 91.792639 | | 1157.286877 | 95.044603 | | 1157.286877 | 87.565027 |
| 1161.1445 | 91.741263 | | 1161.1445 | 95.075839 | | 1161.1445 | 87.545664 |
| 1165.002123 | 92.1751 | | 1165.002123 | 95.303061 | | 1165.002123 | 87.859078 |
| 1168.859746 | 92.842162 | | 1168.859746 | 95.599691 | | 1168.859746 | 88.442435 |
| 1172.717369 | 93.574991 | | 1172.717369 | 95.92971 | | 1172.717369 | 89.286032 |
| 1176.574992 | 94.340899 | | 1176.574992 | 96.299399 | | 1176.574992 | 90.356954 |
| 1180.432615 | 95.063065 | | 1180.432615 | 96.6699 | | 1180.432615 | 91.421766 |
| 1184.290238 | 95.552058 | | 1184.290238 | 96.953013 | | 1184.290238 | 92.124498 |
| 1188.147861 | 95.615604 | | 1188.147861 | 97.068574 | | 1188.147861 | 92.120109 |
| 1192.005484 | 95.142687 | | 1192.005484 | 96.978779 | | 1192.005484 | 91.119654 |
| 1195.863107 | 94.033379 | | 1195.863107 | 96.652637 | | 1195.863107 | 88.877008 |
| 1199.72073 | 92.110661 | | 1199.72073 | 96.032763 | | 1199.72073 | 85.116762 |
| 1203.578353 | 89.145082 | | 1203.578353 | 95.01481 | | 1203.578353 | 79.65801 |
| 1207.435975 | 85.085935 | | 1207.435975 | 93.507365 | | 1207.435975 | 72.989466 |
| 1211.293598 | 80.334924 | | 1211.293598 | 91.568331 | | 1211.293598 | 66.452793 |
| 1215.151221 | 75.707271 | | 1215.151221 | 89.45344 | | 1215.151221 | 61.389306 |
| 1219.008844 | 71.961261 | | 1219.008844 | 87.490354 | | 1219.008844 | 58.236172 |
| 1222.866467 | 69.341842 | | 1222.866467 | 85.88058 | | 1222.866467 | 56.597248 |
| 1226.72409 | 67.608983 | | 1226.72409 | 84.587498 | | 1226.72409 | 55.92478 |
| 1230.581713 | 66.511397 | | 1230.581713 | 83.477583 | | 1230.581713 | 56.06947 |
| 1234.439336 | 66.094941 | | 1234.439336 | 82.553329 | | 1234.439336 | 57.221252 |
| 1238.296959 | 66.519521 | | 1238.296959 | 81.960593 | | 1238.296959 | 59.423364 |
| 1242.154582 | 67.789458 | | 1242.154582 | 81.824665 | | 1242.154582 | 62.422341 |
| 1246.012205 | 69.71479 | | 1246.012205 | 82.160964 | | 1246.012205 | 65.836724 |
| 1249.869828 | 72.085654 | | 1249.869828 | 82.906029 | | 1249.869828 | 69.429972 |
| 1253.727451 | 74.785664 | | 1253.727451 | 84.006743 | | 1253.727451 | 73.107838 |
| 1257.585073 | 77.685876 | | 1257.585073 | 85.421033 | | 1257.585073 | 76.73203 |
| 1261.442696 | 80.652677 | | 1261.442696 | 87.076722 | | 1261.442696 | 80.1957 |
| 1265.300319 | 83.555623 | | 1265.300319 | 88.833872 | | 1265.300319 | 83.46603 |
| 1269.157942 | 86.287476 | | 1269.157942 | 90.562054 | | 1269.157942 | 86.516716 |
| 1273.015565 | 88.885504 | | 1273.015565 | 92.250696 | | 1273.015565 | 89.354678 |
| 1276.873188 | 91.258088 | | 1276.873188 | 93.789019 | | 1276.873188 | 91.853084 |
| 1280.730811 | 93.222979 | | 1280.730811 | 95.033865 | | 1280.730811 | 93.888156 |
| 1284.588434 | 94.785668 | | 1284.588434 | 96.025891 | | 1284.588434 | 95.530412 |
| 1288.446057 | 96.006172 | | 1288.446057 | 96.812115 | | 1288.446057 | 96.847608 |
| 1292.30368 | 96.929896 | | 1292.30368 | 97.401468 | | 1292.30368 | 97.887607 |

Table B-1.—FTIR data of the CA versus CA-GMA membranes presented on figure 10 and CA versus CA-GMA-IDA presented on figure 11

| CA | | | CA-GMA | | | CA-GMA-IDA | |
|---|---|---|---|---|---|---|---|
| 1296.161303 | 97.645222 | | 1296.161303 | 97.850878 | | 1296.161303 | 98.730604 |
| 1300.018926 | 98.191517 | | 1300.018926 | 98.191985 | | 1300.018926 | 99.380473 |
| 1303.876549 | 98.535358 | | 1303.876549 | 98.418626 | | 1303.876549 | 99.790995 |
| 1307.734172 | 98.660631 | | 1307.734172 | 98.528233 | | 1307.734172 | 99.949826 |
| 1311.591794 | 98.627922 | | 1311.591794 | 98.545605 | | 1311.591794 | 99.917977 |
| 1315.449417 | 98.531929 | | 1315.449417 | 98.514986 | | 1315.449417 | 99.822851 |
| 1319.30704 | 98.460117 | | 1319.30704 | 98.48067 | | 1319.30704 | 99.787912 |
| 1323.164663 | 98.478357 | | 1323.164663 | 98.479977 | | 1323.164663 | 99.862945 |
| 1327.022286 | 98.604623 | | 1327.022286 | 98.529494 | | 1327.022286 | 100.019862 |
| 1330.879909 | 98.807576 | | 1330.879909 | 98.620867 | | 1330.879909 | 100.208518 |
| 1334.737532 | 99.033307 | | 1334.737532 | 98.733998 | | 1334.737532 | 100.391358 |
| 1338.595155 | 99.207911 | | 1338.595155 | 98.837483 | | 1338.595155 | 100.508654 |
| 1342.452778 | 99.256049 | | 1342.452778 | 98.896522 | | 1342.452778 | 100.491354 |
| 1346.310401 | 99.122891 | | 1346.310401 | 98.887729 | | 1346.310401 | 100.249769 |
| 1350.168024 | 98.6806 | | 1350.168024 | 98.747725 | | 1350.168024 | 99.513757 |
| 1354.025647 | 97.637499 | | 1354.025647 | 98.332322 | | 1354.025647 | 97.744226 |
| 1357.88327 | 95.659071 | | 1357.88327 | 97.47805 | | 1357.88327 | 94.498083 |
| 1361.740892 | 92.863972 | | 1361.740892 | 96.189789 | | 1361.740892 | 90.329203 |
| 1365.598515 | 90.24742 | | 1365.598515 | 94.865658 | | 1365.598515 | 86.984171 |
| 1369.456138 | 88.922611 | | 1369.456138 | 94.06649 | | 1369.456138 | 85.801933 |
| 1373.313761 | 88.998763 | | 1373.313761 | 93.956611 | | 1373.313761 | 86.504785 |
| 1377.171384 | 89.851013 | | 1377.171384 | 94.278846 | | 1377.171384 | 88.110902 |
| 1381.029007 | 91.105232 | | 1381.029007 | 94.830669 | | 1381.029007 | 90.138948 |
| 1384.88663 | 92.841412 | | 1384.88663 | 95.661989 | | 1384.88663 | 92.619186 |
| 1388.744253 | 94.920869 | | 1388.744253 | 96.72402 | | 1388.744253 | 95.341601 |
| 1392.601876 | 96.838956 | | 1392.601876 | 97.743385 | | 1392.601876 | 97.752591 |
| 1396.459499 | 98.240427 | | 1396.459499 | 98.50804 | | 1396.459499 | 99.454711 |
| 1400.317122 | 99.04053 | | 1400.317122 | 98.964054 | | 1400.317122 | 100.365497 |
| 1404.174745 | 99.36071 | | 1404.174745 | 99.183335 | | 1404.174745 | 100.695079 |
| 1408.032368 | 99.418926 | | 1408.032368 | 99.283277 | | 1408.032368 | 100.738146 |
| 1411.88999 | 99.350395 | | 1411.88999 | 99.32764 | | 1411.88999 | 100.639417 |
| 1415.747613 | 99.195861 | | 1415.747613 | 99.331343 | | 1415.747613 | 100.427908 |
| 1419.605236 | 98.951642 | | 1419.605236 | 99.266893 | | 1419.605236 | 100.087952 |
| 1423.462859 | 98.635901 | | 1423.462859 | 99.121542 | | 1423.462859 | 99.628214 |
| 1427.320482 | 98.32489 | | 1427.320482 | 98.946019 | | 1427.320482 | 99.14921 |
| 1431.178105 | 98.128133 | | 1431.178105 | 98.809765 | | 1431.178105 | 98.812459 |
| 1435.035728 | 98.140793 | | 1435.035728 | 98.772499 | | 1435.035728 | 98.762384 |
| 1438.893351 | 98.368515 | | 1438.893351 | 98.845004 | | 1438.893351 | 99.020546 |
| 1442.750974 | 98.719377 | | 1442.750974 | 98.988428 | | 1442.750974 | 99.467364 |
| 1446.608597 | 99.082102 | | 1446.608597 | 99.156703 | | 1446.608597 | 99.967209 |

Table B-1.—FTIR data of the CA versus CA-GMA membranes presented on figure 10 and CA versus CA-GMA-IDA presented on figure 11

| CA | | | CA-GMA | | | CA-GMA-IDA | |
|---|---|---|---|---|---|---|---|
| 1450.46622 | 99.370032 | | 1450.46622 | 99.297645 | | 1450.46622 | 100.425197 |
| 1454.323843 | 99.574968 | | 1454.323843 | 99.39612 | | 1454.323843 | 100.840189 |
| 1458.181466 | 99.772355 | | 1458.181466 | 99.478457 | | 1458.181466 | 101.27541 |
| 1462.039089 | 100.02409 | | 1462.039089 | 99.561255 | | 1462.039089 | 101.72335 |
| 1465.896711 | 100.33541 | | 1465.896711 | 99.664386 | | 1465.896711 | 102.183804 |
| 1469.754334 | 100.663903 | | 1469.754334 | 99.790748 | | 1469.754334 | 102.682436 |
| 1473.611957 | 100.935166 | | 1473.611957 | 99.884614 | | 1473.611957 | 103.153579 |
| 1477.46958 | 101.086794 | | 1477.46958 | 99.87784 | | 1477.46958 | 103.449097 |
| 1481.327203 | 101.123545 | | 1481.327203 | 99.780804 | | 1481.327203 | 103.521023 |
| 1485.184826 | 101.092994 | | 1485.184826 | 99.653459 | | 1485.184826 | 103.480817 |
| 1489.042449 | 101.025655 | | 1489.042449 | 99.540795 | | 1489.042449 | 103.440786 |
| 1492.900072 | 100.953365 | | 1492.900072 | 99.472784 | | 1492.900072 | 103.434689 |
| 1496.757695 | 100.892886 | | 1496.757695 | 99.428167 | | 1496.757695 | 103.404144 |
| 1500.615318 | 100.847711 | | 1500.615318 | 99.380131 | | 1500.615318 | 103.293241 |
| 1504.472941 | 100.822928 | | 1504.472941 | 99.346877 | | 1504.472941 | 103.110426 |
| 1508.330564 | 100.797249 | | 1508.330564 | 99.31156 | | 1508.330564 | 102.838853 |
| 1512.188187 | 100.764172 | | 1512.188187 | 99.256615 | | 1512.188187 | 102.49715 |
| 1516.045809 | 100.746743 | | 1516.045809 | 99.218521 | | 1516.045809 | 102.20511 |
| 1519.903432 | 100.73952 | | 1519.903432 | 99.194874 | | 1519.903432 | 102.038711 |
| 1523.761055 | 100.72215 | | 1523.761055 | 99.156893 | | 1523.761055 | 101.926257 |
| 1527.618678 | 100.696579 | | 1527.618678 | 99.11409 | | 1527.618678 | 101.779311 |
| 1531.476301 | 100.677238 | | 1531.476301 | 99.081846 | | 1531.476301 | 101.618575 |
| 1535.333924 | 100.671429 | | 1535.333924 | 99.068586 | | 1535.333924 | 101.489442 |
| 1539.191547 | 100.674578 | | 1539.191547 | 99.068242 | | 1539.191547 | 101.401163 |
| 1543.04917 | 100.679484 | | 1543.04917 | 99.04999 | | 1543.04917 | 101.347968 |
| 1546.906793 | 100.698215 | | 1546.906793 | 99.023634 | | 1546.906793 | 101.379331 |
| 1550.764416 | 100.747199 | | 1550.764416 | 99.027854 | | 1550.764416 | 101.586785 |
| 1554.622039 | 100.8261 | | 1554.622039 | 99.072235 | | 1554.622039 | 102.001866 |
| 1558.479662 | 100.927368 | | 1558.479662 | 99.140694 | | 1558.479662 | 102.580583 |
| 1562.337285 | 101.031051 | | 1562.337285 | 99.19655 | | 1562.337285 | 103.184986 |
| 1566.194907 | 101.143748 | | 1566.194907 | 99.248236 | | 1566.194907 | 103.735295 |
| 1570.05253 | 101.261712 | | 1570.05253 | 99.306513 | | 1570.05253 | 104.237484 |
| 1573.910153 | 101.337964 | | 1573.910153 | 99.325767 | | 1573.910153 | 104.63795 |
| 1577.767776 | 101.342081 | | 1577.767776 | 99.263535 | | 1577.767776 | 104.92052 |
| 1581.625399 | 101.250828 | | 1581.625399 | 99.100061 | | 1581.625399 | 105.078868 |
| 1585.483022 | 101.060814 | | 1585.483022 | 98.841378 | | 1585.483022 | 105.10067 |
| 1589.340645 | 100.753787 | | 1589.340645 | 98.461287 | | 1589.340645 | 104.955524 |
| 1593.198268 | 100.320427 | | 1593.198268 | 97.950346 | | 1593.198268 | 104.631575 |
| 1597.055891 | 99.767913 | | 1597.055891 | 97.321579 | | 1597.055891 | 104.153407 |
| 1600.913514 | 99.094882 | | 1600.913514 | 96.578781 | | 1600.913514 | 103.520198 |

Table B-1.—FTIR data of the CA versus CA-GMA membranes presented on figure 10 and CA versus CA-GMA-IDA presented on figure 11

| CA | | | CA-GMA | | | CA-GMA-IDA | |
|---|---|---|---|---|---|---|---|
| 1604.771137 | 98.303897 | | 1604.771137 | 95.728621 | | 1604.771137 | 102.732665 |
| 1608.62876 | 97.394625 | | 1608.62876 | 94.766913 | | 1608.62876 | 101.77259 |
| 1612.486383 | 96.415428 | | 1612.486383 | 93.74623 | | 1612.486383 | 100.687492 |
| 1616.344005 | 95.384574 | | 1616.344005 | 92.684034 | | 1616.344005 | 99.528357 |
| 1620.201628 | 94.358285 | | 1620.201628 | 91.621291 | | 1620.201628 | 98.380893 |
| 1624.059251 | 93.405538 | | 1624.059251 | 90.628511 | | 1624.059251 | 97.323603 |
| 1627.916874 | 92.55619 | | 1627.916874 | 89.743049 | | 1627.916874 | 96.377056 |
| 1631.774497 | 91.878848 | | 1631.774497 | 89.032594 | | 1631.774497 | 95.598978 |
| 1635.63212 | 91.38347 | | 1635.63212 | 88.511191 | | 1635.63212 | 94.962774 |
| 1639.489743 | 91.071387 | | 1639.489743 | 88.184332 | | 1639.489743 | 94.44493 |
| 1643.347366 | 90.954304 | | 1643.347366 | 88.071976 | | 1643.347366 | 94.05715 |
| 1647.204989 | 91.029484 | | 1647.204989 | 88.175313 | | 1647.204989 | 93.847424 |
| 1651.062612 | 91.278969 | | 1651.062612 | 88.470242 | | 1651.062612 | 93.943849 |
| 1654.920235 | 91.659249 | | 1654.920235 | 88.904888 | | 1654.920235 | 94.403404 |
| 1658.777858 | 92.117041 | | 1658.777858 | 89.42204 | | 1658.777858 | 95.104215 |
| 1662.635481 | 92.645345 | | 1662.635481 | 90.030215 | | 1662.635481 | 95.890153 |
| 1666.493104 | 93.212078 | | 1666.493104 | 90.701837 | | 1666.493104 | 96.628151 |
| 1670.350726 | 93.74795 | | 1670.350726 | 91.361517 | | 1670.350726 | 97.223528 |
| 1674.208349 | 94.235178 | | 1674.208349 | 91.990763 | | 1674.208349 | 97.676502 |
| 1678.065972 | 94.641193 | | 1678.065972 | 92.56195 | | 1678.065972 | 97.979285 |
| 1681.923595 | 94.972155 | | 1681.923595 | 93.100122 | | 1681.923595 | 98.170556 |
| 1685.781218 | 95.222871 | | 1685.781218 | 93.598123 | | 1685.781218 | 98.236516 |
| 1689.638841 | 95.345681 | | 1689.638841 | 94.001284 | | 1689.638841 | 98.107309 |
| 1693.496464 | 95.355844 | | 1693.496464 | 94.346549 | | 1693.496464 | 97.792585 |
| 1697.354087 | 95.192284 | | 1697.354087 | 94.610766 | | 1697.354087 | 97.176771 |
| 1701.21171 | 94.732362 | | 1701.21171 | 94.702271 | | 1701.21171 | 96.065802 |
| 1705.069333 | 93.869268 | | 1705.069333 | 94.573264 | | 1705.069333 | 94.271278 |
| 1708.926956 | 92.472406 | | 1708.926956 | 94.183049 | | 1708.926956 | 91.590997 |
| 1712.784579 | 90.452234 | | 1712.784579 | 93.493933 | | 1712.784579 | 87.968475 |
| 1716.642202 | 87.771401 | | 1716.642202 | 92.45864 | | 1716.642202 | 83.478344 |
| 1720.499824 | 84.689205 | | 1720.499824 | 91.133172 | | 1720.499824 | 78.68329 |
| 1724.357447 | 81.747515 | | 1724.357447 | 89.742897 | | 1724.357447 | 74.506629 |
| 1728.21507 | 79.411496 | | 1728.21507 | 88.54901 | | 1728.21507 | 71.568745 |
| 1732.072693 | 77.970007 | | 1732.072693 | 87.749425 | | 1732.072693 | 70.087702 |
| 1735.930316 | 77.466445 | | 1735.930316 | 87.404308 | | 1735.930316 | 69.907573 |
| 1739.787939 | 77.773169 | | 1739.787939 | 87.469807 | | 1739.787939 | 70.710167 |
| 1743.645562 | 78.669251 | | 1743.645562 | 87.840192 | | 1743.645562 | 72.17078 |
| 1747.503185 | 79.965778 | | 1747.503185 | 88.391771 | | 1747.503185 | 74.074257 |
| 1751.360808 | 81.799899 | | 1751.360808 | 89.192082 | | 1751.360808 | 76.595063 |
| 1755.218431 | 84.56715 | | 1755.218431 | 90.577632 | | 1755.218431 | 80.168506 |

Table B-1.—FTIR data of the CA versus CA-GMA membranes presented on figure 10 and CA versus CA-GMA-IDA presented on figure 11

| CA | | | CA-GMA | | | CA-GMA-IDA | |
|---|---|---|---|---|---|---|---|
| 1759.076054 | 88.401249 | | 1759.076054 | 92.778783 | | 1759.076054 | 84.974798 |
| 1762.933677 | 92.692585 | | 1762.933677 | 95.420231 | | 1762.933677 | 90.466618 |
| 1766.7913 | 96.264742 | | 1766.7913 | 97.657431 | | 1766.7913 | 95.348245 |
| 1770.648922 | 98.582402 | | 1770.648922 | 99.100452 | | 1770.648922 | 98.820265 |
| 1774.506545 | 99.903229 | | 1774.506545 | 99.912912 | | 1774.506545 | 100.964382 |
| 1778.364168 | 100.63916 | | 1778.364168 | 100.362703 | | 1778.364168 | 102.211355 |
| 1782.221791 | 101.09099 | | 1782.221791 | 100.645412 | | 1782.221791 | 102.985266 |
| 1786.079414 | 101.383922 | | 1786.079414 | 100.836311 | | 1786.079414 | 103.48611 |
| 1789.937037 | 101.59664 | | 1789.937037 | 100.982264 | | 1789.937037 | 103.835132 |
| 1793.79466 | 101.765094 | | 1793.79466 | 101.100247 | | 1793.79466 | 104.090793 |
| 1797.652283 | 101.899943 | | 1797.652283 | 101.191983 | | 1797.652283 | 104.283953 |
| 1801.509906 | 102.019916 | | 1801.509906 | 101.272975 | | 1801.509906 | 104.451355 |
| 1805.367529 | 102.132822 | | 1805.367529 | 101.35104 | | 1805.367529 | 104.604341 |
| 1809.225152 | 102.24503 | | 1809.225152 | 101.430321 | | 1809.225152 | 104.751539 |
| 1813.082775 | 102.354224 | | 1813.082775 | 101.50565 | | 1813.082775 | 104.889853 |
| 1816.940398 | 102.455318 | | 1816.940398 | 101.577217 | | 1816.940398 | 105.01719 |
| 1820.798021 | 102.546647 | | 1820.798021 | 101.644946 | | 1820.798021 | 105.130883 |
| 1824.655643 | 102.631595 | | 1824.655643 | 101.705068 | | 1824.655643 | 105.231503 |
| 1828.513266 | 102.708727 | | 1828.513266 | 101.761007 | | 1828.513266 | 105.321702 |
| 1832.370889 | 102.772597 | | 1832.370889 | 101.808007 | | 1832.370889 | 105.393628 |
| 1836.228512 | 102.820345 | | 1836.228512 | 101.842634 | | 1836.228512 | 105.442976 |
| 1840.086135 | 102.856951 | | 1840.086135 | 101.874811 | | 1840.086135 | 105.482446 |
| 1843.943758 | 102.89039 | | 1843.943758 | 101.905191 | | 1843.943758 | 105.517443 |
| 1847.801381 | 102.915309 | | 1847.801381 | 101.927015 | | 1847.801381 | 105.537695 |
| 1851.659004 | 102.933568 | | 1851.659004 | 101.945607 | | 1851.659004 | 105.555117 |
| 1855.516627 | 102.951553 | | 1855.516627 | 101.964162 | | 1855.516627 | 105.576578 |
| 1859.37425 | 102.97092 | | 1859.37425 | 101.980567 | | 1859.37425 | 105.594542 |
| 1863.231873 | 102.991144 | | 1863.231873 | 101.996157 | | 1863.231873 | 105.61135 |
| 1867.089496 | 103.008002 | | 1867.089496 | 102.012484 | | 1867.089496 | 105.629134 |
| 1870.947119 | 103.021892 | | 1870.947119 | 102.026783 | | 1870.947119 | 105.644222 |
| 1874.804741 | 103.035691 | | 1874.804741 | 102.03834 | | 1874.804741 | 105.656677 |
| 1878.662364 | 103.051657 | | 1878.662364 | 102.051122 | | 1878.662364 | 105.673116 |
| 1882.519987 | 103.06717 | | 1882.519987 | 102.063288 | | 1882.519987 | 105.689807 |
| 1886.37761 | 103.076953 | | 1886.37761 | 102.070702 | | 1886.37761 | 105.699858 |
| 1890.235233 | 103.081007 | | 1890.235233 | 102.072964 | | 1890.235233 | 105.703315 |
| 1894.092856 | 103.083999 | | 1894.092856 | 102.076487 | | 1894.092856 | 105.7047 |
| 1897.950479 | 103.083482 | | 1897.950479 | 102.081196 | | 1897.950479 | 105.702426 |
| 1901.808102 | 103.076163 | | 1901.808102 | 102.079927 | | 1901.808102 | 105.693811 |
| 1905.665725 | 103.068587 | | 1905.665725 | 102.076331 | | 1905.665725 | 105.6869 |
| 1909.523348 | 103.060857 | | 1909.523348 | 102.071969 | | 1909.523348 | 105.679455 |

Table B-1.—FTIR data of the CA versus CA-GMA membranes presented on figure 10 and CA versus CA-GMA-IDA presented on figure 11

| CA | | | CA-GMA | | | CA-GMA-IDA | |
|---|---|---|---|---|---|---|---|
| 1913.380971 | 103.05135 | | 1913.380971 | 102.065977 | | 1913.380971 | 105.670685 |
| 1917.238594 | 103.043933 | | 1917.238594 | 102.06163 | | 1917.238594 | 105.664135 |
| 1921.096217 | 103.038431 | | 1921.096217 | 102.058226 | | 1921.096217 | 105.657628 |
| 1924.953839 | 103.0313 | | 1924.953839 | 102.052423 | | 1924.953839 | 105.653564 |
| 1928.811462 | 103.024302 | | 1928.811462 | 102.04459 | | 1928.811462 | 105.651841 |
| 1932.669085 | 103.0213 | | 1932.669085 | 102.038117 | | 1932.669085 | 105.650642 |
| 1936.526708 | 103.019213 | | 1936.526708 | 102.031474 | | 1936.526708 | 105.648881 |
| 1940.384331 | 103.015619 | | 1940.384331 | 102.023666 | | 1940.384331 | 105.647998 |
| 1944.241954 | 103.008598 | | 1944.241954 | 102.015561 | | 1944.241954 | 105.648303 |
| 1948.099577 | 102.998336 | | 1948.099577 | 102.004212 | | 1948.099577 | 105.647109 |
| 1951.9572 | 102.989986 | | 1951.9572 | 101.990733 | | 1951.9572 | 105.645931 |
| 1955.814823 | 102.986639 | | 1955.814823 | 101.980745 | | 1955.814823 | 105.647162 |
| 1959.672446 | 102.986046 | | 1959.672446 | 101.972504 | | 1959.672446 | 105.652807 |
| 1963.530069 | 102.984937 | | 1963.530069 | 101.962983 | | 1963.530069 | 105.663461 |
| 1967.387692 | 102.983704 | | 1967.387692 | 101.952908 | | 1967.387692 | 105.67471 |
| 1971.245315 | 102.983193 | | 1971.245315 | 101.94128 | | 1971.245315 | 105.684249 |
| 1975.102938 | 102.986908 | | 1975.102938 | 101.931662 | | 1975.102938 | 105.698349 |
| 1978.96056 | 102.991633 | | 1978.96056 | 101.922615 | | 1978.96056 | 105.716203 |
| 1982.818183 | 102.989524 | | 1982.818183 | 101.909156 | | 1982.818183 | 105.730032 |
| 1986.675806 | 102.983831 | | 1986.675806 | 101.894818 | | 1986.675806 | 105.7411 |
| 1990.533429 | 102.977361 | | 1990.533429 | 101.879324 | | 1990.533429 | 105.749108 |
| 1994.391052 | 102.970034 | | 1994.391052 | 101.861693 | | 1994.391052 | 105.749963 |
| 1998.248675 | 102.960282 | | 1998.248675 | 101.843896 | | 1998.248675 | 105.746866 |
| 2002.106298 | 102.945779 | | 2002.106298 | 101.824929 | | 2002.106298 | 105.743412 |
| 2005.963921 | 102.928581 | | 2005.963921 | 101.803124 | | 2005.963921 | 105.735639 |
| 2009.821544 | 102.909035 | | 2009.821544 | 101.779093 | | 2009.821544 | 105.722583 |
| 2013.679167 | 102.888778 | | 2013.679167 | 101.755348 | | 2013.679167 | 105.708233 |
| 2017.53679 | 102.870243 | | 2017.53679 | 101.731914 | | 2017.53679 | 105.694901 |
| 2021.394413 | 102.851208 | | 2021.394413 | 101.707775 | | 2021.394413 | 105.683212 |
| 2025.252036 | 102.833135 | | 2025.252036 | 101.6846 | | 2025.252036 | 105.673275 |
| 2029.109658 | 102.818638 | | 2029.109658 | 101.663752 | | 2029.109658 | 105.666796 |
| 2032.967281 | 102.804345 | | 2032.967281 | 101.642668 | | 2032.967281 | 105.660481 |
| 2036.824904 | 102.789217 | | 2036.824904 | 101.619986 | | 2036.824904 | 105.651427 |
| 2040.682527 | 102.776608 | | 2040.682527 | 101.598134 | | 2040.682527 | 105.6446 |
| 2044.54015 | 102.766071 | | 2044.54015 | 101.577313 | | 2044.54015 | 105.641293 |
| 2048.397773 | 102.753946 | | 2048.397773 | 101.556085 | | 2048.397773 | 105.638427 |
| 2052.255396 | 102.740651 | | 2052.255396 | 101.534769 | | 2052.255396 | 105.634018 |
| 2056.113019 | 102.729765 | | 2056.113019 | 101.516169 | | 2056.113019 | 105.629368 |
| 2059.970642 | 102.720858 | | 2059.970642 | 101.500731 | | 2059.970642 | 105.625716 |
| 2063.828265 | 102.710345 | | 2063.828265 | 101.484651 | | 2063.828265 | 105.622345 |

Table B-1.—FTIR data of the CA versus CA-GMA membranes presented on figure 10 and CA versus CA-GMA-IDA presented on figure 11

| CA | | | CA-GMA | | | CA-GMA-IDA | |
|---|---|---|---|---|---|---|---|
| 2067.685888 | 102.696633 | | 2067.685888 | 101.466729 | | 2067.685888 | 105.620123 |
| 2071.543511 | 102.681639 | | 2071.543511 | 101.44828 | | 2071.543511 | 105.614954 |
| 2075.401134 | 102.666476 | | 2075.401134 | 101.42947 | | 2075.401134 | 105.603435 |
| 2079.258756 | 102.650208 | | 2079.258756 | 101.411489 | | 2079.258756 | 105.5914 |
| 2083.116379 | 102.631263 | | 2083.116379 | 101.393607 | | 2083.116379 | 105.576958 |
| 2086.974002 | 102.61344 | | 2086.974002 | 101.375516 | | 2086.974002 | 105.560438 |
| 2090.831625 | 102.601997 | | 2090.831625 | 101.36204 | | 2090.831625 | 105.549458 |
| 2094.689248 | 102.589122 | | 2094.689248 | 101.350563 | | 2094.689248 | 105.535002 |
| 2098.546871 | 102.571966 | | 2098.546871 | 101.335373 | | 2098.546871 | 105.515723 |
| 2102.404494 | 102.558685 | | 2102.404494 | 101.321627 | | 2102.404494 | 105.502106 |
| 2106.262117 | 102.546771 | | 2106.262117 | 101.311367 | | 2106.262117 | 105.490789 |
| 2110.11974 | 102.532319 | | 2110.11974 | 101.300981 | | 2110.11974 | 105.478894 |
| 2113.977363 | 102.519927 | | 2113.977363 | 101.292923 | | 2113.977363 | 105.468287 |
| 2117.834986 | 102.512129 | | 2117.834986 | 101.287977 | | 2117.834986 | 105.462789 |
| 2121.692609 | 102.507157 | | 2121.692609 | 101.283833 | | 2121.692609 | 105.464255 |
| 2125.550232 | 102.506227 | | 2125.550232 | 101.283 | | 2125.550232 | 105.468749 |
| 2129.407854 | 102.509841 | | 2129.407854 | 101.285372 | | 2129.407854 | 105.47598 |
| 2133.265477 | 102.516789 | | 2133.265477 | 101.289226 | | 2133.265477 | 105.488563 |
| 2137.1231 | 102.527918 | | 2137.1231 | 101.296823 | | 2137.1231 | 105.50779 |
| 2140.980723 | 102.541443 | | 2140.980723 | 101.30852 | | 2140.980723 | 105.530249 |
| 2144.838346 | 102.559648 | | 2144.838346 | 101.322826 | | 2144.838346 | 105.552082 |
| 2148.695969 | 102.583639 | | 2148.695969 | 101.338676 | | 2148.695969 | 105.575997 |
| 2152.553592 | 102.605387 | | 2152.553592 | 101.355966 | | 2152.553592 | 105.602254 |
| 2156.411215 | 102.625898 | | 2156.411215 | 101.37503 | | 2156.411215 | 105.626193 |
| 2160.268838 | 102.651677 | | 2160.268838 | 101.39645 | | 2160.268838 | 105.651483 |
| 2164.126461 | 102.681793 | | 2164.126461 | 101.421707 | | 2164.126461 | 105.684296 |
| 2167.984084 | 102.714079 | | 2167.984084 | 101.449613 | | 2167.984084 | 105.72007 |
| 2171.841707 | 102.742718 | | 2171.841707 | 101.474997 | | 2171.841707 | 105.751468 |
| 2175.69933 | 102.766757 | | 2175.69933 | 101.497208 | | 2175.69933 | 105.775207 |
| 2179.556953 | 102.795508 | | 2179.556953 | 101.523109 | | 2179.556953 | 105.796242 |
| 2183.414575 | 102.825875 | | 2183.414575 | 101.552646 | | 2183.414575 | 105.820379 |
| 2187.272198 | 102.851266 | | 2187.272198 | 101.579527 | | 2187.272198 | 105.843114 |
| 2191.129821 | 102.877602 | | 2191.129821 | 101.602822 | | 2191.129821 | 105.860342 |
| 2194.987444 | 102.905547 | | 2194.987444 | 101.628601 | | 2194.987444 | 105.874764 |
| 2198.845067 | 102.930638 | | 2198.845067 | 101.659899 | | 2198.845067 | 105.891391 |
| 2202.70269 | 102.954902 | | 2202.70269 | 101.688059 | | 2202.70269 | 105.909878 |
| 2206.560313 | 102.978092 | | 2206.560313 | 101.711465 | | 2206.560313 | 105.924593 |
| 2210.417936 | 102.998696 | | 2210.417936 | 101.735511 | | 2210.417936 | 105.938563 |
| 2214.275559 | 103.023385 | | 2214.275559 | 101.764228 | | 2214.275559 | 105.95865 |
| 2218.133182 | 103.050684 | | 2218.133182 | 101.80062 | | 2218.133182 | 105.979681 |

Table B-1.—FTIR data of the CA versus CA-GMA membranes presented on figure 10 and CA versus CA-GMA-IDA presented on figure 11

| CA | | | CA-GMA | | | CA-GMA-IDA | |
|---|---|---|---|---|---|---|---|
| 2221.990805 | 103.072443 | | 2221.990805 | 101.833728 | | 2221.990805 | 105.996682 |
| 2225.848428 | 103.092432 | | 2225.848428 | 101.860686 | | 2225.848428 | 106.013889 |
| 2229.706051 | 103.112994 | | 2229.706051 | 101.887713 | | 2229.706051 | 106.029722 |
| 2233.563673 | 103.13201 | | 2233.563673 | 101.911343 | | 2233.563673 | 106.040862 |
| 2237.421296 | 103.153081 | | 2237.421296 | 101.937366 | | 2237.421296 | 106.05175 |
| 2241.278919 | 103.177197 | | 2241.278919 | 101.966996 | | 2241.278919 | 106.065026 |
| 2245.136542 | 103.198962 | | 2245.136542 | 101.993054 | | 2245.136542 | 106.076584 |
| 2248.994165 | 103.218358 | | 2248.994165 | 102.021206 | | 2248.994165 | 106.084469 |
| 2252.851788 | 103.238573 | | 2252.851788 | 102.049726 | | 2252.851788 | 106.091569 |
| 2256.709411 | 103.257249 | | 2256.709411 | 102.071717 | | 2256.709411 | 106.097505 |
| 2260.567034 | 103.274632 | | 2260.567034 | 102.095563 | | 2260.567034 | 106.103176 |
| 2264.424657 | 103.290772 | | 2264.424657 | 102.12345 | | 2264.424657 | 106.110012 |
| 2268.28228 | 103.304989 | | 2268.28228 | 102.14846 | | 2268.28228 | 106.115593 |
| 2272.139903 | 103.320649 | | 2272.139903 | 102.173183 | | 2272.139903 | 106.123757 |
| 2275.997526 | 103.338471 | | 2275.997526 | 102.197878 | | 2275.997526 | 106.136744 |
| 2279.855149 | 103.356356 | | 2279.855149 | 102.221788 | | 2279.855149 | 106.148175 |
| 2283.712771 | 103.372492 | | 2283.712771 | 102.246652 | | 2283.712771 | 106.157416 |
| 2287.570394 | 103.390122 | | 2287.570394 | 102.267625 | | 2287.570394 | 106.170978 |
| 2291.428017 | 103.409066 | | 2291.428017 | 102.287803 | | 2291.428017 | 106.187054 |
| 2295.28564 | 103.424884 | | 2295.28564 | 102.310418 | | 2295.28564 | 106.196746 |
| 2299.143263 | 103.444874 | | 2299.143263 | 102.335294 | | 2299.143263 | 106.209051 |
| 2303.000886 | 103.471842 | | 2303.000886 | 102.367059 | | 2303.000886 | 106.234409 |
| 2306.858509 | 103.496378 | | 2306.858509 | 102.396889 | | 2306.858509 | 106.258041 |
| 2310.716132 | 103.516199 | | 2310.716132 | 102.419173 | | 2310.716132 | 106.274016 |
| 2314.573755 | 103.533028 | | 2314.573755 | 102.437479 | | 2314.573755 | 106.289005 |
| 2318.431378 | 103.549357 | | 2318.431378 | 102.453087 | | 2318.431378 | 106.306204 |
| 2322.289001 | 103.570603 | | 2322.289001 | 102.476219 | | 2322.289001 | 106.332098 |
| 2326.146624 | 103.591102 | | 2326.146624 | 102.503141 | | 2326.146624 | 106.357211 |
| 2330.004247 | 103.60534 | | 2330.004247 | 102.522205 | | 2330.004247 | 106.374055 |
| 2333.86187 | 103.619954 | | 2333.86187 | 102.538862 | | 2333.86187 | 106.386793 |
| 2337.719492 | 103.633409 | | 2337.719492 | 102.556247 | | 2337.719492 | 106.38919 |
| 2341.577115 | 103.641826 | | 2341.577115 | 102.57442 | | 2341.577115 | 106.381854 |
| 2345.434738 | 103.648149 | | 2345.434738 | 102.593527 | | 2345.434738 | 106.366205 |
| 2349.292361 | 103.654363 | | 2349.292361 | 102.611371 | | 2349.292361 | 106.354626 |
| 2353.149984 | 103.66658 | | 2353.149984 | 102.63082 | | 2353.149984 | 106.378034 |
| 2357.007607 | 103.68651 | | 2357.007607 | 102.648869 | | 2357.007607 | 106.424948 |
| 2360.86523 | 103.707632 | | 2360.86523 | 102.663067 | | 2360.86523 | 106.453372 |
| 2364.722853 | 103.722882 | | 2364.722853 | 102.681258 | | 2364.722853 | 106.456401 |
| 2368.580476 | 103.729622 | | 2368.580476 | 102.700028 | | 2368.580476 | 106.445024 |
| 2372.438099 | 103.736766 | | 2372.438099 | 102.714958 | | 2372.438099 | 106.422566 |

Table B-1.—FTIR data of the CA versus CA-GMA membranes presented on figure 10 and CA versus CA-GMA-IDA presented on figure 11

| CA | | | CA-GMA | | | CA-GMA-IDA | |
|---|---|---|---|---|---|---|---|
| 2376.295722 | 103.748331 | | 2376.295722 | 102.734291 | | 2376.295722 | 106.398463 |
| 2380.153345 | 103.75788 | | 2380.153345 | 102.756399 | | 2380.153345 | 106.380435 |
| 2384.010968 | 103.763938 | | 2384.010968 | 102.774332 | | 2384.010968 | 106.370659 |
| 2387.86859 | 103.767137 | | 2387.86859 | 102.786377 | | 2387.86859 | 106.367499 |
| 2391.726213 | 103.771568 | | 2391.726213 | 102.795378 | | 2391.726213 | 106.360219 |
| 2395.583836 | 103.779832 | | 2395.583836 | 102.806908 | | 2395.583836 | 106.351006 |
| 2399.441459 | 103.785962 | | 2399.441459 | 102.817734 | | 2399.441459 | 106.347253 |
| 2403.299082 | 103.788362 | | 2403.299082 | 102.825789 | | 2403.299082 | 106.341024 |
| 2407.156705 | 103.790088 | | 2407.156705 | 102.836171 | | 2407.156705 | 106.332773 |
| 2411.014328 | 103.79243 | | 2411.014328 | 102.848452 | | 2411.014328 | 106.327346 |
| 2414.871951 | 103.798287 | | 2414.871951 | 102.85947 | | 2414.871951 | 106.324528 |
| 2418.729574 | 103.808274 | | 2418.729574 | 102.869939 | | 2418.729574 | 106.32668 |
| 2422.587197 | 103.819071 | | 2422.587197 | 102.883265 | | 2422.587197 | 106.331655 |
| 2426.44482 | 103.829542 | | 2426.44482 | 102.898978 | | 2426.44482 | 106.336526 |
| 2430.302443 | 103.839801 | | 2430.302443 | 102.913189 | | 2430.302443 | 106.339398 |
| 2434.160066 | 103.849677 | | 2434.160066 | 102.926352 | | 2434.160066 | 106.34187 |
| 2438.017688 | 103.860802 | | 2438.017688 | 102.938744 | | 2438.017688 | 106.347018 |
| 2441.875311 | 103.871852 | | 2441.875311 | 102.945978 | | 2441.875311 | 106.348396 |
| 2445.732934 | 103.882383 | | 2445.732934 | 102.954655 | | 2445.732934 | 106.347996 |
| 2449.590557 | 103.889782 | | 2449.590557 | 102.969236 | | 2449.590557 | 106.348855 |
| 2453.44818 | 103.890876 | | 2453.44818 | 102.978655 | | 2453.44818 | 106.344716 |
| 2457.305803 | 103.894342 | | 2457.305803 | 102.987752 | | 2457.305803 | 106.339282 |
| 2461.163426 | 103.901568 | | 2461.163426 | 103.001578 | | 2461.163426 | 106.335912 |
| 2465.021049 | 103.905903 | | 2465.021049 | 103.009514 | | 2465.021049 | 106.335348 |
| 2468.878672 | 103.911785 | | 2468.878672 | 103.015885 | | 2468.878672 | 106.337612 |
| 2472.736295 | 103.920901 | | 2472.736295 | 103.025748 | | 2472.736295 | 106.335862 |
| 2476.593918 | 103.931087 | | 2476.593918 | 103.038364 | | 2476.593918 | 106.336374 |
| 2480.451541 | 103.939464 | | 2480.451541 | 103.052059 | | 2480.451541 | 106.341474 |
| 2484.309164 | 103.944063 | | 2484.309164 | 103.059229 | | 2484.309164 | 106.340459 |
| 2488.166786 | 103.951159 | | 2488.166786 | 103.064731 | | 2488.166786 | 106.338946 |
| 2492.024409 | 103.959503 | | 2492.024409 | 103.074875 | | 2492.024409 | 106.341547 |
| 2495.882032 | 103.966173 | | 2495.882032 | 103.087494 | | 2495.882032 | 106.344559 |
| 2499.739655 | 103.976568 | | 2499.739655 | 103.101694 | | 2499.739655 | 106.35025 |
| 2503.597278 | 103.984257 | | 2503.597278 | 103.111835 | | 2503.597278 | 106.354228 |
| 2507.454901 | 103.989612 | | 2507.454901 | 103.119404 | | 2507.454901 | 106.355756 |
| 2511.312524 | 104.003175 | | 2511.312524 | 103.131473 | | 2511.312524 | 106.358246 |
| 2515.170147 | 104.013661 | | 2515.170147 | 103.144004 | | 2515.170147 | 106.358202 |
| 2519.02777 | 104.015615 | | 2519.02777 | 103.1507 | | 2519.02777 | 106.355655 |
| 2522.885393 | 104.018837 | | 2522.885393 | 103.154138 | | 2522.885393 | 106.35479 |
| 2526.743016 | 104.020428 | | 2526.743016 | 103.160766 | | 2526.743016 | 106.357336 |

Table B-1.—FTIR data of the CA versus CA-GMA membranes presented on figure 10 and CA versus CA-GMA-IDA presented on figure 11

| CA | | | CA-GMA | | | CA-GMA-IDA | |
|---|---|---|---|---|---|---|---|
| 2530.600639 | 104.024206 | | 2530.600639 | 103.16858 | | 2530.600639 | 106.357545 |
| 2534.458262 | 104.032347 | | 2534.458262 | 103.17238 | | 2534.458262 | 106.354943 |
| 2538.315885 | 104.034767 | | 2538.315885 | 103.17723 | | 2538.315885 | 106.353619 |
| 2542.173507 | 104.03779 | | 2542.173507 | 103.188123 | | 2542.173507 | 106.352146 |
| 2546.03113 | 104.046337 | | 2546.03113 | 103.199759 | | 2546.03113 | 106.356738 |
| 2549.888753 | 104.053099 | | 2549.888753 | 103.207739 | | 2549.888753 | 106.360918 |
| 2553.746376 | 104.055674 | | 2553.746376 | 103.211873 | | 2553.746376 | 106.35374 |
| 2557.603999 | 104.053517 | | 2557.603999 | 103.211444 | | 2557.603999 | 106.345893 |
| 2561.461622 | 104.053191 | | 2561.461622 | 103.214203 | | 2561.461622 | 106.342116 |
| 2565.319245 | 104.056232 | | 2565.319245 | 103.22142 | | 2565.319245 | 106.337631 |
| 2569.176868 | 104.056291 | | 2569.176868 | 103.224047 | | 2569.176868 | 106.330205 |
| 2573.034491 | 104.059425 | | 2573.034491 | 103.227848 | | 2573.034491 | 106.324758 |
| 2576.892114 | 104.064871 | | 2576.892114 | 103.235751 | | 2576.892114 | 106.324011 |
| 2580.749737 | 104.061131 | | 2580.749737 | 103.238443 | | 2580.749737 | 106.317125 |
| 2584.60736 | 104.05372 | | 2584.60736 | 103.236259 | | 2584.60736 | 106.308782 |
| 2588.464983 | 104.050007 | | 2588.464983 | 103.23665 | | 2588.464983 | 106.30538 |
| 2592.322605 | 104.044124 | | 2592.322605 | 103.240743 | | 2592.322605 | 106.296364 |
| 2596.180228 | 104.041102 | | 2596.180228 | 103.245336 | | 2596.180228 | 106.287644 |
| 2600.037851 | 104.046656 | | 2600.037851 | 103.253409 | | 2600.037851 | 106.284072 |
| 2603.895474 | 104.048663 | | 2603.895474 | 103.26033 | | 2603.895474 | 106.277297 |
| 2607.753097 | 104.046716 | | 2607.753097 | 103.25895 | | 2607.753097 | 106.271908 |
| 2611.61072 | 104.046241 | | 2611.61072 | 103.256873 | | 2611.61072 | 106.265784 |
| 2615.468343 | 104.040565 | | 2615.468343 | 103.258369 | | 2615.468343 | 106.255845 |
| 2619.325966 | 104.031158 | | 2619.325966 | 103.260143 | | 2619.325966 | 106.250431 |
| 2623.183589 | 104.02364 | | 2623.183589 | 103.257264 | | 2623.183589 | 106.243039 |
| 2627.041212 | 104.020935 | | 2627.041212 | 103.249775 | | 2627.041212 | 106.230057 |
| 2630.898835 | 104.021469 | | 2630.898835 | 103.247042 | | 2630.898835 | 106.219093 |
| 2634.756458 | 104.016196 | | 2634.756458 | 103.254432 | | 2634.756458 | 106.214248 |
| 2638.614081 | 104.010253 | | 2638.614081 | 103.265615 | | 2638.614081 | 106.216706 |
| 2642.471703 | 104.010829 | | 2642.471703 | 103.267856 | | 2642.471703 | 106.216549 |
| 2646.329326 | 104.008805 | | 2646.329326 | 103.264323 | | 2646.329326 | 106.212479 |
| 2650.186949 | 104.005271 | | 2650.186949 | 103.263434 | | 2650.186949 | 106.213917 |
| 2654.044572 | 104.009356 | | 2654.044572 | 103.262798 | | 2654.044572 | 106.220045 |
| 2657.902195 | 104.0153 | | 2657.902195 | 103.265408 | | 2657.902195 | 106.22802 |
| 2661.759818 | 104.016482 | | 2661.759818 | 103.268803 | | 2661.759818 | 106.234681 |
| 2665.617441 | 104.016562 | | 2665.617441 | 103.27193 | | 2665.617441 | 106.239288 |
| 2669.475064 | 104.017642 | | 2669.475064 | 103.280483 | | 2669.475064 | 106.24534 |
| 2673.332687 | 104.015243 | | 2673.332687 | 103.284553 | | 2673.332687 | 106.248705 |
| 2677.19031 | 104.009583 | | 2677.19031 | 103.280502 | | 2677.19031 | 106.246308 |
| 2681.047933 | 104.007586 | | 2681.047933 | 103.27751 | | 2681.047933 | 106.244669 |

Table B-1.—FTIR data of the CA versus CA-GMA membranes presented on figure 10 and CA versus CA-GMA-IDA presented on figure 11

| CA | | | CA-GMA | | | CA-GMA-IDA | |
|---|---|---|---|---|---|---|---|
| 2684.905556 | 104.007004 | | 2684.905556 | 103.27659 | | 2684.905556 | 106.242973 |
| 2688.763179 | 104.002392 | | 2688.763179 | 103.275451 | | 2688.763179 | 106.237293 |
| 2692.620802 | 103.997281 | | 2692.620802 | 103.275141 | | 2692.620802 | 106.235515 |
| 2696.478424 | 103.99051 | | 2696.478424 | 103.275072 | | 2696.478424 | 106.236296 |
| 2700.336047 | 103.979194 | | 2700.336047 | 103.27151 | | 2700.336047 | 106.229867 |
| 2704.19367 | 103.96825 | | 2704.19367 | 103.267437 | | 2704.19367 | 106.216697 |
| 2708.051293 | 103.95984 | | 2708.051293 | 103.264925 | | 2708.051293 | 106.201305 |
| 2711.908916 | 103.948405 | | 2711.908916 | 103.256894 | | 2711.908916 | 106.185288 |
| 2715.766539 | 103.931161 | | 2715.766539 | 103.243368 | | 2715.766539 | 106.167543 |
| 2719.624162 | 103.915487 | | 2719.624162 | 103.229915 | | 2719.624162 | 106.15315 |
| 2723.481785 | 103.903646 | | 2723.481785 | 103.220216 | | 2723.481785 | 106.146934 |
| 2727.339408 | 103.891006 | | 2727.339408 | 103.214629 | | 2727.339408 | 106.141294 |
| 2731.197031 | 103.887102 | | 2731.197031 | 103.212578 | | 2731.197031 | 106.137759 |
| 2735.054654 | 103.894026 | | 2735.054654 | 103.213851 | | 2735.054654 | 106.146721 |
| 2738.912277 | 103.896088 | | 2738.912277 | 103.210706 | | 2738.912277 | 106.159024 |
| 2742.7699 | 103.898595 | | 2742.7699 | 103.206868 | | 2742.7699 | 106.165089 |
| 2746.627522 | 103.908621 | | 2746.627522 | 103.211138 | | 2746.627522 | 106.173018 |
| 2750.485145 | 103.910875 | | 2750.485145 | 103.209749 | | 2750.485145 | 106.180411 |
| 2754.342768 | 103.903523 | | 2754.342768 | 103.19561 | | 2754.342768 | 106.180107 |
| 2758.200391 | 103.893271 | | 2758.200391 | 103.179979 | | 2758.200391 | 106.177543 |
| 2762.058014 | 103.884069 | | 2762.058014 | 103.169215 | | 2762.058014 | 106.175921 |
| 2765.915637 | 103.880529 | | 2765.915637 | 103.160592 | | 2765.915637 | 106.172564 |
| 2769.77326 | 103.876669 | | 2769.77326 | 103.152456 | | 2769.77326 | 106.168798 |
| 2773.630883 | 103.871899 | | 2773.630883 | 103.147907 | | 2773.630883 | 106.169515 |
| 2777.488506 | 103.863389 | | 2777.488506 | 103.142857 | | 2777.488506 | 106.167291 |
| 2781.346129 | 103.845708 | | 2781.346129 | 103.133624 | | 2781.346129 | 106.156712 |
| 2785.203752 | 103.82892 | | 2785.203752 | 103.120752 | | 2785.203752 | 106.14638 |
| 2789.061375 | 103.813517 | | 2789.061375 | 103.102647 | | 2789.061375 | 106.132911 |
| 2792.918998 | 103.799243 | | 2792.918998 | 103.086631 | | 2792.918998 | 106.116215 |
| 2796.77662 | 103.789402 | | 2796.77662 | 103.073785 | | 2796.77662 | 106.10192 |
| 2800.634243 | 103.770974 | | 2800.634243 | 103.052012 | | 2800.634243 | 106.082047 |
| 2804.491866 | 103.746389 | | 2804.491866 | 103.025243 | | 2804.491866 | 106.062027 |
| 2808.349489 | 103.730712 | | 2808.349489 | 103.007949 | | 2808.349489 | 106.049774 |
| 2812.207112 | 103.716791 | | 2812.207112 | 102.992911 | | 2812.207112 | 106.03611 |
| 2816.064735 | 103.695789 | | 2816.064735 | 102.967719 | | 2816.064735 | 106.019237 |
| 2819.922358 | 103.672595 | | 2819.922358 | 102.943029 | | 2819.922358 | 106.000201 |
| 2823.779981 | 103.649222 | | 2823.779981 | 102.922653 | | 2823.779981 | 105.972641 |
| 2827.637604 | 103.6251 | | 2827.637604 | 102.893327 | | 2827.637604 | 105.938251 |
| 2831.495227 | 103.595907 | | 2831.495227 | 102.851932 | | 2831.495227 | 105.895936 |
| 2835.35285 | 103.553895 | | 2835.35285 | 102.798658 | | 2835.35285 | 105.819615 |

Table B-1.—FTIR data of the CA versus CA-GMA membranes presented on figure 10 and CA versus CA-GMA-IDA presented on figure 11

| CA | | | CA-GMA | | | CA-GMA-IDA | |
|---|---|---|---|---|---|---|---|
| 2839.210473 | 103.498352 | | 2839.210473 | 102.728788 | | 2839.210473 | 105.694809 |
| 2843.068096 | 103.41461 | | 2843.068096 | 102.615918 | | 2843.068096 | 105.470912 |
| 2846.925719 | 103.290868 | | 2846.925719 | 102.439001 | | 2846.925719 | 105.077371 |
| 2850.783341 | 103.171105 | | 2850.783341 | 102.274763 | | 2850.783341 | 104.695507 |
| 2854.640964 | 103.106486 | | 2854.640964 | 102.219862 | | 2854.640964 | 104.582989 |
| 2858.498587 | 103.080498 | | 2858.498587 | 102.246099 | | 2858.498587 | 104.655617 |
| 2862.35621 | 103.048812 | | 2862.35621 | 102.277847 | | 2862.35621 | 104.730416 |
| 2866.213833 | 102.994025 | | 2866.213833 | 102.276508 | | 2866.213833 | 104.744506 |
| 2870.071456 | 102.920937 | | 2870.071456 | 102.234515 | | 2870.071456 | 104.687829 |
| 2873.929079 | 102.848566 | | 2873.929079 | 102.182847 | | 2873.929079 | 104.625535 |
| 2877.786702 | 102.786964 | | 2877.786702 | 102.142914 | | 2877.786702 | 104.592681 |
| 2881.644325 | 102.724753 | | 2881.644325 | 102.097045 | | 2881.644325 | 104.558958 |
| 2885.501948 | 102.66105 | | 2885.501948 | 102.029444 | | 2885.501948 | 104.504982 |
| 2889.359571 | 102.599278 | | 2889.359571 | 101.945835 | | 2889.359571 | 104.432676 |
| 2893.217194 | 102.539987 | | 2893.217194 | 101.862739 | | 2893.217194 | 104.360617 |
| 2897.074817 | 102.495464 | | 2897.074817 | 101.783402 | | 2897.074817 | 104.289031 |
| 2900.932439 | 102.459559 | | 2900.932439 | 101.698917 | | 2900.932439 | 104.209214 |
| 2904.790062 | 102.417995 | | 2904.790062 | 101.609507 | | 2904.790062 | 104.112712 |
| 2908.647685 | 102.366844 | | 2908.647685 | 101.498491 | | 2908.647685 | 103.953067 |
| 2912.505308 | 102.285438 | | 2912.505308 | 101.329641 | | 2912.505308 | 103.651935 |
| 2916.362931 | 102.176546 | | 2916.362931 | 101.124495 | | 2916.362931 | 103.238669 |
| 2920.220554 | 102.08362 | | 2920.220554 | 100.956509 | | 2920.220554 | 102.922942 |
| 2924.078177 | 102.031594 | | 2924.078177 | 100.863504 | | 2924.078177 | 102.831421 |
| 2927.9358 | 102.00495 | | 2927.9358 | 100.838241 | | 2927.9358 | 102.869607 |
| 2931.793423 | 101.970482 | | 2931.793423 | 100.848069 | | 2931.793423 | 102.934629 |
| 2935.651046 | 101.909228 | | 2935.651046 | 100.853621 | | 2935.651046 | 103.001275 |
| 2939.508669 | 101.82589 | | 2939.508669 | 100.838913 | | 2939.508669 | 103.07332 |
| 2943.366292 | 101.745827 | | 2943.366292 | 100.799611 | | 2943.366292 | 103.159704 |
| 2947.223915 | 101.68594 | | 2947.223915 | 100.732873 | | 2947.223915 | 103.243208 |
| 2951.081537 | 101.62529 | | 2951.081537 | 100.639929 | | 2951.081537 | 103.28266 |
| 2954.93916 | 101.554444 | | 2954.93916 | 100.537051 | | 2954.93916 | 103.272279 |
| 2958.796783 | 101.505285 | | 2958.796783 | 100.465648 | | 2958.796783 | 103.291067 |
| 2962.654406 | 101.512272 | | 2962.654406 | 100.453682 | | 2962.654406 | 103.423054 |
| 2966.512029 | 101.582516 | | 2966.512029 | 100.490127 | | 2966.512029 | 103.666431 |
| 2970.369652 | 101.685713 | | 2970.369652 | 100.541987 | | 2970.369652 | 103.965526 |
| 2974.227275 | 101.777171 | | 2974.227275 | 100.57604 | | 2974.227275 | 104.24904 |
| 2978.084898 | 101.838113 | | 2978.084898 | 100.58338 | | 2978.084898 | 104.472156 |
| 2981.942521 | 101.864277 | | 2981.942521 | 100.553356 | | 2981.942521 | 104.619586 |
| 2985.800144 | 101.846994 | | 2985.800144 | 100.472021 | | 2985.800144 | 104.687101 |
| 2989.657767 | 101.79981 | | 2989.657767 | 100.362991 | | 2989.657767 | 104.7084 |

Table B-1.—FTIR data of the CA versus CA-GMA membranes presented on figure 10 and CA versus CA-GMA-IDA presented on figure 11

| CA | | | CA-GMA | | | CA-GMA-IDA | |
|---|---|---|---|---|---|---|---|
| 2993.51539 | 101.74004 | | 2993.51539 | 100.239863 | | 2993.51539 | 104.714404 |
| 2997.373013 | 101.664626 | | 2997.373013 | 100.099563 | | 2997.373013 | 104.711029 |
| 3001.230635 | 101.585383 | | 3001.230635 | 99.966747 | | 3001.230635 | 104.709853 |
| 3005.088258 | 101.510698 | | 3005.088258 | 99.848 | | 3005.088258 | 104.717576 |
| 3008.945881 | 101.426093 | | 3008.945881 | 99.723034 | | 3008.945881 | 104.732327 |
| 3012.803504 | 101.328966 | | 3012.803504 | 99.580936 | | 3012.803504 | 104.736988 |
| 3016.661127 | 101.228609 | | 3016.661127 | 99.434645 | | 3016.661127 | 104.735024 |
| 3020.51875 | 101.129481 | | 3020.51875 | 99.306471 | | 3020.51875 | 104.755883 |
| 3024.376373 | 101.033059 | | 3024.376373 | 99.182012 | | 3024.376373 | 104.787004 |
| 3028.233996 | 100.940183 | | 3028.233996 | 99.038989 | | 3028.233996 | 104.806216 |
| 3032.091619 | 100.845146 | | 3032.091619 | 98.882563 | | 3032.091619 | 104.814667 |
| 3035.949242 | 100.750406 | | 3035.949242 | 98.727 | | 3035.949242 | 104.826376 |
| 3039.806865 | 100.661026 | | 3039.806865 | 98.573495 | | 3039.806865 | 104.84588 |
| 3043.664488 | 100.561044 | | 3043.664488 | 98.402366 | | 3043.664488 | 104.842442 |
| 3047.522111 | 100.444753 | | 3047.522111 | 98.215103 | | 3047.522111 | 104.815235 |
| 3051.379734 | 100.320642 | | 3051.379734 | 98.025918 | | 3051.379734 | 104.779221 |
| 3055.237356 | 100.192095 | | 3055.237356 | 97.826734 | | 3055.237356 | 104.72691 |
| 3059.094979 | 100.064771 | | 3059.094979 | 97.617227 | | 3059.094979 | 104.679396 |
| 3062.952602 | 99.93494 | | 3062.952602 | 97.403767 | | 3062.952602 | 104.643136 |
| 3066.810225 | 99.789148 | | 3066.810225 | 97.180164 | | 3066.810225 | 104.599928 |
| 3070.667848 | 99.626096 | | 3070.667848 | 96.945986 | | 3070.667848 | 104.556666 |
| 3074.525471 | 99.462097 | | 3074.525471 | 96.710346 | | 3074.525471 | 104.521944 |
| 3078.383094 | 99.300037 | | 3078.383094 | 96.467783 | | 3078.383094 | 104.486249 |
| 3082.240717 | 99.125669 | | 3082.240717 | 96.209285 | | 3082.240717 | 104.43495 |
| 3086.09834 | 98.94286 | | 3086.09834 | 95.94272 | | 3086.09834 | 104.378859 |
| 3089.955963 | 98.762721 | | 3089.955963 | 95.672454 | | 3089.955963 | 104.332501 |
| 3093.813586 | 98.581199 | | 3093.813586 | 95.395723 | | 3093.813586 | 104.287202 |
| 3097.671209 | 98.387653 | | 3097.671209 | 95.105619 | | 3097.671209 | 104.234375 |
| 3101.528832 | 98.185126 | | 3101.528832 | 94.803398 | | 3101.528832 | 104.168415 |
| 3105.386454 | 97.979092 | | 3105.386454 | 94.503102 | | 3105.386454 | 104.0963 |
| 3109.244077 | 97.759422 | | 3109.244077 | 94.193005 | | 3109.244077 | 104.021177 |
| 3113.1017 | 97.534448 | | 3113.1017 | 93.86972 | | 3113.1017 | 103.938456 |
| 3116.959323 | 97.312375 | | 3116.959323 | 93.547173 | | 3116.959323 | 103.854563 |
| 3120.816946 | 97.075693 | | 3120.816946 | 93.205978 | | 3120.816946 | 103.759385 |
| 3124.674569 | 96.829789 | | 3124.674569 | 92.852246 | | 3124.674569 | 103.649929 |
| 3128.532192 | 96.589034 | | 3128.532192 | 92.50917 | | 3128.532192 | 103.543593 |
| 3132.389815 | 96.346379 | | 3132.389815 | 92.160478 | | 3132.389815 | 103.437662 |
| 3136.247438 | 96.094478 | | 3136.247438 | 91.802207 | | 3136.247438 | 103.322379 |
| 3140.105061 | 95.83118 | | 3140.105061 | 91.44113 | | 3140.105061 | 103.205156 |
| 3143.962684 | 95.563659 | | 3143.962684 | 91.077856 | | 3143.962684 | 103.093262 |

Table B-1.—FTIR data of the CA versus CA-GMA membranes presented on figure 10 and CA versus CA-GMA-IDA presented on figure 11

| CA | | | CA-GMA | | | CA-GMA-IDA | |
|---|---|---|---|---|---|---|---|
| 3147.820307 | 95.299888 | | 3147.820307 | 90.712738 | | 3147.820307 | 102.973535 |
| 3151.67793 | 95.030575 | | 3151.67793 | 90.338535 | | 3151.67793 | 102.838803 |
| 3155.535552 | 94.749654 | | 3155.535552 | 89.954384 | | 3155.535552 | 102.700627 |
| 3159.393175 | 94.467198 | | 3159.393175 | 89.564267 | | 3159.393175 | 102.564043 |
| 3163.250798 | 94.184432 | | 3163.250798 | 89.1852 | | 3163.250798 | 102.431093 |
| 3167.108421 | 93.899848 | | 3167.108421 | 88.814159 | | 3167.108421 | 102.299926 |
| 3170.966044 | 93.617431 | | 3170.966044 | 88.426995 | | 3170.966044 | 102.160356 |
| 3174.823667 | 93.326244 | | 3174.823667 | 88.038881 | | 3174.823667 | 102.008759 |
| 3178.68129 | 93.027002 | | 3178.68129 | 87.659112 | | 3178.68129 | 101.851056 |
| 3182.538913 | 92.732295 | | 3182.538913 | 87.277127 | | 3182.538913 | 101.69022 |
| 3186.396536 | 92.440252 | | 3186.396536 | 86.900244 | | 3186.396536 | 101.526894 |
| 3190.254159 | 92.149064 | | 3190.254159 | 86.530818 | | 3190.254159 | 101.369468 |
| 3194.111782 | 91.849654 | | 3194.111782 | 86.165341 | | 3194.111782 | 101.212799 |
| 3197.969405 | 91.544269 | | 3197.969405 | 85.802945 | | 3197.969405 | 101.048094 |
| 3201.827028 | 91.254299 | | 3201.827028 | 85.449911 | | 3201.827028 | 100.888584 |
| 3205.684651 | 90.979094 | | 3205.684651 | 85.107353 | | 3205.684651 | 100.735181 |
| 3209.542273 | 90.709319 | | 3209.542273 | 84.765347 | | 3209.542273 | 100.582328 |
| 3213.399896 | 90.440566 | | 3213.399896 | 84.4356 | | 3213.399896 | 100.431977 |
| 3217.257519 | 90.171717 | | 3217.257519 | 84.128043 | | 3217.257519 | 100.272191 |
| 3221.115142 | 89.910004 | | 3221.115142 | 83.828355 | | 3221.115142 | 100.108054 |
| 3224.972765 | 89.654094 | | 3224.972765 | 83.533922 | | 3224.972765 | 99.955311 |
| 3228.830388 | 89.405837 | | 3228.830388 | 83.250605 | | 3228.830388 | 99.79995 |
| 3232.688011 | 89.177697 | | 3232.688011 | 82.983033 | | 3232.688011 | 99.632319 |
| 3236.545634 | 88.962766 | | 3236.545634 | 82.736208 | | 3236.545634 | 99.46635 |
| 3240.403257 | 88.751415 | | 3240.403257 | 82.503161 | | 3240.403257 | 99.307708 |
| 3244.26088 | 88.552711 | | 3244.26088 | 82.284779 | | 3244.26088 | 99.147225 |
| 3248.118503 | 88.367838 | | 3248.118503 | 82.087345 | | 3248.118503 | 98.981338 |
| 3251.976126 | 88.189821 | | 3251.976126 | 81.894596 | | 3251.976126 | 98.814702 |
| 3255.833749 | 88.018732 | | 3255.833749 | 81.702517 | | 3255.833749 | 98.649681 |
| 3259.691371 | 87.858842 | | 3259.691371 | 81.532929 | | 3259.691371 | 98.49216 |
| 3263.548994 | 87.711175 | | 3263.548994 | 81.386367 | | 3263.548994 | 98.347968 |
| 3267.406617 | 87.57114 | | 3267.406617 | 81.243396 | | 3267.406617 | 98.209939 |
| 3271.26424 | 87.441435 | | 3271.26424 | 81.103053 | | 3271.26424 | 98.075926 |
| 3275.121863 | 87.318919 | | 3275.121863 | 80.969082 | | 3275.121863 | 97.954281 |
| 3278.979486 | 87.191482 | | 3278.979486 | 80.831708 | | 3278.979486 | 97.846927 |
| 3282.837109 | 87.060463 | | 3282.837109 | 80.693303 | | 3282.837109 | 97.752407 |
| 3286.694732 | 86.932622 | | 3286.694732 | 80.563529 | | 3286.694732 | 97.668118 |
| 3290.552355 | 86.814228 | | 3290.552355 | 80.443323 | | 3290.552355 | 97.605683 |
| 3294.409978 | 86.703375 | | 3294.409978 | 80.335387 | | 3294.409978 | 97.571492 |
| 3298.267601 | 86.583878 | | 3298.267601 | 80.22729 | | 3298.267601 | 97.53057 |

Table B-1.—FTIR data of the CA versus CA-GMA membranes presented on figure 10 and CA versus CA-GMA-IDA presented on figure 11

| CA | | | CA-GMA | | | CA-GMA-IDA | |
|---|---|---|---|---|---|---|---|
| 3302.125224 | 86.458151 | | 3302.125224 | 80.108023 | | 3302.125224 | 97.483055 |
| 3305.982847 | 86.338923 | | 3305.982847 | 79.987811 | | 3305.982847 | 97.449103 |
| 3309.840469 | 86.214375 | | 3309.840469 | 79.863977 | | 3309.840469 | 97.397986 |
| 3313.698092 | 86.083296 | | 3313.698092 | 79.734187 | | 3313.698092 | 97.341105 |
| 3317.555715 | 85.963954 | | 3317.555715 | 79.609747 | | 3317.555715 | 97.305173 |
| 3321.413338 | 85.844824 | | 3321.413338 | 79.48854 | | 3321.413338 | 97.263755 |
| 3325.270961 | 85.708525 | | 3325.270961 | 79.359253 | | 3325.270961 | 97.212527 |
| 3329.128584 | 85.568914 | | 3329.128584 | 79.225649 | | 3329.128584 | 97.156647 |
| 3332.986207 | 85.440356 | | 3332.986207 | 79.106057 | | 3332.986207 | 97.10104 |
| 3336.84383 | 85.313836 | | 3336.84383 | 78.995067 | | 3336.84383 | 97.053707 |
| 3340.701453 | 85.177396 | | 3340.701453 | 78.877222 | | 3340.701453 | 96.988882 |
| 3344.559076 | 85.038613 | | 3344.559076 | 78.759476 | | 3344.559076 | 96.909286 |
| 3348.416699 | 84.901621 | | 3348.416699 | 78.645773 | | 3348.416699 | 96.838012 |
| 3352.274322 | 84.760048 | | 3352.274322 | 78.534092 | | 3352.274322 | 96.758704 |
| 3356.131945 | 84.627852 | | 3356.131945 | 78.432031 | | 3356.131945 | 96.671027 |
| 3359.989568 | 84.506613 | | 3359.989568 | 78.339575 | | 3359.989568 | 96.586511 |
| 3363.84719 | 84.380551 | | 3363.84719 | 78.243775 | | 3363.84719 | 96.496692 |
| 3367.704813 | 84.257365 | | 3367.704813 | 78.149382 | | 3367.704813 | 96.400852 |
| 3371.562436 | 84.139479 | | 3371.562436 | 78.071421 | | 3371.562436 | 96.302582 |
| 3375.420059 | 84.028262 | | 3375.420059 | 78.011621 | | 3375.420059 | 96.213136 |
| 3379.277682 | 83.929446 | | 3379.277682 | 77.966374 | | 3379.277682 | 96.125718 |
| 3383.135305 | 83.840732 | | 3383.135305 | 77.928019 | | 3383.135305 | 96.019309 |
| 3386.992928 | 83.776627 | | 3386.992928 | 77.905879 | | 3386.992928 | 95.9219 |
| 3390.850551 | 83.722731 | | 3390.850551 | 77.901477 | | 3390.850551 | 95.843052 |
| 3394.708174 | 83.66878 | | 3394.708174 | 77.905207 | | 3394.708174 | 95.762449 |
| 3398.565797 | 83.641222 | | 3398.565797 | 77.933126 | | 3398.565797 | 95.690172 |
| 3402.42342 | 83.627764 | | 3402.42342 | 77.979503 | | 3402.42342 | 95.617056 |
| 3406.281043 | 83.620883 | | 3406.281043 | 78.032673 | | 3406.281043 | 95.536734 |
| 3410.138666 | 83.626674 | | 3410.138666 | 78.10513 | | 3410.138666 | 95.462929 |
| 3413.996288 | 83.638824 | | 3413.996288 | 78.196271 | | 3413.996288 | 95.395324 |
| 3417.853911 | 83.673213 | | 3417.853911 | 78.301875 | | 3417.853911 | 95.344773 |
| 3421.711534 | 83.727298 | | 3421.711534 | 78.417636 | | 3421.711534 | 95.306753 |
| 3425.569157 | 83.786234 | | 3425.569157 | 78.54091 | | 3425.569157 | 95.265424 |
| 3429.42678 | 83.853997 | | 3429.42678 | 78.67831 | | 3429.42678 | 95.227824 |
| 3433.284403 | 83.933288 | | 3433.284403 | 78.834934 | | 3433.284403 | 95.196505 |
| 3437.142026 | 84.020356 | | 3437.142026 | 79.003794 | | 3437.142026 | 95.17098 |
| 3440.999649 | 84.115216 | | 3440.999649 | 79.179983 | | 3440.999649 | 95.15346 |
| 3444.857272 | 84.227972 | | 3444.857272 | 79.372619 | | 3444.857272 | 95.143418 |
| 3448.714895 | 84.353299 | | 3448.714895 | 79.570886 | | 3448.714895 | 95.142918 |
| 3452.572518 | 84.482829 | | 3452.572518 | 79.763036 | | 3452.572518 | 95.151124 |

Table B-1.—FTIR data of the CA versus CA-GMA membranes presented on figure 10 and CA versus CA-GMA-IDA presented on figure 11

| CA | | | CA-GMA | | | CA-GMA-IDA | |
|---|---|---|---|---|---|---|---|
| 3456.430141 | 84.622206 | | 3456.430141 | 79.962538 | | 3456.430141 | 95.168663 |
| 3460.287764 | 84.768915 | | 3460.287764 | 80.174281 | | 3460.287764 | 95.194558 |
| 3464.145386 | 84.927284 | | 3464.145386 | 80.399098 | | 3464.145386 | 95.226813 |
| 3468.003009 | 85.092906 | | 3468.003009 | 80.629574 | | 3468.003009 | 95.263432 |
| 3471.860632 | 85.249389 | | 3471.860632 | 80.848539 | | 3471.860632 | 95.297693 |
| 3475.718255 | 85.410423 | | 3475.718255 | 81.069011 | | 3475.718255 | 95.335236 |
| 3479.575878 | 85.582925 | | 3479.575878 | 81.303999 | | 3479.575878 | 95.37852 |
| 3483.433501 | 85.751627 | | 3483.433501 | 81.538174 | | 3483.433501 | 95.417215 |
| 3487.291124 | 85.927914 | | 3487.291124 | 81.767547 | | 3487.291124 | 95.46188 |
| 3491.148747 | 86.122197 | | 3491.148747 | 82.002551 | | 3491.148747 | 95.526442 |
| 3495.00637 | 86.304437 | | 3495.00637 | 82.248501 | | 3495.00637 | 95.599729 |
| 3498.863993 | 86.4715 | | 3498.863993 | 82.500712 | | 3498.863993 | 95.668411 |
| 3502.721616 | 86.659625 | | 3502.721616 | 82.750238 | | 3502.721616 | 95.734393 |
| 3506.579239 | 86.861555 | | 3506.579239 | 83.001892 | | 3506.579239 | 95.807843 |
| 3510.436862 | 87.058844 | | 3510.436862 | 83.259737 | | 3510.436862 | 95.891597 |
| 3514.294484 | 87.255212 | | 3514.294484 | 83.51427 | | 3514.294484 | 95.972692 |
| 3518.152107 | 87.453042 | | 3518.152107 | 83.771077 | | 3518.152107 | 96.057503 |
| 3522.00973 | 87.668983 | | 3522.00973 | 84.047061 | | 3522.00973 | 96.163394 |
| 3525.867353 | 87.894186 | | 3525.867353 | 84.332426 | | 3525.867353 | 96.269845 |
| 3529.724976 | 88.116346 | | 3529.724976 | 84.614913 | | 3529.724976 | 96.374946 |
| 3533.582599 | 88.34644 | | 3533.582599 | 84.900964 | | 3533.582599 | 96.494955 |
| 3537.440222 | 88.56478 | | 3537.440222 | 85.183249 | | 3537.440222 | 96.603202 |
| 3541.297845 | 88.77515 | | 3541.297845 | 85.459566 | | 3541.297845 | 96.700556 |
| 3545.155468 | 89.006892 | | 3545.155468 | 85.748075 | | 3545.155468 | 96.817924 |
| 3549.013091 | 89.241261 | | 3549.013091 | 86.045072 | | 3549.013091 | 96.945419 |
| 3552.870714 | 89.4624 | | 3552.870714 | 86.333459 | | 3552.870714 | 97.065456 |
| 3556.728337 | 89.68681 | | 3556.728337 | 86.608685 | | 3556.728337 | 97.181825 |
| 3560.58596 | 89.920381 | | 3560.58596 | 86.884744 | | 3560.58596 | 97.304346 |
| 3564.443583 | 90.156729 | | 3564.443583 | 87.182524 | | 3564.443583 | 97.437957 |
| 3568.301205 | 90.393838 | | 3568.301205 | 87.487386 | | 3568.301205 | 97.57812 |
| 3572.158828 | 90.634945 | | 3572.158828 | 87.77655 | | 3572.158828 | 97.718526 |
| 3576.016451 | 90.870593 | | 3576.016451 | 88.060339 | | 3576.016451 | 97.851094 |
| 3579.874074 | 91.095721 | | 3579.874074 | 88.346369 | | 3579.874074 | 97.976044 |
| 3583.731697 | 91.341267 | | 3583.731697 | 88.641532 | | 3583.731697 | 98.11431 |
| 3587.58932 | 91.607044 | | 3587.58932 | 88.943962 | | 3587.58932 | 98.262392 |
| 3591.446943 | 91.860273 | | 3591.446943 | 89.234669 | | 3591.446943 | 98.397868 |
| 3595.304566 | 92.110345 | | 3595.304566 | 89.527022 | | 3595.304566 | 98.538144 |
| 3599.162189 | 92.370193 | | 3599.162189 | 89.832639 | | 3599.162189 | 98.695775 |
| 3603.019812 | 92.634653 | | 3603.019812 | 90.132068 | | 3603.019812 | 98.853861 |
| 3606.877435 | 92.908165 | | 3606.877435 | 90.436785 | | 3606.877435 | 99.014744 |

Table B-1.—FTIR data of the CA versus CA-GMA membranes presented on figure 10 and CA versus CA-GMA-IDA presented on figure 11

| CA | | | CA-GMA | | | CA-GMA-IDA | |
|---|---|---|---|---|---|---|---|
| 3610.735058 | 93.18884 | | 3610.735058 | 90.750051 | | 3610.735058 | 99.184481 |
| 3614.592681 | 93.481593 | | 3614.592681 | 91.058424 | | 3614.592681 | 99.36469 |
| 3618.450303 | 93.792778 | | 3618.450303 | 91.381347 | | 3618.450303 | 99.562044 |
| 3622.307926 | 94.101492 | | 3622.307926 | 91.712336 | | 3622.307926 | 99.764601 |
| 3626.165549 | 94.415203 | | 3626.165549 | 92.052406 | | 3626.165549 | 99.976128 |
| 3630.023172 | 94.758 | | 3630.023172 | 92.413783 | | 3630.023172 | 100.216743 |
| 3633.880795 | 95.110287 | | 3633.880795 | 92.765462 | | 3633.880795 | 100.462023 |
| 3637.738418 | 95.469632 | | 3637.738418 | 93.127664 | | 3637.738418 | 100.705722 |
| 3641.596041 | 95.841821 | | 3641.596041 | 93.517896 | | 3641.596041 | 100.976855 |
| 3645.453664 | 96.233558 | | 3645.453664 | 93.926193 | | 3645.453664 | 101.27283 |
| 3649.311287 | 96.65547 | | 3649.311287 | 94.36862 | | 3649.311287 | 101.581049 |
| 3653.16891 | 97.069308 | | 3653.16891 | 94.811743 | | 3653.16891 | 101.886002 |
| 3657.026533 | 97.473439 | | 3657.026533 | 95.247216 | | 3657.026533 | 102.18248 |
| 3660.884156 | 97.883653 | | 3660.884156 | 95.695245 | | 3660.884156 | 102.477231 |
| 3664.741779 | 98.281044 | | 3664.741779 | 96.134942 | | 3664.741779 | 102.763385 |
| 3668.599401 | 98.674288 | | 3668.599401 | 96.575482 | | 3668.599401 | 103.046497 |
| 3672.457024 | 99.057958 | | 3672.457024 | 97.014945 | | 3672.457024 | 103.319484 |
| 3676.314647 | 99.41871 | | 3676.314647 | 97.429208 | | 3676.314647 | 103.562756 |
| 3680.17227 | 99.736194 | | 3680.17227 | 97.79899 | | 3680.17227 | 103.774474 |
| 3684.029893 | 100.000981 | | 3684.029893 | 98.123231 | | 3684.029893 | 103.963216 |
| 3687.887516 | 100.252582 | | 3687.887516 | 98.433476 | | 3687.887516 | 104.13912 |
| 3691.745139 | 100.489499 | | 3691.745139 | 98.714493 | | 3691.745139 | 104.289875 |
| 3695.602762 | 100.689138 | | 3695.602762 | 98.943848 | | 3695.602762 | 104.416253 |
| 3699.460385 | 100.863342 | | 3699.460385 | 99.148631 | | 3699.460385 | 104.533969 |
| 3703.318008 | 101.013864 | | 3703.318008 | 99.329997 | | 3703.318008 | 104.627775 |
| 3707.175631 | 101.144038 | | 3707.175631 | 99.488188 | | 3707.175631 | 104.711409 |
| 3711.033254 | 101.263488 | | 3711.033254 | 99.641588 | | 3711.033254 | 104.807496 |
| 3714.890877 | 101.365571 | | 3714.890877 | 99.77264 | | 3714.890877 | 104.886032 |
| 3718.7485 | 101.446035 | | 3718.7485 | 99.87136 | | 3718.7485 | 104.942381 |
| 3722.606122 | 101.518004 | | 3722.606122 | 99.96193 | | 3722.606122 | 104.998153 |
| 3726.463745 | 101.589071 | | 3726.463745 | 100.05205 | | 3726.463745 | 105.04715 |
| 3730.321368 | 101.65936 | | 3730.321368 | 100.140714 | | 3730.321368 | 105.094922 |
| 3734.178991 | 101.727225 | | 3734.178991 | 100.221944 | | 3734.178991 | 105.146555 |
| 3738.036614 | 101.782178 | | 3738.036614 | 100.283873 | | 3738.036614 | 105.187207 |
| 3741.894237 | 101.826325 | | 3741.894237 | 100.33662 | | 3741.894237 | 105.220212 |
| 3745.75186 | 101.875474 | | 3745.75186 | 100.39231 | | 3745.75186 | 105.260765 |
| 3749.609483 | 101.924545 | | 3749.609483 | 100.445288 | | 3749.609483 | 105.30824 |
| 3753.467106 | 101.961272 | | 3753.467106 | 100.489922 | | 3753.467106 | 105.346551 |
| 3757.324729 | 101.999234 | | 3757.324729 | 100.529961 | | 3757.324729 | 105.372206 |
| 3761.182352 | 102.038053 | | 3761.182352 | 100.566394 | | 3761.182352 | 105.39626 |

Table B-1.—FTIR data of the CA versus CA-GMA membranes presented on figure 10 and CA versus CA-GMA-IDA presented on figure 11

| CA | | | CA-GMA | | | CA-GMA-IDA | |
|---|---|---|---|---|---|---|---|
| 3765.039975 | 102.061496 | | 3765.039975 | 100.600052 | | 3765.039975 | 105.419408 |
| 3768.897598 | 102.088995 | | 3768.897598 | 100.640752 | | 3768.897598 | 105.441637 |
| 3772.75522 | 102.12686 | | 3772.75522 | 100.683238 | | 3772.75522 | 105.466929 |
| 3776.612843 | 102.155496 | | 3776.612843 | 100.719665 | | 3776.612843 | 105.495329 |
| 3780.470466 | 102.179062 | | 3780.470466 | 100.753241 | | 3780.470466 | 105.518467 |
| 3784.328089 | 102.2001 | | 3784.328089 | 100.779935 | | 3784.328089 | 105.532088 |
| 3788.185712 | 102.216893 | | 3788.185712 | 100.799526 | | 3788.185712 | 105.543509 |
| 3792.043335 | 102.235535 | | 3792.043335 | 100.815271 | | 3792.043335 | 105.553704 |
| 3795.900958 | 102.259901 | | 3795.900958 | 100.837726 | | 3795.900958 | 105.570844 |
| 3799.758581 | 102.289034 | | 3799.758581 | 100.874915 | | 3799.758581 | 105.60048 |
| 3803.616204 | 102.315314 | | 3803.616204 | 100.913013 | | 3803.616204 | 105.630664 |
| 3807.473827 | 102.337507 | | 3807.473827 | 100.942772 | | 3807.473827 | 105.6523 |
| 3811.33145 | 102.356924 | | 3811.33145 | 100.967221 | | 3811.33145 | 105.668536 |
| 3815.189073 | 102.376097 | | 3815.189073 | 100.995158 | | 3815.189073 | 105.693984 |
| 3819.046696 | 102.395399 | | 3819.046696 | 101.020296 | | 3819.046696 | 105.717255 |
| 3822.904318 | 102.409188 | | 3822.904318 | 101.029878 | | 3822.904318 | 105.724993 |
| 3826.761941 | 102.423355 | | 3826.761941 | 101.040569 | | 3826.761941 | 105.735423 |
| 3830.619564 | 102.444087 | | 3830.619564 | 101.057946 | | 3830.619564 | 105.749765 |
| 3834.477187 | 102.468919 | | 3834.477187 | 101.078292 | | 3834.477187 | 105.769026 |
| 3838.33481 | 102.493475 | | 3838.33481 | 101.108524 | | 3838.33481 | 105.794901 |
| 3842.192433 | 102.5124 | | 3842.192433 | 101.126563 | | 3842.192433 | 105.808535 |
| 3846.050056 | 102.523591 | | 3846.050056 | 101.12866 | | 3846.050056 | 105.815088 |
| 3849.907679 | 102.534512 | | 3849.907679 | 101.152348 | | 3849.907679 | 105.833701 |
| 3853.765302 | 102.548303 | | 3853.765302 | 101.188354 | | 3853.765302 | 105.856872 |
| 3857.622925 | 102.549676 | | 3857.622925 | 101.200052 | | 3857.622925 | 105.863929 |
| 3861.480548 | 102.549084 | | 3861.480548 | 101.198832 | | 3861.480548 | 105.862597 |
| 3865.338171 | 102.568775 | | 3865.338171 | 101.20516 | | 3865.338171 | 105.874145 |
| 3869.195794 | 102.593641 | | 3869.195794 | 101.225948 | | 3869.195794 | 105.892368 |
| 3873.053417 | 102.605276 | | 3873.053417 | 101.248561 | | 3873.053417 | 105.905821 |
| 3876.911039 | 102.604181 | | 3876.911039 | 101.250447 | | 3876.911039 | 105.916761 |
| 3880.768662 | 102.606424 | | 3880.768662 | 101.250634 | | 3880.768662 | 105.923742 |
| 3884.626285 | 102.626281 | | 3884.626285 | 101.270059 | | 3884.626285 | 105.934147 |
| 3888.483908 | 102.646892 | | 3888.483908 | 101.285501 | | 3888.483908 | 105.946224 |
| 3892.341531 | 102.657028 | | 3892.341531 | 101.285998 | | 3892.341531 | 105.946085 |
| 3896.199154 | 102.665915 | | 3896.199154 | 101.295965 | | 3896.199154 | 105.95655 |
| 3900.056777 | 102.676321 | | 3900.056777 | 101.320518 | | 3900.056777 | 105.984039 |
| 3903.9144 | 102.68805 | | 3903.9144 | 101.337344 | | 3903.9144 | 105.997144 |
| 3907.772023 | 102.692427 | | 3907.772023 | 101.33645 | | 3907.772023 | 105.99822 |
| 3911.629646 | 102.690358 | | 3911.629646 | 101.329654 | | 3911.629646 | 106.000794 |
| 3915.487269 | 102.703166 | | 3915.487269 | 101.337979 | | 3915.487269 | 106.007909 |

Table B-1.—FTIR data of the CA versus CA-GMA membranes presented on figure 10 and CA versus CA-GMA-IDA presented on figure 11

| CA | | | CA-GMA | | | CA-GMA-IDA | |
|---|---|---|---|---|---|---|---|
| 3919.344892 | 102.720092 | | 3919.344892 | 101.358659 | | 3919.344892 | 106.024185 |
| 3923.202515 | 102.718402 | | 3923.202515 | 101.368418 | | 3923.202515 | 106.0382 |
| 3927.060137 | 102.715995 | | 3927.060137 | 101.371457 | | 3927.060137 | 106.041908 |
| 3930.91776 | 102.723511 | | 3930.91776 | 101.378797 | | 3930.91776 | 106.04042 |
| 3934.775383 | 102.729943 | | 3934.775383 | 101.382621 | | 3934.775383 | 106.040631 |
| 3938.633006 | 102.739189 | | 3938.633006 | 101.388196 | | 3938.633006 | 106.053234 |
| 3942.490629 | 102.751092 | | 3942.490629 | 101.4035 | | 3942.490629 | 106.072899 |
| 3946.348252 | 102.755337 | | 3946.348252 | 101.409491 | | 3946.348252 | 106.080979 |
| 3950.205875 | 102.755327 | | 3950.205875 | 101.401044 | | 3950.205875 | 106.083372 |
| 3954.063498 | 102.760342 | | 3954.063498 | 101.402969 | | 3954.063498 | 106.090291 |
| 3957.921121 | 102.77251 | | 3957.921121 | 101.419032 | | 3957.921121 | 106.096549 |
| 3961.778744 | 102.787478 | | 3961.778744 | 101.431385 | | 3961.778744 | 106.107054 |
| 3965.636367 | 102.796453 | | 3965.636367 | 101.43531 | | 3965.636367 | 106.117578 |
| 3969.49399 | 102.802054 | | 3969.49399 | 101.443848 | | 3969.49399 | 106.123284 |
| 3973.351613 | 102.812346 | | 3973.351613 | 101.457847 | | 3973.351613 | 106.135417 |
| 3977.209235 | 102.8188 | | 3977.209235 | 101.461341 | | 3977.209235 | 106.145246 |
| 3981.066858 | 102.818672 | | 3981.066858 | 101.462407 | | 3981.066858 | 106.148929 |
| 3984.924481 | 102.824626 | | 3984.924481 | 101.474284 | | 3984.924481 | 106.160698 |
| 3988.782104 | 102.839096 | | 3988.782104 | 101.487171 | | 3988.782104 | 106.17962 |
| 3992.639727 | 102.850161 | | 3992.639727 | 101.493524 | | 3992.639727 | 106.192065 |
| 3996.49735 | 102.855414 | | 3996.49735 | 101.499321 | | 3996.49735 | 106.195233 |
| 4000.354973 | 102.868196 | | 4000.354973 | 101.515097 | | 4000.354973 | 106.209826 |

Table B-2.—FTIR peaks data for figure 20: FTIR spectra comparing clean membranes and fouled membranes

| Clean membrane | | | Biofouled membrane | |
|---|---|---|---|---|
| XLabel | Wavenumber | | XLabel | Wavenumber |
| YLabel | %Transmittance | | YLabel | %Transmittance |
| FileType | %Transmittance | | FileType | %Transmittance |
| DisplayDirection | 20300 | | DisplayDirection | 20300 |
| PeakDirection | 20311 | | PeakDirection | 20311 |
| 698.229749 | 98.764786 | | 698.229749 | 96.102003 |
| 702.087372 | 98.753744 | | 702.087372 | 96.095694 |
| 705.944995 | 98.781873 | | 705.944995 | 96.062559 |
| 709.802618 | 98.765525 | | 709.802618 | 96.049093 |
| 713.660241 | 98.742882 | | 713.660241 | 96.027987 |
| 717.517864 | 98.7604 | | 717.517864 | 95.978629 |
| 721.375487 | 98.788761 | | 721.375487 | 95.94108 |
| 725.23311 | 98.802746 | | 725.23311 | 95.946683 |
| 729.090733 | 98.813375 | | 729.090733 | 95.99157 |
| 732.948356 | 98.836373 | | 732.948356 | 96.050815 |
| 736.805979 | 98.881672 | | 736.805979 | 96.121781 |
| 740.663602 | 98.905397 | | 740.663602 | 96.225195 |
| 744.521224 | 98.907958 | | 744.521224 | 96.334039 |
| 748.378847 | 98.9406 | | 748.378847 | 96.411654 |
| 752.23647 | 98.950268 | | 752.23647 | 96.472146 |
| 756.094093 | 98.938593 | | 756.094093 | 96.522933 |
| 759.951716 | 98.955082 | | 759.951716 | 96.566265 |
| 763.809339 | 98.959846 | | 763.809339 | 96.645492 |
| 767.666962 | 98.960005 | | 767.666962 | 96.767706 |
| 771.524585 | 98.982195 | | 771.524585 | 96.857893 |
| 775.382208 | 99.006888 | | 775.382208 | 96.909358 |
| 779.239831 | 99.021048 | | 779.239831 | 96.987905 |
| 783.097454 | 99.032713 | | 783.097454 | 97.087064 |
| 786.955077 | 99.055577 | | 786.955077 | 97.19424 |
| 790.8127 | 99.082457 | | 790.8127 | 97.302944 |
| 794.670323 | 99.117813 | | 794.670323 | 97.391837 |
| 798.527945 | 99.158311 | | 798.527945 | 97.498598 |
| 802.385568 | 99.182598 | | 802.385568 | 97.613923 |
| 806.243191 | 99.197549 | | 806.243191 | 97.694347 |
| 810.100814 | 99.212209 | | 810.100814 | 97.770809 |
| 813.958437 | 99.219585 | | 813.958437 | 97.858426 |
| 817.81606 | 99.228471 | | 817.81606 | 97.939511 |

Table B-2.—FTIR peaks data for figure 20: FTIR spectra comparing clean membranes and fouled membranes

| Clean membrane | | | Biofouled membrane | |
|---|---|---|---|---|
| 821.673683 | 99.25944 | | 821.673683 | 98.012577 |
| 825.531306 | 99.29228 | | 825.531306 | 98.087615 |
| 829.388929 | 99.314846 | | 829.388929 | 98.175795 |
| 833.246552 | 99.349261 | | 833.246552 | 98.281666 |
| 837.104175 | 99.379829 | | 837.104175 | 98.391106 |
| 840.961798 | 99.392885 | | 840.961798 | 98.49972 |
| 844.819421 | 99.401904 | | 844.819421 | 98.631432 |
| 848.677043 | 99.416628 | | 848.677043 | 98.783249 |
| 852.534666 | 99.436323 | | 852.534666 | 98.933957 |
| 856.392289 | 99.459722 | | 856.392289 | 99.038311 |
| 860.249912 | 99.495269 | | 860.249912 | 99.049822 |
| 864.107535 | 99.51896 | | 864.107535 | 99.018511 |
| 867.965158 | 99.526561 | | 867.965158 | 98.997597 |
| 871.822781 | 99.541473 | | 871.822781 | 99.004788 |
| 875.680404 | 99.542357 | | 875.680404 | 99.042341 |
| 879.538027 | 99.537437 | | 879.538027 | 99.089816 |
| 883.39565 | 99.557411 | | 883.39565 | 99.145586 |
| 887.253273 | 99.578226 | | 887.253273 | 99.208596 |
| 891.110896 | 99.59719 | | 891.110896 | 99.261037 |
| 894.968519 | 99.623661 | | 894.968519 | 99.302346 |
| 898.826141 | 99.635185 | | 898.826141 | 99.353321 |
| 902.683764 | 99.639866 | | 902.683764 | 99.417207 |
| 906.541387 | 99.656711 | | 906.541387 | 99.472005 |
| 910.39901 | 99.679192 | | 910.39901 | 99.518246 |
| 914.256633 | 99.696714 | | 914.256633 | 99.564939 |
| 918.114256 | 99.703953 | | 918.114256 | 99.618849 |
| 921.971879 | 99.708374 | | 921.971879 | 99.685242 |
| 925.829502 | 99.714469 | | 925.829502 | 99.744874 |
| 929.687125 | 99.716502 | | 929.687125 | 99.798668 |
| 933.544748 | 99.711269 | | 933.544748 | 99.874183 |
| 937.402371 | 99.702381 | | 937.402371 | 99.959199 |
| 941.259994 | 99.704129 | | 941.259994 | 100.024055 |
| 945.117617 | 99.720105 | | 945.117617 | 100.087712 |
| 948.97524 | 99.735139 | | 948.97524 | 100.167616 |
| 952.832862 | 99.743247 | | 952.832862 | 100.237692 |
| 956.690485 | 99.752808 | | 956.690485 | 100.274977 |
| 960.548108 | 99.763399 | | 960.548108 | 100.289221 |

Table B-2.—FTIR peaks data for figure 20: FTIR spectra comparing clean membranes and fouled membranes

| Clean membrane | | | Biofouled membrane | |
|---|---|---|---|---|
| 964.405731 | 99.76571 | | 964.405731 | 100.321678 |
| 968.263354 | 99.761766 | | 968.263354 | 100.361721 |
| 972.120977 | 99.758319 | | 972.120977 | 100.364842 |
| 975.9786 | 99.762236 | | 975.9786 | 100.367398 |
| 979.836223 | 99.775752 | | 979.836223 | 100.392463 |
| 983.693846 | 99.789353 | | 983.693846 | 100.42222 |
| 987.551469 | 99.801647 | | 987.551469 | 100.473044 |
| 991.409092 | 99.805464 | | 991.409092 | 100.533739 |
| 995.266715 | 99.792156 | | 995.266715 | 100.591595 |
| 999.124338 | 99.790263 | | 999.124338 | 100.671888 |
| 1002.98196 | 99.808632 | | 1002.98196 | 100.75521 |
| 1006.839583 | 99.814883 | | 1006.839583 | 100.811283 |
| 1010.697206 | 99.816651 | | 1010.697206 | 100.841083 |
| 1014.554829 | 99.831052 | | 1014.554829 | 100.821632 |
| 1018.412452 | 99.834168 | | 1018.412452 | 100.761249 |
| 1022.270075 | 99.825839 | | 1022.270075 | 100.699087 |
| 1026.127698 | 99.827358 | | 1026.127698 | 100.625406 |
| 1029.985321 | 99.837711 | | 1029.985321 | 100.551903 |
| 1033.842944 | 99.845524 | | 1033.842944 | 100.499066 |
| 1037.700567 | 99.849662 | | 1037.700567 | 100.454267 |
| 1041.55819 | 99.85679 | | 1041.55819 | 100.436762 |
| 1045.415813 | 99.855265 | | 1045.415813 | 100.466676 |
| 1049.273436 | 99.839022 | | 1049.273436 | 100.521858 |
| 1053.131058 | 99.82336 | | 1053.131058 | 100.562319 |
| 1056.988681 | 99.815485 | | 1056.988681 | 100.577243 |
| 1060.846304 | 99.823574 | | 1060.846304 | 100.609877 |
| 1064.703927 | 99.835917 | | 1064.703927 | 100.660662 |
| 1068.56155 | 99.825152 | | 1068.56155 | 100.687446 |
| 1072.419173 | 99.808194 | | 1072.419173 | 100.691812 |
| 1076.276796 | 99.808884 | | 1076.276796 | 100.67827 |
| 1080.134419 | 99.815708 | | 1080.134419 | 100.660815 |
| 1083.992042 | 99.82583 | | 1083.992042 | 100.670095 |
| 1087.849665 | 99.840086 | | 1087.849665 | 100.681334 |
| 1091.707288 | 99.83356 | | 1091.707288 | 100.667723 |
| 1095.564911 | 99.810934 | | 1095.564911 | 100.647558 |
| 1099.422534 | 99.801794 | | 1099.422534 | 100.623718 |
| 1103.280156 | 99.796269 | | 1103.280156 | 100.590896 |

Table B-2.—FTIR peaks data for figure 20: FTIR spectra comparing clean membranes and fouled membranes

| Clean membrane | | | Biofouled membrane | |
|---|---|---|---|---|
| 1107.137779 | 99.790457 | | 1107.137779 | 100.567748 |
| 1110.995402 | 99.800296 | | 1110.995402 | 100.549393 |
| 1114.853025 | 99.813646 | | 1114.853025 | 100.513328 |
| 1118.710648 | 99.821203 | | 1118.710648 | 100.47998 |
| 1122.568271 | 99.826824 | | 1122.568271 | 100.472136 |
| 1126.425894 | 99.81686 | | 1126.425894 | 100.491232 |
| 1130.283517 | 99.797727 | | 1130.283517 | 100.545775 |
| 1134.14114 | 99.795132 | | 1134.14114 | 100.618644 |
| 1137.998763 | 99.790892 | | 1137.998763 | 100.68001 |
| 1141.856386 | 99.774095 | | 1141.856386 | 100.73091 |
| 1145.714009 | 99.769633 | | 1145.714009 | 100.774208 |
| 1149.571632 | 99.771651 | | 1149.571632 | 100.795037 |
| 1153.429255 | 99.774194 | | 1153.429255 | 100.798534 |
| 1157.286877 | 99.785588 | | 1157.286877 | 100.803333 |
| 1161.1445 | 99.787912 | | 1161.1445 | 100.803894 |
| 1165.002123 | 99.775772 | | 1165.002123 | 100.794712 |
| 1168.859746 | 99.772294 | | 1168.859746 | 100.775281 |
| 1172.717369 | 99.776221 | | 1172.717369 | 100.742899 |
| 1176.574992 | 99.76939 | | 1176.574992 | 100.707777 |
| 1180.432615 | 99.764726 | | 1180.432615 | 100.670305 |
| 1184.290238 | 99.767562 | | 1184.290238 | 100.623363 |
| 1188.147861 | 99.768047 | | 1188.147861 | 100.575726 |
| 1192.005484 | 99.775755 | | 1192.005484 | 100.547011 |
| 1195.863107 | 99.783619 | | 1195.863107 | 100.541806 |
| 1199.72073 | 99.781037 | | 1199.72073 | 100.548576 |
| 1203.578353 | 99.782699 | | 1203.578353 | 100.563942 |
| 1207.435975 | 99.787867 | | 1207.435975 | 100.585799 |
| 1211.293598 | 99.781852 | | 1211.293598 | 100.618332 |
| 1215.151221 | 99.777278 | | 1215.151221 | 100.656364 |
| 1219.008844 | 99.787417 | | 1219.008844 | 100.680435 |
| 1222.866467 | 99.79811 | | 1222.866467 | 100.709308 |
| 1226.72409 | 99.803314 | | 1226.72409 | 100.75485 |
| 1230.581713 | 99.801303 | | 1230.581713 | 100.793181 |
| 1234.439336 | 99.794709 | | 1234.439336 | 100.823386 |
| 1238.296959 | 99.794634 | | 1238.296959 | 100.850396 |
| 1242.154582 | 99.796337 | | 1242.154582 | 100.870531 |
| 1246.012205 | 99.807723 | | 1246.012205 | 100.894052 |

Table B-2.—FTIR peaks data for figure 20: FTIR spectra comparing clean membranes and fouled membranes

| Clean membrane | | | Biofouled membrane | |
|---|---|---|---|---|
| 1249.869828 | 99.823093 | | 1249.869828 | 100.908508 |
| 1253.727451 | 99.823073 | | 1253.727451 | 100.873253 |
| 1257.585073 | 99.824595 | | 1257.585073 | 100.782844 |
| 1261.442696 | 99.825046 | | 1261.442696 | 100.660964 |
| 1265.300319 | 99.810787 | | 1265.300319 | 100.532534 |
| 1269.157942 | 99.80122 | | 1269.157942 | 100.428826 |
| 1273.015565 | 99.810006 | | 1273.015565 | 100.359058 |
| 1276.873188 | 99.819816 | | 1276.873188 | 100.310863 |
| 1280.730811 | 99.811363 | | 1280.730811 | 100.261081 |
| 1284.588434 | 99.794258 | | 1284.588434 | 100.204095 |
| 1288.446057 | 99.783405 | | 1288.446057 | 100.167006 |
| 1292.30368 | 99.780706 | | 1292.30368 | 100.141263 |
| 1296.161303 | 99.783185 | | 1296.161303 | 100.108407 |
| 1300.018926 | 99.790323 | | 1300.018926 | 100.080386 |
| 1303.876549 | 99.800602 | | 1303.876549 | 100.052564 |
| 1307.734172 | 99.808681 | | 1307.734172 | 100.027204 |
| 1311.591794 | 99.81077 | | 1311.591794 | 100.014075 |
| 1315.449417 | 99.809765 | | 1315.449417 | 100.003594 |
| 1319.30704 | 99.818573 | | 1319.30704 | 100.000175 |
| 1323.164663 | 99.826655 | | 1323.164663 | 100.012891 |
| 1327.022286 | 99.822821 | | 1327.022286 | 100.032233 |
| 1330.879909 | 99.827222 | | 1330.879909 | 100.04654 |
| 1334.737532 | 99.830279 | | 1334.737532 | 100.049399 |
| 1338.595155 | 99.817509 | | 1338.595155 | 100.040823 |
| 1342.452778 | 99.806979 | | 1342.452778 | 100.032834 |
| 1346.310401 | 99.807467 | | 1346.310401 | 100.032695 |
| 1350.168024 | 99.812278 | | 1350.168024 | 100.030796 |
| 1354.025647 | 99.807491 | | 1354.025647 | 100.028594 |
| 1357.88327 | 99.800614 | | 1357.88327 | 100.039734 |
| 1361.740892 | 99.815522 | | 1361.740892 | 100.061534 |
| 1365.598515 | 99.841284 | | 1365.598515 | 100.084778 |
| 1369.456138 | 99.84596 | | 1369.456138 | 100.107229 |
| 1373.313761 | 99.832944 | | 1373.313761 | 100.12302 |
| 1377.171384 | 99.833127 | | 1377.171384 | 100.125873 |
| 1381.029007 | 99.839542 | | 1381.029007 | 100.114102 |
| 1384.88663 | 99.832138 | | 1384.88663 | 100.096665 |
| 1388.744253 | 99.824749 | | 1388.744253 | 100.084548 |

Table B-2.—FTIR peaks data for figure 20: FTIR spectra comparing clean membranes and fouled membranes

| Clean membrane | | | Biofouled membrane | |
|---|---|---|---|---|
| 1392.601876 | 99.825628 | | 1392.601876 | 100.062168 |
| 1396.459499 | 99.826737 | | 1396.459499 | 100.018444 |
| 1400.317122 | 99.831479 | | 1400.317122 | 99.970844 |
| 1404.174745 | 99.847129 | | 1404.174745 | 99.924666 |
| 1408.032368 | 99.86491 | | 1408.032368 | 99.882819 |
| 1411.88999 | 99.869383 | | 1411.88999 | 99.848645 |
| 1415.747613 | 99.859303 | | 1415.747613 | 99.811808 |
| 1419.605236 | 99.847699 | | 1419.605236 | 99.798296 |
| 1423.462859 | 99.843875 | | 1423.462859 | 99.827014 |
| 1427.320482 | 99.842625 | | 1427.320482 | 99.853497 |
| 1431.178105 | 99.841855 | | 1431.178105 | 99.873957 |
| 1435.035728 | 99.846339 | | 1435.035728 | 99.912575 |
| 1438.893351 | 99.851895 | | 1438.893351 | 99.93698 |
| 1442.750974 | 99.840837 | | 1442.750974 | 99.927796 |
| 1446.608597 | 99.818934 | | 1446.608597 | 99.894602 |
| 1450.46622 | 99.812672 | | 1450.46622 | 99.844613 |
| 1454.323843 | 99.805498 | | 1454.323843 | 99.807071 |
| 1458.181466 | 99.797615 | | 1458.181466 | 99.806801 |
| 1462.039089 | 99.814673 | | 1462.039089 | 99.821357 |
| 1465.896711 | 99.826305 | | 1465.896711 | 99.818658 |
| 1469.754334 | 99.810203 | | 1469.754334 | 99.814315 |
| 1473.611957 | 99.791889 | | 1473.611957 | 99.812807 |
| 1477.46958 | 99.793138 | | 1477.46958 | 99.795711 |
| 1481.327203 | 99.803311 | | 1481.327203 | 99.779262 |
| 1485.184826 | 99.796932 | | 1485.184826 | 99.768775 |
| 1489.042449 | 99.779217 | | 1489.042449 | 99.758175 |
| 1492.900072 | 99.769153 | | 1492.900072 | 99.743092 |
| 1496.757695 | 99.76598 | | 1496.757695 | 99.714467 |
| 1500.615318 | 99.755792 | | 1500.615318 | 99.68216 |
| 1504.472941 | 99.734654 | | 1504.472941 | 99.654446 |
| 1508.330564 | 99.726692 | | 1508.330564 | 99.633893 |
| 1512.188187 | 99.740227 | | 1512.188187 | 99.613691 |
| 1516.045809 | 99.742709 | | 1516.045809 | 99.577981 |
| 1519.903432 | 99.726527 | | 1519.903432 | 99.53856 |
| 1523.761055 | 99.722905 | | 1523.761055 | 99.499633 |
| 1527.618678 | 99.734584 | | 1527.618678 | 99.445569 |
| 1531.476301 | 99.734371 | | 1531.476301 | 99.383501 |

Table B-2.—FTIR peaks data for figure 20: FTIR spectra comparing clean membranes and fouled membranes

| Clean membrane | | | Biofouled membrane | |
|---|---|---|---|---|
| 1535.333924 | 99.711207 | | 1535.333924 | 99.318738 |
| 1539.191547 | 99.684628 | | 1539.191547 | 99.247799 |
| 1543.04917 | 99.684575 | | 1543.04917 | 99.17671 |
| 1546.906793 | 99.700949 | | 1546.906793 | 99.102836 |
| 1550.764416 | 99.699307 | | 1550.764416 | 99.022193 |
| 1554.622039 | 99.673434 | | 1554.622039 | 98.940291 |
| 1558.479662 | 99.652696 | | 1558.479662 | 98.8608 |
| 1562.337285 | 99.659536 | | 1562.337285 | 98.786583 |
| 1566.194907 | 99.672512 | | 1566.194907 | 98.712785 |
| 1570.05253 | 99.666157 | | 1570.05253 | 98.632607 |
| 1573.910153 | 99.642612 | | 1573.910153 | 98.553319 |
| 1577.767776 | 99.627859 | | 1577.767776 | 98.491299 |
| 1581.625399 | 99.629107 | | 1581.625399 | 98.439044 |
| 1585.483022 | 99.621615 | | 1585.483022 | 98.376412 |
| 1589.340645 | 99.609042 | | 1589.340645 | 98.303122 |
| 1593.198268 | 99.607815 | | 1593.198268 | 98.211465 |
| 1597.055891 | 99.600646 | | 1597.055891 | 98.092625 |
| 1600.913514 | 99.562578 | | 1600.913514 | 97.952511 |
| 1604.771137 | 99.507371 | | 1604.771137 | 97.790835 |
| 1608.62876 | 99.454123 | | 1608.62876 | 97.609335 |
| 1612.486383 | 99.387614 | | 1612.486383 | 97.393192 |
| 1616.344005 | 99.322864 | | 1616.344005 | 97.148466 |
| 1620.201628 | 99.273216 | | 1620.201628 | 96.928514 |
| 1624.059251 | 99.207267 | | 1624.059251 | 96.735961 |
| 1627.916874 | 99.135102 | | 1627.916874 | 96.561206 |
| 1631.774497 | 99.076902 | | 1631.774497 | 96.428611 |
| 1635.63212 | 99.030486 | | 1635.63212 | 96.341599 |
| 1639.489743 | 99.006575 | | 1639.489743 | 96.314502 |
| 1643.347366 | 99.002546 | | 1643.347366 | 96.359831 |
| 1647.204989 | 99.003202 | | 1647.204989 | 96.453306 |
| 1651.062612 | 99.007962 | | 1651.062612 | 96.581258 |
| 1654.920235 | 99.043784 | | 1654.920235 | 96.756198 |
| 1658.777858 | 99.105154 | | 1658.777858 | 96.960933 |
| 1662.635481 | 99.146435 | | 1662.635481 | 97.169093 |
| 1666.493104 | 99.177926 | | 1666.493104 | 97.375073 |
| 1670.350726 | 99.234224 | | 1670.350726 | 97.583069 |
| 1674.208349 | 99.305479 | | 1674.208349 | 97.8046 |

Table B-2.—FTIR peaks data for figure 20: FTIR spectra comparing clean membranes and fouled membranes

| Clean membrane | | | Biofouled membrane | |
|---|---|---|---|---|
| 1678.065972 | 99.366391 | | 1678.065972 | 98.032333 |
| 1681.923595 | 99.417121 | | 1681.923595 | 98.250221 |
| 1685.781218 | 99.477276 | | 1685.781218 | 98.456976 |
| 1689.638841 | 99.536021 | | 1689.638841 | 98.652231 |
| 1693.496464 | 99.573802 | | 1693.496464 | 98.825287 |
| 1697.354087 | 99.61132 | | 1697.354087 | 98.976087 |
| 1701.21171 | 99.662108 | | 1701.21171 | 99.113979 |
| 1705.069333 | 99.709979 | | 1705.069333 | 99.240923 |
| 1708.926956 | 99.745531 | | 1708.926956 | 99.354192 |
| 1712.784579 | 99.768501 | | 1712.784579 | 99.454601 |
| 1716.642202 | 99.793779 | | 1716.642202 | 99.547674 |
| 1720.499824 | 99.825993 | | 1720.499824 | 99.630031 |
| 1724.357447 | 99.846822 | | 1724.357447 | 99.711166 |
| 1728.21507 | 99.856481 | | 1728.21507 | 99.794832 |
| 1732.072693 | 99.851754 | | 1732.072693 | 99.864679 |
| 1735.930316 | 99.841464 | | 1735.930316 | 99.940072 |
| 1739.787939 | 99.856382 | | 1739.787939 | 100.026966 |
| 1743.645562 | 99.874253 | | 1743.645562 | 100.093767 |
| 1747.503185 | 99.88155 | | 1747.503185 | 100.13335 |
| 1751.360808 | 99.896719 | | 1751.360808 | 100.145681 |
| 1755.218431 | 99.912552 | | 1755.218431 | 100.138208 |
| 1759.076054 | 99.935124 | | 1759.076054 | 100.127034 |
| 1762.933677 | 99.957738 | | 1762.933677 | 100.105291 |
| 1766.7913 | 99.954852 | | 1766.7913 | 100.080534 |
| 1770.648922 | 99.9373 | | 1770.648922 | 100.074874 |
| 1774.506545 | 99.929428 | | 1774.506545 | 100.080818 |
| 1778.364168 | 99.932118 | | 1778.364168 | 100.08428 |
| 1782.221791 | 99.936227 | | 1782.221791 | 100.091002 |
| 1786.079414 | 99.933969 | | 1786.079414 | 100.096051 |
| 1789.937037 | 99.925893 | | 1789.937037 | 100.092184 |
| 1793.79466 | 99.927921 | | 1793.79466 | 100.08665 |
| 1797.652283 | 99.935557 | | 1797.652283 | 100.091154 |
| 1801.509906 | 99.937651 | | 1801.509906 | 100.102101 |
| 1805.367529 | 99.939779 | | 1805.367529 | 100.106383 |
| 1809.225152 | 99.937728 | | 1809.225152 | 100.111019 |
| 1813.082775 | 99.939474 | | 1813.082775 | 100.120594 |
| 1816.940398 | 99.946268 | | 1816.940398 | 100.124378 |

Table B-2.—FTIR peaks data for figure 20: FTIR spectra comparing clean membranes and fouled membranes

| Clean membrane | | | Biofouled membrane | |
|---|---|---|---|---|
| 1820.798021 | 99.946819 | | 1820.798021 | 100.125419 |
| 1824.655643 | 99.947864 | | 1824.655643 | 100.134408 |
| 1828.513266 | 99.94167 | | 1828.513266 | 100.147092 |
| 1832.370889 | 99.937893 | | 1832.370889 | 100.15009 |
| 1836.228512 | 99.94829 | | 1836.228512 | 100.154054 |
| 1840.086135 | 99.944435 | | 1840.086135 | 100.16864 |
| 1843.943758 | 99.935662 | | 1843.943758 | 100.171371 |
| 1847.801381 | 99.943869 | | 1847.801381 | 100.163643 |
| 1851.659004 | 99.954237 | | 1851.659004 | 100.1664 |
| 1855.516627 | 99.960356 | | 1855.516627 | 100.16916 |
| 1859.37425 | 99.958955 | | 1859.37425 | 100.164405 |
| 1863.231873 | 99.949908 | | 1863.231873 | 100.166452 |
| 1867.089496 | 99.944713 | | 1867.089496 | 100.1748 |
| 1870.947119 | 99.945695 | | 1870.947119 | 100.177508 |
| 1874.804741 | 99.947113 | | 1874.804741 | 100.178106 |
| 1878.662364 | 99.949598 | | 1878.662364 | 100.180891 |
| 1882.519987 | 99.956181 | | 1882.519987 | 100.183808 |
| 1886.37761 | 99.957672 | | 1886.37761 | 100.18945 |
| 1890.235233 | 99.95203 | | 1890.235233 | 100.1899 |
| 1894.092856 | 99.950235 | | 1894.092856 | 100.178128 |
| 1897.950479 | 99.952409 | | 1897.950479 | 100.169709 |
| 1901.808102 | 99.952291 | | 1901.808102 | 100.173694 |
| 1905.665725 | 99.947953 | | 1905.665725 | 100.178257 |
| 1909.523348 | 99.945106 | | 1909.523348 | 100.175128 |
| 1913.380971 | 99.946165 | | 1913.380971 | 100.167199 |
| 1917.238594 | 99.948449 | | 1917.238594 | 100.160444 |
| 1921.096217 | 99.955936 | | 1921.096217 | 100.152376 |
| 1924.953839 | 99.96491 | | 1924.953839 | 100.143517 |
| 1928.811462 | 99.966199 | | 1928.811462 | 100.145832 |
| 1932.669085 | 99.957451 | | 1932.669085 | 100.147328 |
| 1936.526708 | 99.942734 | | 1936.526708 | 100.135166 |
| 1940.384331 | 99.932241 | | 1940.384331 | 100.125267 |
| 1944.241954 | 99.928639 | | 1944.241954 | 100.121076 |
| 1948.099577 | 99.932758 | | 1948.099577 | 100.117079 |
| 1951.9572 | 99.945744 | | 1951.9572 | 100.11218 |
| 1955.814823 | 99.951239 | | 1955.814823 | 100.108038 |
| 1959.672446 | 99.943395 | | 1959.672446 | 100.109664 |

Table B-2.—FTIR peaks data for figure 20: FTIR spectra comparing clean membranes and fouled membranes

| Clean membrane | | | Biofouled membrane | |
|---|---|---|---|---|
| 1963.530069 | 99.937521 | | 1963.530069 | 100.105689 |
| 1967.387692 | 99.934907 | | 1967.387692 | 100.0937 |
| 1971.245315 | 99.936186 | | 1971.245315 | 100.08747 |
| 1975.102938 | 99.940885 | | 1975.102938 | 100.080972 |
| 1978.96056 | 99.934355 | | 1978.96056 | 100.065975 |
| 1982.818183 | 99.927787 | | 1982.818183 | 100.052628 |
| 1986.675806 | 99.929107 | | 1986.675806 | 100.050623 |
| 1990.533429 | 99.919867 | | 1990.533429 | 100.05173 |
| 1994.391052 | 99.911604 | | 1994.391052 | 100.0446 |
| 1998.248675 | 99.91585 | | 1998.248675 | 100.035046 |
| 2002.106298 | 99.917208 | | 2002.106298 | 100.026072 |
| 2005.963921 | 99.916339 | | 2005.963921 | 100.016541 |
| 2009.821544 | 99.917276 | | 2009.821544 | 100.010605 |
| 2013.679167 | 99.915044 | | 2013.679167 | 99.99704 |
| 2017.53679 | 99.914002 | | 2017.53679 | 99.975413 |
| 2021.394413 | 99.919133 | | 2021.394413 | 99.965007 |
| 2025.252036 | 99.922803 | | 2025.252036 | 99.96161 |
| 2029.109658 | 99.917573 | | 2029.109658 | 99.94958 |
| 2032.967281 | 99.912593 | | 2032.967281 | 99.933695 |
| 2036.824904 | 99.914431 | | 2036.824904 | 99.923918 |
| 2040.682527 | 99.914436 | | 2040.682527 | 99.912197 |
| 2044.54015 | 99.908329 | | 2044.54015 | 99.898211 |
| 2048.397773 | 99.902186 | | 2048.397773 | 99.89273 |
| 2052.255396 | 99.899512 | | 2052.255396 | 99.887603 |
| 2056.113019 | 99.895256 | | 2056.113019 | 99.880938 |
| 2059.970642 | 99.894239 | | 2059.970642 | 99.875816 |
| 2063.828265 | 99.899062 | | 2063.828265 | 99.869681 |
| 2067.685888 | 99.894724 | | 2067.685888 | 99.866279 |
| 2071.543511 | 99.889745 | | 2071.543511 | 99.857262 |
| 2075.401134 | 99.893947 | | 2075.401134 | 99.840723 |
| 2079.258756 | 99.894645 | | 2079.258756 | 99.832782 |
| 2083.116379 | 99.899573 | | 2083.116379 | 99.831756 |
| 2086.974002 | 99.908902 | | 2086.974002 | 99.821866 |
| 2090.831625 | 99.908281 | | 2090.831625 | 99.808021 |
| 2094.689248 | 99.903537 | | 2094.689248 | 99.797919 |
| 2098.546871 | 99.898582 | | 2098.546871 | 99.784848 |
| 2102.404494 | 99.896155 | | 2102.404494 | 99.781224 |

Table B-2.—FTIR peaks data for figure 20: FTIR spectra comparing clean membranes and fouled membranes

| Clean membrane | | | Biofouled membrane | |
|---|---|---|---|---|
| 2106.262117 | 99.895517 | | 2106.262117 | 99.782959 |
| 2110.11974 | 99.885878 | | 2110.11974 | 99.770328 |
| 2113.977363 | 99.87832 | | 2113.977363 | 99.765493 |
| 2117.834986 | 99.887224 | | 2117.834986 | 99.770125 |
| 2121.692609 | 99.899064 | | 2121.692609 | 99.764597 |
| 2125.550232 | 99.899942 | | 2125.550232 | 99.760923 |
| 2129.407854 | 99.898233 | | 2129.407854 | 99.756705 |
| 2133.265477 | 99.903168 | | 2133.265477 | 99.748429 |
| 2137.1231 | 99.905544 | | 2137.1231 | 99.747936 |
| 2140.980723 | 99.900035 | | 2140.980723 | 99.751434 |
| 2144.838346 | 99.897118 | | 2144.838346 | 99.755967 |
| 2148.695969 | 99.899824 | | 2148.695969 | 99.756538 |
| 2152.553592 | 99.899508 | | 2152.553592 | 99.753097 |
| 2156.411215 | 99.898615 | | 2156.411215 | 99.755277 |
| 2160.268838 | 99.907301 | | 2160.268838 | 99.75904 |
| 2164.126461 | 99.912294 | | 2164.126461 | 99.765707 |
| 2167.984084 | 99.905457 | | 2167.984084 | 99.770022 |
| 2171.841707 | 99.904905 | | 2171.841707 | 99.762769 |
| 2175.69933 | 99.907087 | | 2175.69933 | 99.764511 |
| 2179.556953 | 99.910419 | | 2179.556953 | 99.781184 |
| 2183.414575 | 99.921588 | | 2183.414575 | 99.789871 |
| 2187.272198 | 99.923325 | | 2187.272198 | 99.783493 |
| 2191.129821 | 99.923229 | | 2191.129821 | 99.776354 |
| 2194.987444 | 99.925536 | | 2194.987444 | 99.779251 |
| 2198.845067 | 99.918843 | | 2198.845067 | 99.786289 |
| 2202.70269 | 99.922433 | | 2202.70269 | 99.789552 |
| 2206.560313 | 99.928933 | | 2206.560313 | 99.790375 |
| 2210.417936 | 99.928227 | | 2210.417936 | 99.792264 |
| 2214.275559 | 99.936574 | | 2214.275559 | 99.799812 |
| 2218.133182 | 99.941409 | | 2218.133182 | 99.814997 |
| 2221.990805 | 99.937126 | | 2221.990805 | 99.823323 |
| 2225.848428 | 99.935658 | | 2225.848428 | 99.817402 |
| 2229.706051 | 99.944058 | | 2229.706051 | 99.815562 |
| 2233.563673 | 99.961079 | | 2233.563673 | 99.82413 |
| 2237.421296 | 99.966707 | | 2237.421296 | 99.832449 |
| 2241.278919 | 99.961006 | | 2241.278919 | 99.836424 |
| 2245.136542 | 99.958896 | | 2245.136542 | 99.842891 |

Table B-2.—FTIR peaks data for figure 20: FTIR spectra comparing clean membranes and fouled membranes

| Clean membrane | | | Biofouled membrane | |
|---|---|---|---|---|
| 2248.994165 | 99.959544 | | 2248.994165 | 99.85798 |
| 2252.851788 | 99.965269 | | 2252.851788 | 99.872075 |
| 2256.709411 | 99.969967 | | 2256.709411 | 99.88194 |
| 2260.567034 | 99.966159 | | 2260.567034 | 99.889709 |
| 2264.424657 | 99.969215 | | 2264.424657 | 99.882255 |
| 2268.28228 | 99.972519 | | 2268.28228 | 99.865447 |
| 2272.139903 | 99.960871 | | 2272.139903 | 99.863502 |
| 2275.997526 | 99.955762 | | 2275.997526 | 99.873841 |
| 2279.855149 | 99.958345 | | 2279.855149 | 99.880756 |
| 2283.712771 | 99.959631 | | 2283.712771 | 99.881259 |
| 2287.570394 | 99.970538 | | 2287.570394 | 99.881308 |
| 2291.428017 | 99.976935 | | 2291.428017 | 99.891627 |
| 2295.28564 | 99.969608 | | 2295.28564 | 99.904863 |
| 2299.143263 | 99.96481 | | 2299.143263 | 99.902322 |
| 2303.000886 | 99.976567 | | 2303.000886 | 99.891938 |
| 2306.858509 | 99.988881 | | 2306.858509 | 99.893858 |
| 2310.716132 | 99.978647 | | 2310.716132 | 99.907143 |
| 2314.573755 | 99.974018 | | 2314.573755 | 99.912252 |
| 2318.431378 | 99.97945 | | 2318.431378 | 99.898756 |
| 2322.289001 | 99.963088 | | 2322.289001 | 99.880547 |
| 2326.146624 | 99.944563 | | 2326.146624 | 99.873269 |
| 2330.004247 | 99.946795 | | 2330.004247 | 99.874568 |
| 2333.86187 | 99.956525 | | 2333.86187 | 99.875405 |
| 2337.719492 | 99.964197 | | 2337.719492 | 99.869693 |
| 2341.577115 | 99.970577 | | 2341.577115 | 99.866556 |
| 2345.434738 | 99.973606 | | 2345.434738 | 99.886032 |
| 2349.292361 | 99.974224 | | 2349.292361 | 99.904975 |
| 2353.149984 | 99.966042 | | 2353.149984 | 99.890022 |
| 2357.007607 | 99.948375 | | 2357.007607 | 99.867765 |
| 2360.86523 | 99.949656 | | 2360.86523 | 99.861758 |
| 2364.722853 | 99.962118 | | 2364.722853 | 99.862872 |
| 2368.580476 | 99.964563 | | 2368.580476 | 99.875433 |
| 2372.438099 | 99.97305 | | 2372.438099 | 99.896299 |
| 2376.295722 | 99.979717 | | 2376.295722 | 99.909431 |
| 2380.153345 | 99.981743 | | 2380.153345 | 99.915042 |
| 2384.010968 | 99.994204 | | 2384.010968 | 99.916198 |
| 2387.86859 | 100.007908 | | 2387.86859 | 99.913546 |

Table B-2.—FTIR peaks data for figure 20: FTIR spectra comparing clean membranes and fouled membranes

| Clean membrane | | | Biofouled membrane | |
|---|---|---|---|---|
| 2391.726213 | 100.015462 | | 2391.726213 | 99.92075 |
| 2395.583836 | 100.011558 | | 2395.583836 | 99.934439 |
| 2399.441459 | 100.001822 | | 2399.441459 | 99.935716 |
| 2403.299082 | 100.003804 | | 2403.299082 | 99.929875 |
| 2407.156705 | 100.008241 | | 2407.156705 | 99.924611 |
| 2411.014328 | 100.001203 | | 2411.014328 | 99.926054 |
| 2414.871951 | 99.996338 | | 2414.871951 | 99.935933 |
| 2418.729574 | 100.00896 | | 2418.729574 | 99.936794 |
| 2422.587197 | 100.02489 | | 2422.587197 | 99.928349 |
| 2426.44482 | 100.029563 | | 2426.44482 | 99.914925 |
| 2430.302443 | 100.027703 | | 2430.302443 | 99.903113 |
| 2434.160066 | 100.021307 | | 2434.160066 | 99.908602 |
| 2438.017688 | 100.023763 | | 2438.017688 | 99.913989 |
| 2441.875311 | 100.034275 | | 2441.875311 | 99.903093 |
| 2445.732934 | 100.03116 | | 2445.732934 | 99.888505 |
| 2449.590557 | 100.028092 | | 2449.590557 | 99.886754 |
| 2453.44818 | 100.033178 | | 2453.44818 | 99.8949 |
| 2457.305803 | 100.032923 | | 2457.305803 | 99.89249 |
| 2461.163426 | 100.029564 | | 2461.163426 | 99.890588 |
| 2465.021049 | 100.026645 | | 2465.021049 | 99.898517 |
| 2468.878672 | 100.035579 | | 2468.878672 | 99.903192 |
| 2472.736295 | 100.049704 | | 2472.736295 | 99.906474 |
| 2476.593918 | 100.04855 | | 2476.593918 | 99.903001 |
| 2480.451541 | 100.049067 | | 2480.451541 | 99.892786 |
| 2484.309164 | 100.051737 | | 2484.309164 | 99.886113 |
| 2488.166786 | 100.03592 | | 2488.166786 | 99.877144 |
| 2492.024409 | 100.021978 | | 2492.024409 | 99.863465 |
| 2495.882032 | 100.027419 | | 2495.882032 | 99.857282 |
| 2499.739655 | 100.038892 | | 2499.739655 | 99.861547 |
| 2503.597278 | 100.045696 | | 2503.597278 | 99.865488 |
| 2507.454901 | 100.048696 | | 2507.454901 | 99.870676 |
| 2511.312524 | 100.053247 | | 2511.312524 | 99.871628 |
| 2515.170147 | 100.049441 | | 2515.170147 | 99.866102 |
| 2519.02777 | 100.043965 | | 2519.02777 | 99.869452 |
| 2522.885393 | 100.055529 | | 2522.885393 | 99.868975 |
| 2526.743016 | 100.055605 | | 2526.743016 | 99.857505 |
| 2530.600639 | 100.045487 | | 2530.600639 | 99.854918 |

Table B-2.—FTIR peaks data for figure 20: FTIR spectra comparing clean membranes and fouled membranes

| Clean membrane | | | Biofouled membrane | |
|---|---|---|---|---|
| 2534.458262 | 100.056515 | | 2534.458262 | 99.862824 |
| 2538.315885 | 100.065918 | | 2538.315885 | 99.862386 |
| 2542.173507 | 100.064841 | | 2542.173507 | 99.852742 |
| 2546.03113 | 100.065155 | | 2546.03113 | 99.85685 |
| 2549.888753 | 100.063871 | | 2549.888753 | 99.864668 |
| 2553.746376 | 100.066658 | | 2553.746376 | 99.856162 |
| 2557.603999 | 100.066376 | | 2557.603999 | 99.846834 |
| 2561.461622 | 100.060142 | | 2561.461622 | 99.846328 |
| 2565.319245 | 100.056837 | | 2565.319245 | 99.843576 |
| 2569.176868 | 100.048103 | | 2569.176868 | 99.836769 |
| 2573.034491 | 100.042662 | | 2573.034491 | 99.840115 |
| 2576.892114 | 100.054227 | | 2576.892114 | 99.849037 |
| 2580.749737 | 100.062274 | | 2580.749737 | 99.851495 |
| 2584.60736 | 100.059673 | | 2584.60736 | 99.853425 |
| 2588.464983 | 100.060219 | | 2588.464983 | 99.852322 |
| 2592.322605 | 100.063122 | | 2592.322605 | 99.846084 |
| 2596.180228 | 100.065999 | | 2596.180228 | 99.832437 |
| 2600.037851 | 100.063999 | | 2600.037851 | 99.8168 |
| 2603.895474 | 100.052627 | | 2603.895474 | 99.825555 |
| 2607.753097 | 100.042022 | | 2607.753097 | 99.845202 |
| 2611.61072 | 100.044176 | | 2611.61072 | 99.84182 |
| 2615.468343 | 100.055404 | | 2615.468343 | 99.82567 |
| 2619.325966 | 100.06108 | | 2619.325966 | 99.810662 |
| 2623.183589 | 100.07036 | | 2623.183589 | 99.803941 |
| 2627.041212 | 100.087081 | | 2627.041212 | 99.812939 |
| 2630.898835 | 100.079621 | | 2630.898835 | 99.81819 |
| 2634.756458 | 100.055492 | | 2634.756458 | 99.815178 |
| 2638.614081 | 100.054135 | | 2638.614081 | 99.818785 |
| 2642.471703 | 100.073942 | | 2642.471703 | 99.821462 |
| 2646.329326 | 100.089171 | | 2646.329326 | 99.817971 |
| 2650.186949 | 100.082231 | | 2650.186949 | 99.813704 |
| 2654.044572 | 100.066537 | | 2654.044572 | 99.813992 |
| 2657.902195 | 100.064993 | | 2657.902195 | 99.811925 |
| 2661.759818 | 100.064659 | | 2661.759818 | 99.802284 |
| 2665.617441 | 100.054111 | | 2665.617441 | 99.802112 |
| 2669.475064 | 100.048935 | | 2669.475064 | 99.80437 |
| 2673.332687 | 100.056639 | | 2673.332687 | 99.798497 |

Table B-2.—FTIR peaks data for figure 20: FTIR spectra comparing clean membranes and fouled membranes

| Clean membrane | | | Biofouled membrane | |
|---|---|---|---|---|
| 2677.19031 | 100.059476 | | 2677.19031 | 99.800401 |
| 2681.047933 | 100.057881 | | 2681.047933 | 99.797724 |
| 2684.905556 | 100.069247 | | 2684.905556 | 99.779243 |
| 2688.763179 | 100.067425 | | 2688.763179 | 99.773918 |
| 2692.620802 | 100.052869 | | 2692.620802 | 99.78484 |
| 2696.478424 | 100.062343 | | 2696.478424 | 99.77642 |
| 2700.336047 | 100.071443 | | 2700.336047 | 99.755394 |
| 2704.19367 | 100.059303 | | 2704.19367 | 99.752045 |
| 2708.051293 | 100.055162 | | 2708.051293 | 99.753547 |
| 2711.908916 | 100.061551 | | 2711.908916 | 99.746185 |
| 2715.766539 | 100.049134 | | 2715.766539 | 99.735832 |
| 2719.624162 | 100.036252 | | 2719.624162 | 99.727389 |
| 2723.481785 | 100.055368 | | 2723.481785 | 99.71894 |
| 2727.339408 | 100.070568 | | 2727.339408 | 99.703311 |
| 2731.197031 | 100.062191 | | 2731.197031 | 99.69244 |
| 2735.054654 | 100.058488 | | 2735.054654 | 99.688386 |
| 2738.912277 | 100.061758 | | 2738.912277 | 99.686911 |
| 2742.7699 | 100.061415 | | 2742.7699 | 99.694068 |
| 2746.627522 | 100.055684 | | 2746.627522 | 99.689504 |
| 2750.485145 | 100.039309 | | 2750.485145 | 99.67614 |
| 2754.342768 | 100.024468 | | 2754.342768 | 99.671445 |
| 2758.200391 | 100.035807 | | 2758.200391 | 99.65805 |
| 2762.058014 | 100.048788 | | 2762.058014 | 99.642839 |
| 2765.915637 | 100.04525 | | 2765.915637 | 99.634228 |
| 2769.77326 | 100.05062 | | 2769.77326 | 99.617636 |
| 2773.630883 | 100.05646 | | 2773.630883 | 99.607163 |
| 2777.488506 | 100.052592 | | 2777.488506 | 99.60928 |
| 2781.346129 | 100.039497 | | 2781.346129 | 99.601272 |
| 2785.203752 | 100.026769 | | 2785.203752 | 99.591909 |
| 2789.061375 | 100.037084 | | 2789.061375 | 99.596985 |
| 2792.918998 | 100.04578 | | 2792.918998 | 99.592054 |
| 2796.77662 | 100.046179 | | 2796.77662 | 99.57258 |
| 2800.634243 | 100.0489 | | 2800.634243 | 99.552987 |
| 2804.491866 | 100.03271 | | 2804.491866 | 99.530526 |
| 2808.349489 | 100.018362 | | 2808.349489 | 99.523464 |
| 2812.207112 | 100.021253 | | 2812.207112 | 99.521654 |
| 2816.064735 | 100.018262 | | 2816.064735 | 99.494145 |

Table B-2.—FTIR peaks data for figure 20: FTIR spectra comparing clean membranes and fouled membranes

| Clean membrane | | | Biofouled membrane | |
|---|---|---|---|---|
| 2819.922358 | 100.010916 | | 2819.922358 | 99.470053 |
| 2823.779981 | 100.009429 | | 2823.779981 | 99.458707 |
| 2827.637604 | 100.017611 | | 2827.637604 | 99.440529 |
| 2831.495227 | 100.028217 | | 2831.495227 | 99.423145 |
| 2835.35285 | 100.030708 | | 2835.35285 | 99.409449 |
| 2839.210473 | 100.023966 | | 2839.210473 | 99.414113 |
| 2843.068096 | 100.008927 | | 2843.068096 | 99.4221 |
| 2846.925719 | 100.004924 | | 2846.925719 | 99.409079 |
| 2850.783341 | 100.01232 | | 2850.783341 | 99.407188 |
| 2854.640964 | 100.017716 | | 2854.640964 | 99.408439 |
| 2858.498587 | 100.032304 | | 2858.498587 | 99.399763 |
| 2862.35621 | 100.035146 | | 2862.35621 | 99.396562 |
| 2866.213833 | 100.019519 | | 2866.213833 | 99.377652 |
| 2870.071456 | 100.010008 | | 2870.071456 | 99.349457 |
| 2873.929079 | 100.001035 | | 2873.929079 | 99.322759 |
| 2877.786702 | 99.994973 | | 2877.786702 | 99.299695 |
| 2881.644325 | 99.983557 | | 2881.644325 | 99.297585 |
| 2885.501948 | 99.968283 | | 2885.501948 | 99.291297 |
| 2889.359571 | 99.972268 | | 2889.359571 | 99.262869 |
| 2893.217194 | 99.97246 | | 2893.217194 | 99.225739 |
| 2897.074817 | 99.967512 | | 2897.074817 | 99.176572 |
| 2900.932439 | 99.974935 | | 2900.932439 | 99.132477 |
| 2904.790062 | 99.977269 | | 2904.790062 | 99.111399 |
| 2908.647685 | 99.973895 | | 2908.647685 | 99.084987 |
| 2912.505308 | 99.971179 | | 2912.505308 | 99.05478 |
| 2916.362931 | 99.968728 | | 2916.362931 | 99.043404 |
| 2920.220554 | 99.978125 | | 2920.220554 | 99.026032 |
| 2924.078177 | 99.996249 | | 2924.078177 | 98.993906 |
| 2927.9358 | 99.995386 | | 2927.9358 | 98.956942 |
| 2931.793423 | 99.982331 | | 2931.793423 | 98.912876 |
| 2935.651046 | 99.980657 | | 2935.651046 | 98.864373 |
| 2939.508669 | 99.961944 | | 2939.508669 | 98.820892 |
| 2943.366292 | 99.925016 | | 2943.366292 | 98.788664 |
| 2947.223915 | 99.904834 | | 2947.223915 | 98.757645 |
| 2951.081537 | 99.898846 | | 2951.081537 | 98.731914 |
| 2954.93916 | 99.893813 | | 2954.93916 | 98.713381 |
| 2958.796783 | 99.887534 | | 2958.796783 | 98.690428 |

Table B-2.—FTIR peaks data for figure 20: FTIR spectra comparing clean membranes and fouled membranes

| Clean membrane | | | Biofouled membrane | |
|---|---|---|---|---|
| 2962.654406 | 99.89074 | | 2962.654406 | 98.66522 |
| 2966.512029 | 99.892539 | | 2966.512029 | 98.640211 |
| 2970.369652 | 99.86636 | | 2970.369652 | 98.610421 |
| 2974.227275 | 99.835426 | | 2974.227275 | 98.562304 |
| 2978.084898 | 99.82463 | | 2978.084898 | 98.513806 |
| 2981.942521 | 99.813356 | | 2981.942521 | 98.450583 |
| 2985.800144 | 99.7867 | | 2985.800144 | 98.330956 |
| 2989.657767 | 99.763873 | | 2989.657767 | 98.214782 |
| 2993.51539 | 99.750455 | | 2993.51539 | 98.137428 |
| 2997.373013 | 99.732598 | | 2997.373013 | 98.076815 |
| 3001.230635 | 99.717212 | | 3001.230635 | 98.022578 |
| 3005.088258 | 99.706259 | | 3005.088258 | 97.940818 |
| 3008.945881 | 99.692046 | | 3008.945881 | 97.849628 |
| 3012.803504 | 99.672653 | | 3012.803504 | 97.790756 |
| 3016.661127 | 99.645992 | | 3016.661127 | 97.751269 |
| 3020.51875 | 99.628898 | | 3020.51875 | 97.687584 |
| 3024.376373 | 99.620787 | | 3024.376373 | 97.602026 |
| 3028.233996 | 99.596844 | | 3028.233996 | 97.537389 |
| 3032.091619 | 99.573864 | | 3032.091619 | 97.465399 |
| 3035.949242 | 99.564521 | | 3035.949242 | 97.369066 |
| 3039.806865 | 99.543052 | | 3039.806865 | 97.284235 |
| 3043.664488 | 99.513204 | | 3043.664488 | 97.207723 |
| 3047.522111 | 99.49254 | | 3047.522111 | 97.133675 |
| 3051.379734 | 99.479881 | | 3051.379734 | 97.047418 |
| 3055.237356 | 99.459869 | | 3055.237356 | 96.943023 |
| 3059.094979 | 99.422735 | | 3059.094979 | 96.855361 |
| 3062.952602 | 99.401494 | | 3062.952602 | 96.78114 |
| 3066.810225 | 99.400374 | | 3066.810225 | 96.685473 |
| 3070.667848 | 99.374148 | | 3070.667848 | 96.568658 |
| 3074.525471 | 99.331999 | | 3074.525471 | 96.464936 |
| 3078.383094 | 99.309633 | | 3078.383094 | 96.367578 |
| 3082.240717 | 99.293422 | | 3082.240717 | 96.24769 |
| 3086.09834 | 99.264401 | | 3086.09834 | 96.134687 |
| 3089.955963 | 99.235972 | | 3089.955963 | 96.028059 |
| 3093.813586 | 99.218482 | | 3093.813586 | 95.901313 |
| 3097.671209 | 99.201309 | | 3097.671209 | 95.777294 |
| 3101.528832 | 99.169347 | | 3101.528832 | 95.658184 |

Table B-2.—FTIR peaks data for figure 20: FTIR spectra comparing clean membranes and fouled membranes

| Clean membrane | | | Biofouled membrane | |
|---|---|---|---|---|
| 3105.386454 | 99.137352 | | 3105.386454 | 95.53089 |
| 3109.244077 | 99.116954 | | 3109.244077 | 95.397148 |
| 3113.1017 | 99.074309 | | 3113.1017 | 95.262772 |
| 3116.959323 | 99.024556 | | 3116.959323 | 95.136677 |
| 3120.816946 | 99.003199 | | 3120.816946 | 95.005351 |
| 3124.674569 | 98.982659 | | 3124.674569 | 94.864605 |
| 3128.532192 | 98.958532 | | 3128.532192 | 94.732407 |
| 3132.389815 | 98.935895 | | 3132.389815 | 94.609282 |
| 3136.247438 | 98.897032 | | 3136.247438 | 94.47031 |
| 3140.105061 | 98.85184 | | 3140.105061 | 94.310262 |
| 3143.962684 | 98.815863 | | 3143.962684 | 94.15955 |
| 3147.820307 | 98.78687 | | 3147.820307 | 94.02067 |
| 3151.67793 | 98.752914 | | 3151.67793 | 93.878701 |
| 3155.535552 | 98.712724 | | 3155.535552 | 93.73475 |
| 3159.393175 | 98.677505 | | 3159.393175 | 93.585875 |
| 3163.250798 | 98.648338 | | 3163.250798 | 93.43342 |
| 3167.108421 | 98.616261 | | 3167.108421 | 93.280489 |
| 3170.966044 | 98.581497 | | 3170.966044 | 93.129826 |
| 3174.823667 | 98.5501 | | 3174.823667 | 92.986098 |
| 3178.68129 | 98.50961 | | 3178.68129 | 92.842392 |
| 3182.538913 | 98.465981 | | 3182.538913 | 92.68561 |
| 3186.396536 | 98.435999 | | 3186.396536 | 92.524572 |
| 3190.254159 | 98.401804 | | 3190.254159 | 92.376333 |
| 3194.111782 | 98.366616 | | 3194.111782 | 92.239098 |
| 3197.969405 | 98.336683 | | 3197.969405 | 92.118348 |
| 3201.827028 | 98.294003 | | 3201.827028 | 91.998896 |
| 3205.684651 | 98.257159 | | 3205.684651 | 91.859777 |
| 3209.542273 | 98.235719 | | 3209.542273 | 91.729677 |
| 3213.399896 | 98.208752 | | 3213.399896 | 91.616209 |
| 3217.257519 | 98.175859 | | 3217.257519 | 91.503952 |
| 3221.115142 | 98.143437 | | 3221.115142 | 91.392217 |
| 3224.972765 | 98.116678 | | 3224.972765 | 91.278776 |
| 3228.830388 | 98.09319 | | 3228.830388 | 91.173311 |
| 3232.688011 | 98.0626 | | 3232.688011 | 91.075252 |
| 3236.545634 | 98.022246 | | 3236.545634 | 90.991607 |
| 3240.403257 | 97.984001 | | 3240.403257 | 90.919974 |
| 3244.26088 | 97.968802 | | 3244.26088 | 90.823531 |

Table B-2.—FTIR peaks data for figure 20: FTIR spectra comparing clean membranes and fouled membranes

| Clean membrane | | | Biofouled membrane | |
|---|---|---|---|---|
| 3248.118503 | 97.962931 | | 3248.118503 | 90.737416 |
| 3251.976126 | 97.945796 | | 3251.976126 | 90.693202 |
| 3255.833749 | 97.925126 | | 3255.833749 | 90.634203 |
| 3259.691371 | 97.895255 | | 3259.691371 | 90.559384 |
| 3263.548994 | 97.866364 | | 3263.548994 | 90.499379 |
| 3267.406617 | 97.858455 | | 3267.406617 | 90.440649 |
| 3271.26424 | 97.85064 | | 3271.26424 | 90.393389 |
| 3275.121863 | 97.831329 | | 3275.121863 | 90.368179 |
| 3278.979486 | 97.816107 | | 3278.979486 | 90.332476 |
| 3282.837109 | 97.814378 | | 3282.837109 | 90.274142 |
| 3286.694732 | 97.818106 | | 3286.694732 | 90.223328 |
| 3290.552355 | 97.803709 | | 3290.552355 | 90.188401 |
| 3294.409978 | 97.774961 | | 3294.409978 | 90.155408 |
| 3298.267601 | 97.75952 | | 3298.267601 | 90.117384 |
| 3302.125224 | 97.749902 | | 3302.125224 | 90.061917 |
| 3305.982847 | 97.725858 | | 3305.982847 | 89.997087 |
| 3309.840469 | 97.70302 | | 3309.840469 | 89.946559 |
| 3313.698092 | 97.691287 | | 3313.698092 | 89.907521 |
| 3317.555715 | 97.674138 | | 3317.555715 | 89.862657 |
| 3321.413338 | 97.656631 | | 3321.413338 | 89.803656 |
| 3325.270961 | 97.640491 | | 3325.270961 | 89.747548 |
| 3329.128584 | 97.613544 | | 3329.128584 | 89.712059 |
| 3332.986207 | 97.59071 | | 3332.986207 | 89.676175 |
| 3336.84383 | 97.580075 | | 3336.84383 | 89.633744 |
| 3340.701453 | 97.573515 | | 3340.701453 | 89.601948 |
| 3344.559076 | 97.560834 | | 3344.559076 | 89.56369 |
| 3348.416699 | 97.538391 | | 3348.416699 | 89.519319 |
| 3352.274322 | 97.522041 | | 3352.274322 | 89.488014 |
| 3356.131945 | 97.509124 | | 3356.131945 | 89.457701 |
| 3359.989568 | 97.492714 | | 3359.989568 | 89.42343 |
| 3363.84719 | 97.480891 | | 3363.84719 | 89.390805 |
| 3367.704813 | 97.470268 | | 3367.704813 | 89.36972 |
| 3371.562436 | 97.456928 | | 3371.562436 | 89.354617 |
| 3375.420059 | 97.4371 | | 3375.420059 | 89.343046 |
| 3379.277682 | 97.411635 | | 3379.277682 | 89.365288 |
| 3383.135305 | 97.398513 | | 3383.135305 | 89.385839 |
| 3386.992928 | 97.409399 | | 3386.992928 | 89.374708 |

Table B-2.—FTIR peaks data for figure 20: FTIR spectra comparing clean membranes and fouled membranes

| Clean membrane | | | Biofouled membrane | |
|---|---|---|---|---|
| 3390.850551 | 97.422853 | | 3390.850551 | 89.390804 |
| 3394.708174 | 97.416416 | | 3394.708174 | 89.436518 |
| 3398.565797 | 97.408191 | | 3398.565797 | 89.475616 |
| 3402.42342 | 97.413143 | | 3402.42342 | 89.511498 |
| 3406.281043 | 97.418336 | | 3406.281043 | 89.551745 |
| 3410.138666 | 97.422732 | | 3410.138666 | 89.606332 |
| 3413.996288 | 97.439003 | | 3413.996288 | 89.671717 |
| 3417.853911 | 97.461751 | | 3417.853911 | 89.746665 |
| 3421.711534 | 97.47481 | | 3421.711534 | 89.836099 |
| 3425.569157 | 97.492805 | | 3425.569157 | 89.918238 |
| 3429.42678 | 97.524203 | | 3429.42678 | 90.000469 |
| 3433.284403 | 97.536992 | | 3433.284403 | 90.09964 |
| 3437.142026 | 97.5387 | | 3437.142026 | 90.198025 |
| 3440.999649 | 97.554703 | | 3440.999649 | 90.297237 |
| 3444.857272 | 97.569897 | | 3444.857272 | 90.399286 |
| 3448.714895 | 97.599445 | | 3448.714895 | 90.501049 |
| 3452.572518 | 97.646712 | | 3452.572518 | 90.602038 |
| 3456.430141 | 97.673963 | | 3456.430141 | 90.709924 |
| 3460.287764 | 97.698108 | | 3460.287764 | 90.846566 |
| 3464.145386 | 97.73676 | | 3464.145386 | 90.972883 |
| 3468.003009 | 97.76295 | | 3468.003009 | 91.078802 |
| 3471.860632 | 97.77653 | | 3471.860632 | 91.212854 |
| 3475.718255 | 97.80993 | | 3475.718255 | 91.354612 |
| 3479.575878 | 97.865417 | | 3479.575878 | 91.489512 |
| 3483.433501 | 97.90659 | | 3483.433501 | 91.630076 |
| 3487.291124 | 97.936485 | | 3487.291124 | 91.770626 |
| 3491.148747 | 97.967222 | | 3491.148747 | 91.902934 |
| 3495.00637 | 97.980663 | | 3495.00637 | 92.028094 |
| 3498.863993 | 97.990456 | | 3498.863993 | 92.168604 |
| 3502.721616 | 98.00587 | | 3502.721616 | 92.300962 |
| 3506.579239 | 98.027149 | | 3506.579239 | 92.413515 |
| 3510.436862 | 98.060751 | | 3510.436862 | 92.550926 |
| 3514.294484 | 98.09068 | | 3514.294484 | 92.704166 |
| 3518.152107 | 98.116824 | | 3518.152107 | 92.850801 |
| 3522.00973 | 98.129642 | | 3522.00973 | 93.000303 |
| 3525.867353 | 98.140238 | | 3525.867353 | 93.152476 |
| 3529.724976 | 98.196259 | | 3529.724976 | 93.293977 |

Table B-2.—FTIR peaks data for figure 20: FTIR spectra comparing clean membranes and fouled membranes

| **Clean membrane** | | | **Biofouled membrane** | |
|---|---|---|---|---|
| 3533.582599 | 98.267283 | | 3533.582599 | 93.427931 |
| 3537.440222 | 98.318041 | | 3537.440222 | 93.582155 |
| 3541.297845 | 98.358423 | | 3541.297845 | 93.752118 |
| 3545.155468 | 98.392493 | | 3545.155468 | 93.907288 |
| 3549.013091 | 98.435031 | | 3549.013091 | 94.049377 |
| 3552.870714 | 98.473261 | | 3552.870714 | 94.192934 |
| 3556.728337 | 98.49905 | | 3556.728337 | 94.345827 |
| 3560.58596 | 98.531154 | | 3560.58596 | 94.508262 |
| 3564.443583 | 98.565747 | | 3564.443583 | 94.658147 |
| 3568.301205 | 98.60518 | | 3568.301205 | 94.796118 |
| 3572.158828 | 98.659836 | | 3572.158828 | 94.941183 |
| 3576.016451 | 98.714997 | | 3576.016451 | 95.082709 |
| 3579.874074 | 98.748923 | | 3579.874074 | 95.231349 |
| 3583.731697 | 98.781806 | | 3583.731697 | 95.382884 |
| 3587.58932 | 98.820691 | | 3587.58932 | 95.508787 |
| 3591.446943 | 98.843261 | | 3591.446943 | 95.624749 |
| 3595.304566 | 98.876721 | | 3595.304566 | 95.747515 |
| 3599.162189 | 98.934199 | | 3599.162189 | 95.881318 |
| 3603.019812 | 98.990254 | | 3603.019812 | 96.006581 |
| 3606.877435 | 99.034076 | | 3606.877435 | 96.125527 |
| 3610.735058 | 99.065679 | | 3610.735058 | 96.27062 |
| 3614.592681 | 99.105135 | | 3614.592681 | 96.406742 |
| 3618.450303 | 99.154781 | | 3618.450303 | 96.541323 |
| 3622.307926 | 99.188962 | | 3622.307926 | 96.705641 |
| 3626.165549 | 99.213741 | | 3626.165549 | 96.858796 |
| 3630.023172 | 99.260805 | | 3630.023172 | 97.006772 |
| 3633.880795 | 99.323771 | | 3633.880795 | 97.160665 |
| 3637.738418 | 99.371326 | | 3637.738418 | 97.309202 |
| 3641.596041 | 99.405053 | | 3641.596041 | 97.476031 |
| 3645.453664 | 99.441316 | | 3645.453664 | 97.643605 |
| 3649.311287 | 99.482136 | | 3649.311287 | 97.789605 |
| 3653.16891 | 99.527237 | | 3653.16891 | 97.942773 |
| 3657.026533 | 99.587182 | | 3657.026533 | 98.100282 |
| 3660.884156 | 99.664102 | | 3660.884156 | 98.235066 |
| 3664.741779 | 99.728152 | | 3664.741779 | 98.356987 |
| 3668.599401 | 99.766521 | | 3668.599401 | 98.479965 |
| 3672.457024 | 99.803063 | | 3672.457024 | 98.594805 |

Table B-2.—FTIR peaks data for figure 20: FTIR spectra comparing clean membranes and fouled membranes

| Clean membrane | | | Biofouled membrane | |
|---|---|---|---|---|
| 3676.314647 | 99.843073 | | 3676.314647 | 98.691074 |
| 3680.17227 | 99.881952 | | 3680.17227 | 98.77343 |
| 3684.029893 | 99.918924 | | 3684.029893 | 98.846116 |
| 3687.887516 | 99.937995 | | 3687.887516 | 98.902774 |
| 3691.745139 | 99.964844 | | 3691.745139 | 98.94982 |
| 3695.602762 | 100.020272 | | 3695.602762 | 99.007312 |
| 3699.460385 | 100.059045 | | 3699.460385 | 99.075306 |
| 3703.318008 | 100.068903 | | 3703.318008 | 99.133663 |
| 3707.175631 | 100.070952 | | 3707.175631 | 99.171943 |
| 3711.033254 | 100.077265 | | 3711.033254 | 99.189637 |
| 3714.890877 | 100.10221 | | 3714.890877 | 99.204374 |
| 3718.7485 | 100.132791 | | 3718.7485 | 99.229132 |
| 3722.606122 | 100.149526 | | 3722.606122 | 99.245205 |
| 3726.463745 | 100.152273 | | 3726.463745 | 99.261023 |
| 3730.321368 | 100.13969 | | 3730.321368 | 99.275445 |
| 3734.178991 | 100.124158 | | 3734.178991 | 99.271365 |
| 3738.036614 | 100.134556 | | 3738.036614 | 99.265376 |
| 3741.894237 | 100.159157 | | 3741.894237 | 99.251217 |
| 3745.75186 | 100.173101 | | 3745.75186 | 99.249063 |
| 3749.609483 | 100.178321 | | 3749.609483 | 99.285565 |
| 3753.467106 | 100.174107 | | 3753.467106 | 99.302766 |
| 3757.324729 | 100.172821 | | 3757.324729 | 99.284419 |
| 3761.182352 | 100.176497 | | 3761.182352 | 99.284911 |
| 3765.039975 | 100.17612 | | 3765.039975 | 99.307311 |
| 3768.897598 | 100.182331 | | 3768.897598 | 99.319043 |
| 3772.75522 | 100.193733 | | 3772.75522 | 99.33072 |
| 3776.612843 | 100.194749 | | 3776.612843 | 99.354239 |
| 3780.470466 | 100.171348 | | 3780.470466 | 99.365263 |
| 3784.328089 | 100.163199 | | 3784.328089 | 99.365725 |
| 3788.185712 | 100.190849 | | 3788.185712 | 99.361403 |
| 3792.043335 | 100.191801 | | 3792.043335 | 99.335741 |
| 3795.900958 | 100.181842 | | 3795.900958 | 99.313655 |
| 3799.758581 | 100.197984 | | 3799.758581 | 99.318237 |
| 3803.616204 | 100.198772 | | 3803.616204 | 99.33114 |
| 3807.473827 | 100.177176 | | 3807.473827 | 99.350799 |
| 3811.33145 | 100.152055 | | 3811.33145 | 99.364647 |
| 3815.189073 | 100.144852 | | 3815.189073 | 99.350346 |

Table B-2.—FTIR peaks data for figure 20: FTIR spectra comparing clean membranes and fouled membranes

| Clean membrane | | | Biofouled membrane | |
|---|---|---|---|---|
| 3819.046696 | 100.170364 | | 3819.046696 | 99.330719 |
| 3822.904318 | 100.185257 | | 3822.904318 | 99.333874 |
| 3826.761941 | 100.17167 | | 3826.761941 | 99.346256 |
| 3830.619564 | 100.175512 | | 3830.619564 | 99.338351 |
| 3834.477187 | 100.193776 | | 3834.477187 | 99.322238 |
| 3838.33481 | 100.193997 | | 3838.33481 | 99.325526 |
| 3842.192433 | 100.197619 | | 3842.192433 | 99.346404 |
| 3846.050056 | 100.197204 | | 3846.050056 | 99.364635 |
| 3849.907679 | 100.162592 | | 3849.907679 | 99.355718 |
| 3853.765302 | 100.145736 | | 3853.765302 | 99.346936 |
| 3857.622925 | 100.180669 | | 3857.622925 | 99.355864 |
| 3861.480548 | 100.201869 | | 3861.480548 | 99.339542 |
| 3865.338171 | 100.190278 | | 3865.338171 | 99.313284 |
| 3869.195794 | 100.187453 | | 3869.195794 | 99.317623 |
| 3873.053417 | 100.184454 | | 3873.053417 | 99.339235 |
| 3876.911039 | 100.176718 | | 3876.911039 | 99.352135 |
| 3880.768662 | 100.183706 | | 3880.768662 | 99.350839 |
| 3884.626285 | 100.190327 | | 3884.626285 | 99.335921 |
| 3888.483908 | 100.193043 | | 3888.483908 | 99.320386 |
| 3892.341531 | 100.201854 | | 3892.341531 | 99.333556 |
| 3896.199154 | 100.209688 | | 3896.199154 | 99.348616 |
| 3900.056777 | 100.209326 | | 3900.056777 | 99.340461 |
| 3903.9144 | 100.202855 | | 3903.9144 | 99.341021 |
| 3907.772023 | 100.188826 | | 3907.772023 | 99.344085 |
| 3911.629646 | 100.177108 | | 3911.629646 | 99.349128 |
| 3915.487269 | 100.195212 | | 3915.487269 | 99.375386 |
| 3919.344892 | 100.205093 | | 3919.344892 | 99.395825 |
| 3923.202515 | 100.191939 | | 3923.202515 | 99.391474 |
| 3927.060137 | 100.219259 | | 3927.060137 | 99.368604 |
| 3930.91776 | 100.236448 | | 3930.91776 | 99.339067 |
| 3934.775383 | 100.206089 | | 3934.775383 | 99.315896 |
| 3938.633006 | 100.207851 | | 3938.633006 | 99.309534 |
| 3942.490629 | 100.217533 | | 3942.490629 | 99.326253 |
| 3946.348252 | 100.195419 | | 3946.348252 | 99.341326 |
| 3950.205875 | 100.182345 | | 3950.205875 | 99.337083 |
| 3954.063498 | 100.17935 | | 3954.063498 | 99.328452 |
| 3957.921121 | 100.187279 | | 3957.921121 | 99.320825 |

Table B-2.—FTIR peaks data for figure 20: FTIR spectra comparing clean membranes and fouled membranes

| Clean membrane | | | Biofouled membrane | |
|---|---|---|---|---|
| 3961.778744 | 100.199561 | | 3961.778744 | 99.311638 |
| 3965.636367 | 100.194422 | | 3965.636367 | 99.299664 |
| 3969.49399 | 100.201445 | | 3969.49399 | 99.302171 |
| 3973.351613 | 100.21541 | | 3973.351613 | 99.328636 |
| 3977.209235 | 100.20726 | | 3977.209235 | 99.332012 |
| 3981.066858 | 100.201704 | | 3981.066858 | 99.305618 |
| 3984.924481 | 100.198872 | | 3984.924481 | 99.312814 |
| 3988.782104 | 100.178891 | | 3988.782104 | 99.339194 |
| 3992.639727 | 100.167036 | | 3992.639727 | 99.330064 |
| 3996.49735 | 100.17918 | | 3996.49735 | 99.315702 |
| 4000.354973 | 100.199213 | | 4000.354973 | 99.323662 |

# APPENDIX C

## Flux Data

The acronyms, abbreviations, and units of measure as they appear in this appendix are defined as follows:

| | |
|---|---|
| $cm^2$ | square centimeter |
| g/L | grams per liter |
| h | hour |
| L | liter |
| L/h | liters per hour |
| $L/m^2$-h | Liters per square meter per hour |
| $m^2$ | square meter |
| mg/L | milligram per liter |
| mL | milliliter |
| min | minute |
| NaCl | sodium chloride |
| psi | pounds per square inch |
| psia | Pounds per square inch absolute |
| s | second |
| **Symbols** | |
| µm | micron |
| # | number |
| % | percent |

Actual flux data of filtration experiments with distilled (DI) water (0–8 hours), bovine serum albumin (BSA) (8–16 hours), and lipase (16–24 hours) presented on figure 17.

Table C-1.—Flux data of cellulose acetate (CA) membranes with DI water, BSA, and lipase

| | | | $cm^2$ | $m^2$ | | | | |
|---|---|---|---|---|---|---|---|---|
| Effective membrane area | | 21% CA | 4.1 | 0.00041 | | | | |
| Date: 8/21/12 | | Thickness: | **120.904** | microns (µm) | | P (psia) | 70 | |
| **Precompaction** | | | | | | | | |
| **Starting time** | | **#** | **Volume (mL)** | **t (min)** | **t (s)** | **Time (h)** | **Flux ($L/m^2$-h)** | **Flux total time (h)** |
| 8/21, 11:21 AM | | 1 | 2 | 24 | 21 | 0.405833333 | 12.01983272 | 0.00 |
| 12:05 | | 2 | 2 | 25 | 32 | 0.425555556 | 11.46277781 | 0.733 |
| 13:22 | | 3 | 2 | 24 | 43 | 0.411944444 | 11.84152098 | 2.02 |
| 14:02 | | 4 | 2 | 25 | 26 | 0.423888889 | 11.50784771 | 2.68 |
| 15:17 | | 5 | 2 | 26 | 26 | 0.440555556 | 11.07249408 | 3.93 |
| 15:59 | | 6 | 2 | 26 | 31 | 0.441944444 | 11.0376968 | 4.63 |
| 16:40 | | 7 | 2 | 26 | 57 | 0.449166667 | 10.86021992 | 5.32 |
| 13:05 | | 8 | 2 | 27 | 55 | 0.465277778 | 10.48416454 | 6.18 |
| 13:51 | | 9 | 2 | 27 | 58 | 0.466111111 | 10.46542051 | 6.95 |
| **Filtration with BSA – 5 mg/L** | | | | | | | | |
| **Starting time** | | **#** | **Volume (mL)** | **t (min)** | **t (s)** | **Time (h)** | **Flux ($L/m^2$-h)** | **Flux total time (h)** |
| 8/23, 10:38 AM | | 10 | 2 | 48 | 19 | 0.805277778 | 6.057597658 | 7.88 |
| 11:24 | | 11 | 2 | 48 | 35 | 0.809722222 | 6.024348408 | 8.650 |
| 12:12 | | 12 | 2 | 48 | 36 | 0.81 | 6.022282445 | 9.450 |
| 13:23 | | 13 | 2 | 52 | 9 | 0.869166667 | 5.612328415 | 10.633 |
| 14:16 | | 14 | 2 | 53 | 3 | 0.884166667 | 5.517114549 | 11.517 |
| 15:06 | | 15 | 2 | 53 | 31 | 0.891944444 | 5.469005173 | 12.350 |
| 15:55 | | 16 | 2 | 53 | 36 | 0.893333333 | 5.460502366 | 13.17 |
| 11:36 | | 17 | 2 | 54 | 15 | 0.904166667 | 5.395076992 | 14.15 |
| 13:07 | | 18 | 2 | 54 | 16 | 0.904444444 | 5.393420028 | 15.67 |
| **Filtration with lipase - 5 mg/L** | | | | | | | | |
| **Starting time** | | **#** | **Volume (mL)** | **t (min)** | **t (s)** | **Time (h)** | **Flux ($L/m^2$-h)** | **Total time (h)** |
| 8/27, 1:27 PM | | 22 | 2 | 46 | 17 | 0.771388889 | 6.323721862 | 16.87 |
| 14:24 | | 23 | 2 | 47 | 30 | 0.791666667 | 6.161745828 | 17.817 |
| 15:17 | | 24 | 2 | 47 | 2 | 0.783888889 | 6.222882923 | 18.700 |
| 16:10 | | 25 | 2 | 46 | 38 | 0.777222222 | 6.276260046 | 19.583 |
| 11:36 | | 26 | 2 | 45 | 57 | 0.765833333 | 6.369595796 | 20.433 |
| 13:53 | | 27 | 2 | 45 | 21 | 0.755833333 | 6.453868287 | 21.717 |
| 14:48 | | 28 | 2 | 45 | 28 | 0.757777778 | 6.437307775 | 22.633 |
| 15:43 | | 29 | 2 | 45 | 43 | 0.761944444 | 6.402105581 | 23.550 |
| 16:35 | | 30 | 2 | 45 | 58 | 0.766111111 | 6.367286298 | 24.42 |

Table C-2.—Flux data of copper-charged membrane with DI water, BSA, and lipase

| | | | $cm^2$ | $m^2$ | | | | |
|---|---|---|---|---|---|---|---|---|
| Effective membrane area | | | 4.1 | 0.00041 | | | | |
| Date: 12/6/12 | 21% CA | Thickness: | **122.683** | microns (µm) | | P (psia) | 70 | |
| **Precompaction** | | | | | | | | |
| **Starting time** | | **#** | **Volume (mL)** | **t (min)** | **t (s)** | **Time (h)** | **Flux ($L/m^2$-h)** | **Flux total time (h)** |
| 12/6, 11:51 AM | | 1 | 2 | 36 | 31 | 0.608611111 | 8.015050484 | 0.00 |
| 12:47 | | 2 | 2 | 36 | 25 | 0.606944444 | 8.037059776 | 1.050 |
| 13:41 | | 3 | 2 | 36 | 9 | 0.6025 | 8.096346524 | 2.20 |
| 13:35 | | 4 | 2 | 36 | 53 | 0.614722222 | 7.935370813 | 3.27 |
| 15:31 | | 5 | 2 | 36 | 40 | 0.611111111 | 7.982261641 | 4.40 |
| 16:25 | | 6 | 2 | 36 | 23 | 0.606388889 | 8.044423092 | 5.57 |
| 17:21 | | 7 | 2 | 36 | 18 | 0.605 | 8.062890546 | 6.75 |
| 16:30 | | 8 | 2 | 38 | 58 | 0.649444444 | 7.511110184 | 7.73 |
| **Filtration with BSA – 5 mg/L** | | | | | | | | |
| **Starting time** | | **#** | **Volume (mL)** | **t (min)** | **t (s)** | **Time (h)** | **Flux ($L/m^2$-h)** | **Flux total time (h)** |
| 10:46 | | 9 | 2 | 46 | 1 | 0.766944444 | 6.360367841 | 8.68 |
| 13:05 | | 10 | 2 | 47 | 18 | 0.788333333 | 6.187799722 | 11.000 |
| 14:20 | | 11 | 2 | 48 | 58 | 0.816111111 | 5.977187069 | 12.250 |
| 15:22 | | 12 | 2 | 47 | 58 | 0.799444444 | 6.101798336 | 13.283 |
| 16:26 | | 13 | 2 | 49 | 37 | 0.826944444 | 5.898883309 | 14.350 |
| 17:30 | | 14 | 2 | 47 | 37 | 0.793611111 | 6.146648796 | 15.417 |
| 18:29 | | 15 | 2 | 48 | 5 | 0.801388889 | 6.086993279 | 16.400 |
| Date: 12/ 10/12 | | | | | | | | |
| **Filtration with lipase – 5 mg/L** | | | | | | | | |
| **Starting time** | | **#** | **Volume (mL)** | **t (min)** | **t (s)** | **Time (h)** | **Flux ($L/m^2$-h)** | **Flux total time (h)** |
| 12/11, 10:26 AM | | 16 | 2 | 37 | 1 | 0.616944444 | 7.906787758 | 17.65 |
| 11:12 | | 17 | 2 | 37 | 47 | 0.629722222 | 7.74635007 | 18.42 |
| 12:00 | | 18 | 2 | 37 | 34 | 0.626111111 | 7.791027334 | 19.22 |
| 12:47 | | 19 | 2 | 38 | 13 | 0.636944444 | 7.658515312 | 20.00 |
| 13:41 | | 20 | 2 | 37 | 32 | 0.625555556 | 7.797946541 | 20.90 |
| 14:28 | | 21 | 2 | 38 | 25 | 0.640277778 | 7.618644516 | 21.67 |
| 15:16 | | 22 | 2 | 37 | 50 | 0.630555556 | 7.736112603 | 22.48 |

Table C-3.—Flux data for flux decline in 24-hour cross-flow filtration studies with biofoulant of cellulose acetate (CA) membranes for figure 18

| **CA membrane** | | | | | |
|---|---|---|---|---|---|
| **Time (h)** | **1st run** | **2nd run** | **3rd run** | **Average** | **Standard deviation** |
| 0 | 1.0000 | 1.0000 | 1.0000 | 1.0000 | 0.0000 |
| 1 | 0.7165 | 0.4847 | 0.7165 | 0.6392 | 0.1639 |
| 2 | 0.5651 | 0.4270 | 0.5651 | 0.5191 | 0.0977 |
| 4 | 0.5679 | 0.3600 | 0.4299 | 0.4526 | 0.1470 |
| 8.5 | 0.4299 | 0.2800 | 0.4000 | 0.3700 | 0.1060 |
| 18 | 0.3704 | 0.2484 | 0.1200 | 0.2462 | 0.0863 |
| 20 | 0.1013 | 0.2300 | 0.0800 | 0.1371 | 0.0910 |
| 22 | 0.0895 | 0.1800 | 0.0800 | 0.1165 | 0.0640 |
| 24 | 0.1048 | 0.1617 | 0.1000 | 0.1222 | 0.0402 |

Table C-4.— Flux decline data of 24-hour cross-flow filtration studies with biofoulant of copper-charged membranes for figure 18

| **Copper-charged membrane** | | | | | |
|---|---|---|---|---|---|
| **Time (h)** | **1st run** | **2nd run** | **3rd run** | **Average** | **Standard deviation** |
| 0 | 1.0000 | 1.0000 | 1.0000 | 1.0000 | 0.0000 |
| 1 | 0.9900 | 0.7300 | 0.9680 | 0.8600 | 0.1838 |
| 2 | 0.9000 | 0.5900 | 0.8900 | 0.7450 | 0.2192 |
| 4 | 0.7800 | 0.5000 | 0.7700 | 0.6400 | 0.1980 |
| 8.5 | 0.6400 | 0.4400 | 0.5710 | 0.5400 | 0.1414 |
| 18 | 0.4100 | 0.3000 | 0.3100 | 0.3550 | 0.0778 |
| 20 | 0.3600 | 0.2500 | 0.2800 | 0.3050 | 0.0778 |
| 22 | 0.3500 | 0.2200 | 0.2507 | 0.2850 | 0.0919 |
| 24 | 0.3400 | 0.2000 | 0.2346 | 0.2700 | 0.0990 |

Table C-5.—Flux decline data with transparent exopolymeric particles (1 mg/L) in saline water (35 g/L NaCl) of cellulose acetate membranes for figure 19

| Thickness: 129.5 µm | Effective area: 0.00041 $m^2$ | Pressure: 78 psi | | | | |
|---|---|---|---|---|---|---|
| **Cumulative filtration time (h)** | **Infiltration time (s)** | **Time (h)** | **Volume (L)** | **Flow rate (L/h)** | **Flux (L/$m^2$-h)** | **Normalized flux (%)** |
| 0.0000 | 2,298 | 0.6383 | 0.0020 | 0.0031 | 7.6419 | 100 |
| 1.2892 | 2,343 | 0.6508 | 0.0020 | 0.0031 | 7.4951 | 98 |
| 1.9772 | 2,477 | 0.6881 | 0.0020 | 0.0029 | 7.0896 | 93 |
| 2.6842 | 2,545 | 0.7069 | 0.0020 | 0.0028 | 6.9002 | 90 |
| 3.4106 | 2,615 | 0.7264 | 0.0020 | 0.0028 | 6.7155 | 88 |
| | | | | | | |
| Thickness: 128.5 µm | Effective area: 0.00041 $m^2$ | Pressure: 75 psi | | | | |
| **Cumulative filtration time (h)** | **Infiltration time (s)** | **Time (h)** | **Volume (L)** | **Flow rate (L/h)** | **Flux (L/$m^2$-h)** | **Normalized flux (%)** |
| 0.0000 | 4,257 | 1.1825 | 0.0020 | 0.0017 | 4.1252 | 1.0000 |
| 2.4158 | 4,440 | 1.2333 | 0.0020 | 0.0016 | 3.9552 | 0.9588 |
| 2.4806 | 4,490 | 1.2472 | 0.0020 | 0.0016 | 3.9111 | 0.9481 |
| | | | | | | |
| Thickness: 93.5 µm | Effective area: 0.00041 $m^2$ | Pressure: 70 psi | | | | |
| **Cumulative filtration time (h)** | **Infiltration time (s)** | **Time (h)** | **Volume (L)** | **Flow rate (L/h)** | **Flux (L/$m^2$-h)** | **Normalized flux (%)** |
| 0.0000 | 4,871 | 1.3531 | 0.0020 | 0.0015 | 3.6052 | 1.0000 |
| 2.7800 | 5,137 | 1.4269 | 0.0020 | 0.0014 | 3.4185 | 0.9482 |
| 4.2894 | 5,434 | 1.5094 | 0.0020 | 0.0013 | 3.2317 | 0.8964 |

Table C-6.—Flux decline data with transparent exopolymeric particles (1 mg/L) in saline water (35 g/L NaCl) of copper-charged membrane for figure 19

| Thickness: 113 µm | Effective area: 0.00041 $m^2$ | Pressure: 70 psi | | | | |
|---|---|---|---|---|---|---|
| **Cumulative filtration time (h)** | **Infiltration time (s)** | **Infiltration time (h)** | **Volume (L)** | **Flow rate (L/h)** | **Flux (L/$m^2$-h)** | **Normalized flux (%)** |
| 0.0000 | 3,665 | 1.0181 | 0.0020 | 0.0020 | 4.7915 | 100% |
| 2.0689 | 3,783 | 1.0508 | 0.0020 | 0.0019 | 4.6421 | 97% |
| 3.1578 | 3,920 | 1.0889 | 0.0020 | 0.0018 | 4.4798 | 93% |
| | | | | | | |
| Thickness: 178.4 µm | Effective area: 0.00041 $m^2$ | Pressure: 70 psi | | | | |
| **Cumulative filtration time (r)** | **Infiltration time (s)** | **Infiltration time (h)** | **Volume (L)** | **Flow rate (L/h)** | **Flux (L/$m^2$-h)** | **Normalized flux (%)** |
| 0.0000 | 4,765 | 1.3236 | 0.0020 | 0.0015 | 3.6854 | 100% |
| 2.6906 | 4,921 | 1.3669 | 0.0020 | 0.0015 | 3.5686 | 97% |
| 4.0586 | 4,925 | 1.3681 | 0.0020 | 0.0015 | 3.5657 | 97% |
| | | | | | | |
| Thickness: 188.5 µm | Effective area: 0.00041 $m^2$ | Pressure: 70 psi | | | | |
| **Cumulative filtration time (h)** | **Infiltration time (s)** | **Infiltration time (h)** | **Volume (L)** | **Flow rate (L/h)** | **Flux (L/$m^2$-h)** | **Normalized flux (%)** |
| 0.0000 | 4,401 | 1.2225 | 0.0020 | 0.0016 | 3.9902 | 100% |
| 2.5003 | 4,600 | 1.2778 | 0.0020 | 0.0016 | 3.8176 | 96% |
| 3.8336 | 4,800 | 1.3333 | 0.0020 | 0.0015 | 3.6585 | 92% |